



University  
of Glasgow

<https://theses.gla.ac.uk/>

Theses Digitisation:

<https://www.gla.ac.uk/myglasgow/research/enlighten/theses/digitisation/>

This is a digitised version of the original print thesis.

Copyright and moral rights for this work are retained by the author

A copy can be downloaded for personal non-commercial research or study, without prior permission or charge

This work cannot be reproduced or quoted extensively from without first obtaining permission in writing from the author

The content must not be changed in any way or sold commercially in any format or medium without the formal permission of the author

When referring to this work, full bibliographic details including the author, title, awarding institution and date of the thesis must be given

Enlighten: Theses

<https://theses.gla.ac.uk/>  
[research-enlighten@glasgow.ac.uk](mailto:research-enlighten@glasgow.ac.uk)

EXPERIMENTS ON AND RELATING TO THE  
DETECTION OF GRAVITATIONAL RADIATION

by

JOHN R. PUGH

DEPARTMENT OF NATURAL PHILOSOPHY  
UNIVERSITY OF GLASGOW

PRESENTED AS A THESIS FOR THE DEGREE OF  
Ph.D. IN THE UNIVERSITY OF GLASGOW

OCTOBER, 1976

ProQuest Number: 10800620

All rights reserved

INFORMATION TO ALL USERS

The quality of this reproduction is dependent upon the quality of the copy submitted.

In the unlikely event that the author did not send a complete manuscript and there are missing pages, these will be noted. Also, if material had to be removed, a note will indicate the deletion.



ProQuest 10800620

Published by ProQuest LLC (2018). Copyright of the Dissertation is held by the Author.

All rights reserved.

This work is protected against unauthorized copying under Title 17, United States Code  
Microform Edition © ProQuest LLC.

ProQuest LLC.  
789 East Eisenhower Parkway  
P.O. Box 1346  
Ann Arbor, MI 48106 – 1346

Thesis  
4492  
Copy 1.



## CONTENTS

	Page
Preface	
Acknowledgments	
Summary	
Chapter 1	Introduction 1
Chapter 2	An Investigation into the Low Noise Amplification of Signals. 22
Chapter 3	An Investigation into the Sensitivity of Various Gravitational Wave Detectors. 35
Chapter 4	The Consideration and Implementation of Various Techniques to Extract Continuous Signals from Gravitational Radiation Detectors. 66
Chapter 5	A Search for Continuous Gravitational Radiation. 82
Chapter 6	Conclusion 101
Appendix 1	An Investigation into the Possibility of Detecting Periodic Celestial X-Rays by a Ground Based Technique.
References	

## Preface

This thesis contains an account of experimental work performed by the author at the University of Glasgow between August 1973 and September 1976.

The research carried out was concerned with the detection of Gravitational Radiation, and the work at Glasgow was initiated by Professor R.W.P. Drever in 1970.

In the introductory chapter a brief historical note is followed by an elementary introduction to the General Relativity theory used in connection with gravitational waves. The magnitude of the effect expected, due to gravitational waves of extra terrestrial origin, is then summarised for various possible sources, and this offers an indication as to the required sensitivity of gravitational wave detectors. The chapter is then brought to a close with a discussion of various gravitational wave detectors that have been constructed and are in operation throughout the world. The content of this chapter is based on the relevant literature.

Chapter 2 contains a report of an investigation into the low noise amplification of signals from gravitational wave detectors. Firstly the possible noise improvement by cooling field effect transistors was investigated, due to an initial suggestion by Dr. J. Hough. The actual experimental investigation was the work of the author. An investigation was also performed into the noise sources of a superconducting quantum interference device. The operation and measurements on the device, along with the interpretation of the

results, were the work of the author in collaboration with Dr. J. Hough.

Chapter 3 presents in detail calculations of the sensitivities of two possible types of gravitational wave detector. The author was responsible for several calculations of this type in conjunction with colleagues, who calculated the sensitivity independently and the results were then compared. This work included a consideration of the effect of noise in the sensing system affecting the actual detector. In the case of the SQUID the component of possible backward fluctuation noise was estimated as this had not previously been considered in the literature. The proposed mechanism was due to Dr. J. Hough with ideas, on other various aspects of the problem, from the author.

Chapter 4 contains a description of various 'on-line' computer techniques in order to extract continuous signals from noise. The writing of the programmes and implementation of these techniques was the work of the author. In the case of the power spectrum analysis system the actual Fourier transform was a standard programme; however the programmes dealing with the data input-output and the method of integration were those of the writer. The author has been responsible for several innovations and improvements in the general computing system, which has grown over the past three years to a powerful 'on-line' computing facility.

The search for continuous gravitational radiation described in Chapter 5 was initiated by Dr. J. Hough and Professor R.W.P. Drever. The actual programme used for

the experiment was in fact written by the author who was also responsible for writing the programmes used in the calibration. The actual experiment was performed in collaboration with Dr. J. Hough and Dr. R. Bland and the calculations of the gravitational wave upper limit implied were performed by the author and independently by Dr. J. Hough.

The basic apparatus to search for extra terrestrial x-rays (Appendix A) was already in existence from previous experiments performed by others. The extension of this experiment to power spectrum analysis was the work of the author, who was also responsible for the design of the electronic systems required for calibration and testing. The actual search was performed by the author in collaboration with Dr. J. Hough. The calculation of the effect expected by x-rays was due to the author, however this did depend to some extent on the literature.



## Acknowledgments

The author would like to thank Professor J.C. Gunn for his interest and encouragement throughout this work.

This research was carried out under the direct supervision of Professor R.W.P. Drever, and the author is grateful to him for his help and enthusiasm.

Technical help was given by Mr. A. McKellar, Mr. B. McAteer, Miss M. McColgan and by the stores staff under Mr. R.E. Donaldson. The author would like to thank Mrs. C. Martin for the typing of this thesis. He also wishes to thank his wife for her ever present help and encouragement.

The author would especially like to express his gratitude to Dr. J. Hough for many useful discussions, and for his helpful advice throughout the past three years.

During the time that this work was carried out, the author was in receipt of financial support from the University of Glasgow.

## Summary

### Experiments on and relating to the detection of Gravitational Radiation

The fact that an accelerating mass can radiate energy in the form of gravitational waves was predicted by Einstein in 1918, as a result of his General Theory of Relativity. Recently much interest has been shown in the possible detection of this radiation, due to the reported detection of gravitational wave pulses in 1969 by J. Weber.

Work was started at Glasgow in 1970 and by 1973 a search had been made for pulses of radiation expected from stellar collapse. The author joined the group in 1973 and it was clear then that improvements had to be made in the detector sensitivity, if gravitational wave pulses were to be observable at an acceptable rate.

This thesis therefore is an account of research aimed to improve the sensitivity of searches for gravitational radiation.

After a brief historical note various sources of gravitational radiation are considered. Estimates of the expected effects, as measured at the earth, are presented; these illustrate the need for improving detector sensitivity.

One of the first fields considered is the low noise amplification of signals from gravitational wave detectors. The experimental work done on this problem includes investigations into the possible improvements by cooling field effect transistors, and the use of a superconducting quantum interference device as a low noise amplifier.

Using the results of these investigations the sensitivities of two proposed types of gravitational wave detector are then calculated. As a detector is very sensitive to applied forces the effect of noise in the sensing circuit producing a feedback force is considered. This effect has not been taken account of in the majority of previous calculations performed by others, and indeed it is found to be an important factor.

As well as an investigation into possible improvements, a search which sets a more sensitive upper limit to gravitational radiation of a continuous nature is described. This experiment has also proved worthwhile in relation to conclusions about the reported detection of gravitational wave pulses by Weber in 1970.

This work led to a more general consideration of possible methods for the extraction of continuous gravitational wave signals from detector noise, and a discussion of the implementation (by use of an on-line computer) of some of these techniques is presented.

A power spectrum analysis programme developed for the purpose of gravitational wave experiments was also used in a different experiment to search for extra-terrestrial X-rays, and this work is presented in Appendix A.

## Chapter 1

### Introduction

Over the last seven years much interest has been shown in the possible detection of gravitational radiation. This interest has been mainly stimulated by the reported detection of gravitational wave pulses by Weber in 1969.<sup>2)</sup>

The possibility of energy being radiated from an accelerating mass was predicted by Einstein in about 1918 using the General Theory of Relativity, and it was shown that, in a weak gravitational field, the radiation is transverse in nature and propagates at the speed of light.

In 1959 Weber<sup>1)</sup> started his experiments on the detection of gravitational radiation. He calculated that the radiation from laboratory generators was far too small<sup>to be detectable</sup> and that he had to rely on extraterrestrial radiation from possible violent cosmic events in our own galaxy.

Basically his detector consisted of an aluminium cylinder with piezoelectric transducers bonded to its girth, at the centre, to enable any longitudinal motion to be monitored. Gravitational radiation interacting with the detector would induce such a motion in the cylinder. Preliminary experiments with a detector at the University of Maryland encouraged him to build another one, which was operated about 1000 km away at the Argonne National Laboratory. The distance between the two detectors tends to rule out simultaneous excitation by terrestrial effects.

In 1969 Weber performed a coincidence experiment and

reported 17 events, which forced him to conclude that "The data were consistent with the conclusion that the detectors are being excited by gravitational radiation." He reinforced this argument with plots of detector coincidences as a function of sidereal time and found that the source of the coincidences was anisotropic.<sup>3)</sup>

Other groups entered the field around this time and performed their own experiments designed to detect gravitational radiation. Although most were similar to those of Weber's no one in fact repeated Weber's experiment completely. In 1972 a group led by Braginski<sup>4)</sup> in Moscow presented the first independent experimental results.

Braginski's detectors although similar to Weber's differed in that they used capacitive transducers rather than piezoelectric crystals to monitor the detector motion. The Russians found no coincidences that corresponded to excitation by gravitational radiation, although the search was of the same order of sensitivity as Weber's experiment.

In 1973 the group at Glasgow University<sup>5)</sup> published the results of a search for pulses of gravitational radiation. The experiment, (designed to obtain further information about the radiation), was slightly more sensitive than Weber's, and it also had a much wider bandwidth compared with the previous searches.

The conclusion of the search was that "it is unlikely that the pulses reported by Weber in 1970 were due to pulses of gravitational radiation of duration less than a few milliseconds." This conclusion was important as, from a con-

2.

sideration of possible sources, this type of gravitational wave pulse was the most likely form of radiation. They did however report an event and there was "no experimental reason to reject the hypothesis that this signal was caused by gravitational radiation."

Other negative results have now also been reported by  
6-7) 9) 8-13)  
Garwin, Tyson and Douglass and others.

This presents a contradiction, as the experiments were at least as, if not more, sensitive than Weber's experiment, and indeed it does cast doubt on the fact that the coincidences reported by Weber were due to gravitational radiation. Due to the differing methods of signal processing used by all the groups however there are some possible signals that Weber may be more sensitive to. Such a type of signal was a high flux of very small pulses, and although the experiment described in Chapter 5 was not designed to offer comment on Weber's pulses, it did prove extremely valuable in showing that an explanation in terms of a large flux of small pulses was unlikely.

Although most experimental work has been done on the detection of pulses of gravitational radiation some experiments have investigated the existence of continuous radiation. 14-20) 14)  
In 1961 Forward et al reported an upper limit to continuous random radiation of period about 1 hour. This was done by using the earth as a gravitational wave detector. 16-19)  
These types of searches using the earth, and more recently the moon, are still underway and indeed Sadeh and Meidav 17)  
claim to detect gravitational waves from the (CP 1133) pulsar. 16)  
However Mast et al have performed a

similar experiment and their results contradict those of Sadeh.

These experiments have investigated gravitational waves of period about 1 hour but searches at higher frequencies have been reported. Mast et al<sup>19)</sup> have searched up to a frequency of 125 Hz, again using the earth as a detector.

An upper limit had been set by a laser strain meter operating in the frequency region above 1 kHz<sup>20)</sup> with a reported energy flux sensitivity of  $6.3 \times 10^9 \text{ W} \cdot \text{m}^{-2} \text{ Hz}^{-1}$ .

There was therefore a need for a more sensitive experiment in this field and the experiment described in Chapter 5 is a search for continuous radiation in the frequency region around 1 kHz. From an analysis of the experiment the sensitivity was found to be  $6.8 \times 10^3 \text{ W} \cdot \text{m}^{-2} \text{ Hz}^{-1}$ , and this sets a much more sensitive upper limit in this frequency region.

Gravitational radiation is the propagation (at the speed of light) of deviations from flat space-time, and it induces a strain ( $\frac{\Delta l}{l}$ ) in the detectors. The present sensitivity of the detectors working in the 1 kHz region is of the order of ( $\frac{\Delta l}{l}$ ) =  $5 \times 10^{-16}$  -  $5 \times 10^{-17}$ , and this figure will be compared with the strain expected from various gravitational wave sources.

However firstly an elementary introduction to the theory will have to be presented.

#### Elementary Introduction to the General Relativity Used

As gravitational radiation is a prediction from general relativity certain concepts of the subject have to be used,

and in this section it is hoped to introduce these ideas.

In general a physical event may be described by four quantities, three for the position of the event and one for the time of occurrence. In the absence of gravitational fields and accelerations the four quantities may be interpreted as coordinates in a four dimensional Euclidean space, this space being called Minkowski Space-time. The four coordinates  $x^i$  ( $i=0$  to  $3$ ) are  $ct$ ,  $x$ ,  $y$  and  $z$  where  $c$  is the velocity of light.

In order to proceed with the geometric interpretation further, a metric of the space has to be defined, and is a definition of the 'distance' between two events. For the Special Relativity case of no gravitational field and accelerations, the metric is as follows.

$$ds^2 = (dx^0)^2 + (dx^1)^2 + (dx^2)^2 + (dx^3)^2 - c^2 dt^2 \quad -(1.1.)$$

or as  $ds^2 = g_{ik} dx^i dx^k$

Note: The Einstein summation convention is used here.

where  $g_{ik} = \begin{bmatrix} -1 & 0 \\ 0 & 1 \\ 0 & 1 \\ 0 & 1 \end{bmatrix}$

On the introduction of matter to the system the space-time ceases to be Euclidean; however, an event in space-time may still be detailed by four coordinates ( $x^0$  is not necessarily equal to  $ct$ ). The metric is still described by the following formula; this form of the metric means that the space is Riemannian.

$$ds^2 = g_{ik} dx^i dx^k \quad -(1.2.)$$

However  $g_{ik}$  has a different form from the special



relativity case.

According to Einstein's general theory of relativity geodesics in the space-time represent the history of particles moving freely in a gravitational field.

The space-time, in which the particle moves, is curved and according to the theory of relativity the amount of curvature depends on the matter that is present. Therefore in considering systems with gravitational interactions the problem may be reduced to that of finding geodesics in a curved space. In the theory of curved spaces an important quantity is the Riemann - Christoffel (R - C) tensor  $R^\sigma_{\lambda\mu\nu}$  which is formed from the metric tensor  $g_{ik}$ . This tensor is a measure of the 'flatness' of the space and indeed the space is flat if, and only if, the R - C tensor is zero.

#### The Behaviour of Two Free Test Masses to a Change in the Riemann Curvature Tensor

The history of a body may be described by a path through space-time, this path being called its world line. If one considers two particles their world lines will follow geodesics and the task is to measure the separation between them as a function of changes in the Riemann curvature tensor. This may be done by light signals sent to one particle and reflected back again.

The separation between geodesics with relation to the curvature tensor is given by the geodesic equation

$$\frac{d^2 \eta^a}{d\tau^2} + R^a_{bcd} \frac{dx^b}{d\tau} \eta^c \frac{dx^d}{d\tau} = 0 \quad -(1.3.)$$

where  $\eta$  is the separation between geodesics.

Now in a Euclidean space

$$x^0 = ct \quad \text{and} \quad x^1, x^2, x^3 = \text{position}$$

in the actual space

$$\frac{dx^0}{dt} = c \quad \frac{dx^i}{dt} = v^i \ll c$$

$\therefore$  the most important term is

$$\frac{d^2 \eta^a}{dt^2} + R_{0c0}^a c^2 \eta^c = 0 \quad -(1.4.)$$

This could be considered as a force between the masses of

$$\underline{F^j = m c^2 R_{0k0}^j \eta^k} \quad -(1.5.)$$

This result has been derived by Weber.<sup>(1)</sup>

### Gravitational Radiation

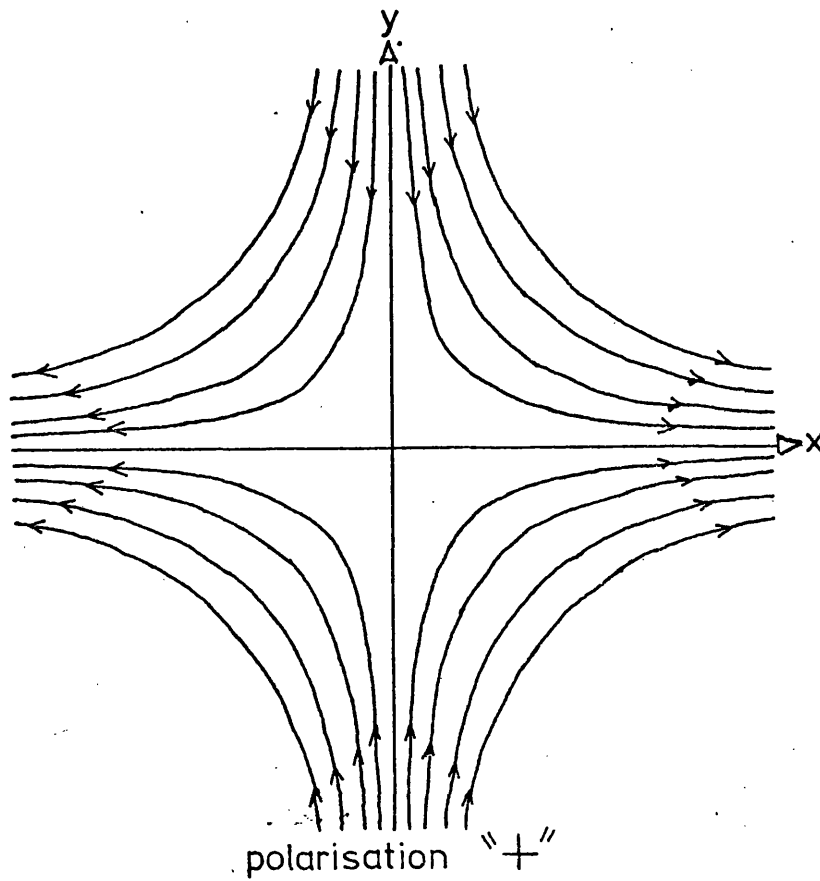
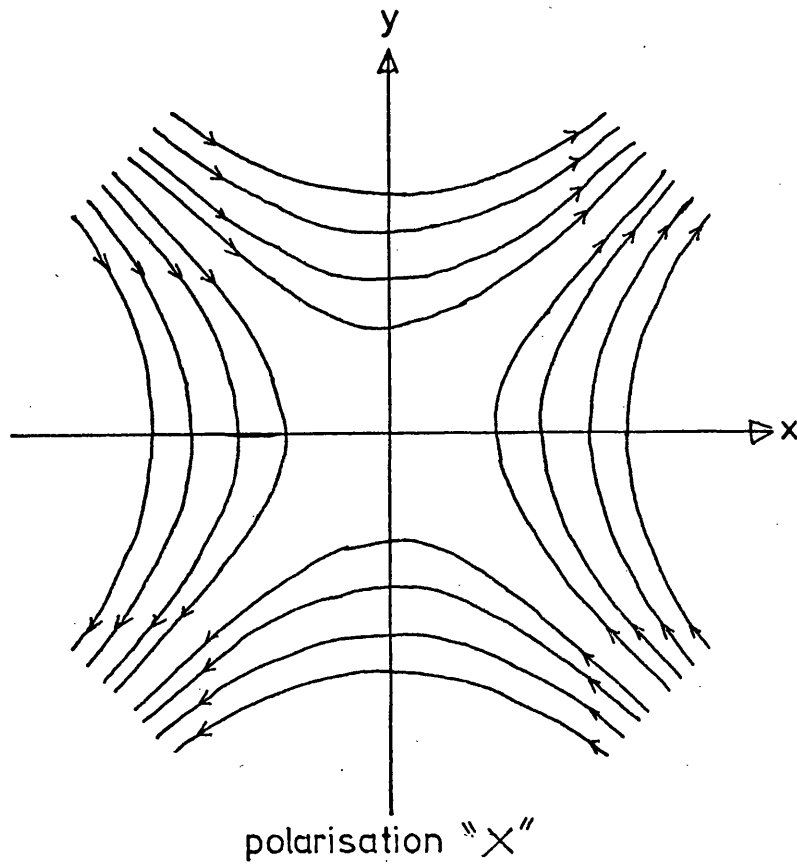
A result of Einstein's general theory of relativity is that fluctuations in the Riemann curvature tensor will be propagated at the speed of light as transverse waves. In solving the weak field solution of general relativity one finds that the curvature tensor in the form of gravitational waves has the following form

$$R_{x_0 x_0} = -R_{y_0 y_0} = -\frac{1}{2} \frac{1}{c^2} \ddot{h}_+(t - z/c) \quad -(1.6.)$$

$$R_{x_0 y_0} = R_{y_0 x_0} = -\frac{1}{2} \frac{1}{c^2} \ddot{h}_\times(t - z/c)$$

where  $h_{ik}$  is the perturbation in the metric tensor  
i.e.  $g_{ik} = \overset{(flat)}{g_{ik}} + h_{ik}$  and is assumed small.

The two polarisations of R are shown in Fig 1.1.



THE POLARISATIONS OF A GRAVITATIONAL WAVE

The energy flux carried by a gravitational wave is well defined when it is averaged over several wavelengths (Isaacson 1968)<sup>22) 34)</sup>, and the flux is given by the following formula

$$\bar{F} = \frac{c^3}{16\pi G} \langle \dot{h}_+^2 + \dot{h}_\times^2 \rangle \quad -(1.7.)$$

where  $\langle \rangle$  signifies the average over several wavelengths and where  $h_+$  and  $h_\times$  are the instantaneous amplitudes of the deviations from the flat metric tensor.

### The Generation of Gravitational Radiation

Gravitational radiation has to be at least quadrupole in nature; dipole radiation is excluded by the conservation of momentum.

The power radiated by a system is as follows

$$\frac{d\mathcal{E}}{dt} = \frac{G}{45 c^5} \ddot{D}_{\alpha\beta}^2 \quad -(1.8.)$$

where

$$D_{\alpha\beta} = \int \rho (3 x_\alpha x_\beta - \delta_{\alpha\beta} x_\gamma^2) dV$$

and this is called the reduced quadrupole moment.

This equation may be simplified in the manner of Misner Thorne and Wheeler<sup>23)</sup>, and they estimate the luminosity of a gravitational wave radiator by the following formula

$$\frac{d\mathcal{E}}{dt} \approx \frac{G}{c^5} \left( \frac{\text{nonspherical part of Kinetic Energy}}{\text{time for the change}} \right)^2 \quad -(1.9.)$$

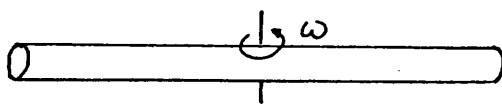
### Sources of Gravitational Radiation

#### Terrestrial Sources

In experiments on the detection of gravitational

radiation, the most convenient situation would be to construct an experiment similar to that of Hertz in the electromagnetic case. This experiment consisted of both a generator and detector. However the following calculation shows that a laboratory generator of gravitational waves does not seem possible at present.

Consider the case of a steel bar rotated about an axis as shown in the diagram.



moment of inertia =  $I$

$$\text{Non spherical part of Kinetic Energy} = \frac{1}{2} I \omega^2$$

$$\text{and the time of change} = \frac{\pi}{\omega}$$

$$\frac{dE}{dt} \approx \frac{G}{c^5} \frac{I^2 \omega^6}{4 \pi^2} \quad \text{---(1.10.)}$$

This case has been considered by Misner, Thorne and Wheeler for a bar 20 m long, 1 m radius, mass = 490 tonnes, and they find that the maximum rotation before exceeding breaking stress is  $\omega = 28 \text{ rad s}^{-1}$  and the power radiated from such a system is  $10^{-31} \text{ W}$ . Such a system 1 km away would produce a strain of  $\frac{\Delta l}{l} = 10^{-38}$ .

From calculations of this type it seems that the best sources of gravitational radiation are extra terrestrial, although some different types of terrestrial sources are still considered.<sup>24) 25)</sup>

There are two types of extra-terrestrial gravitational radiation to be considered, those of pulsed and continuous forms.

## Sources of Pulses of Gravitational Radiation

### The Collapse of Stars

When a star collapses the final state of the system may be either a white dwarf, a neutron star or a black hole depending on how much matter is left in the core after collapse. To emit gravitational radiation the collapse to a neutron star or black hole has not to be spherically symmetrical, and it is the amount of asymmetry that theorists have considered. For a star collapsing into a black hole the following formula, for the gravitational wave amplitude at the earth, has been presented by Thorne.<sup>26)</sup>

$$h = (4 \times 10^{-21}) \left( \frac{M}{2M_{\odot}} \right) \left( \frac{10 \text{ Mpc}}{r} \right) \quad \text{---(1.11.)}$$

where

$M_{\odot}$  - The mass of the sun

$M$  - The mass of the collapsing star

$r$  - Distance from the source

The power spectrum of the pulse peaks at a frequency of

$$f = 5 \text{ kHz} \left( \frac{2M_{\odot}}{M} \right)$$

and the waveform of the radiation is predicted to be a large pulse followed by a ringing tail.

If the star collapses to a neutron star instead of a black hole the frequency of the ringing will be lower and, due to the loss of radiation efficiency, the oscillations will last longer. This tends to mean that most of the gravitational wave energy will be carried off by the oscillations rather than the initial burst. In this type

of collapse Thorne points out that about 1% of the rest mass energy would be emitted in the initial pulse. Thorne<sup>27)</sup> and Ostriker present a less optimistic outlook for this type of collapse and they predict a maximum emission of .5% - .02% of the rest mass energy. Using Thorne's predictions of the collapse into a neutron star the wave amplitude at the earth is given by

$$h = (2 \times 10^{-21}) \left( \frac{M}{M_{\odot}} \right)^{1/2} \left( \frac{10 \text{ Mpc}}{r} \right) \quad -(1.12.)$$

at the power spectrum of the pulse peaks at a frequency of about 2 kHz.

If a  $5 M_{\odot}$  star collapsed to a black hole at the galactic centre ( $8 \times 10^3$  ps away) the gravitational wave amplitude at the earth would be expected to be  $1.3 \times 10^{-17}$ , (Eqn. 1.11.), and the same order of magnitude would be expected from a star collapsing to a neutron star. Bursts of this amplitude could be detected by present detectors, however the predicted rate of occurrence is very small ( $\sim 1$  event in 30 years).

If the sensitivity of the detector is such that a collapse 10 Mpc away could be detected the event rate would be expected to be about 1 per year (Talbot)<sup>28)</sup>. A further increase in sensitivity to detect collapses 30 Mpc away would include events in the Virgo cluster of galaxies and an event rate as high as 20 per year could be expected.

#### Particles Falling into Black Holes

The problem of a particle mass  $m$ , falling into a black hole of mass  $M$  has been analysed by Ruffini<sup>29)</sup> among

others. He predicts that for the above situation the energy emitted is

$$E_{\text{tot}} = \frac{.01 m}{M} \times mc^2$$

and the spectrum of this radiation has a peak value at <sup>-(1.13.)</sup>

$$\omega = \frac{.32 c^3}{GM}$$

which for a  $5 M_\odot$  black hole is about 2 kHz. The detailed shape of the pulses has also been calculated (Davis et al.)<sup>30)</sup> and is a sharp burst with a ringing tail.

As an example the gravitational wave amplitude, at the earth, was calculated for a  $1 M_\odot$  object falling into a  $10 M_\odot$  black hole at the galactic centre. The result of this calculation indicated that a pulse of amplitude  $\sim 5 \times 10^{-18}$  would be expected, with a characteristic frequency of about 1 kHz. The above analysis is performed for a non-rotating black hole and for a particle starting from rest at infinity. Analysis has been done on particles with initial relativistic energy by Ruffini and it is predicted that there is a significant energy increase with not much change in the spectrum.

#### Fly-by as a Source of Gravitational Radiation

The gravitational interaction between two bodies moving close together can cause gravitational radiation.

This method has been discussed by several including Rees, Ruffini and Wheeler,<sup>31)</sup> who predict that for a particle  $m$  moving past a much larger mass  $M$ , the velocity of the particle being much less than  $c$ .



$$\frac{\Delta E}{4\pi} = \frac{64}{5} \frac{G^3}{c^6} \frac{m^2 M^2}{b^2} \quad -(1.14.)$$

where  $b$  is the distance of closest approach,  
The upper cut off frequency of the radiation is

$$\nu = \left( \frac{\pi \times 37}{192} \right) \left( \frac{\beta c}{b} \right)$$

where  $\beta = \frac{v}{c}$

and  $v$  - velocity of particle  
 $c$  - velocity of light

The total energy emitted as gravitational radiation is  
therefore equal to

$$\Delta E = (7.7) \frac{G^3}{c^4} \frac{m^2 M^2}{b^3} \beta \quad -(1.15.)$$

in a pulse of length about  $1.7 \times \frac{b}{\beta c}$  secs

Rees, Ruffini and Wheeler point out that typical parameters  
could be

$$\begin{aligned} M &= 1 M_{\odot} \\ m &= 1 M_{\odot} \\ b &= 100 \text{ km} \\ \beta &= .01 \end{aligned}$$

for an event taking place in a dense galactic nucleus.

For this situation

$$\Delta E = 4.5 \times 10^{40} \text{ J}$$

with a pulse length of 50 ms.

Such a situation at our galactic centre would produce

a gravitational wave amplitude of  $6 \times 10^{-20}$ .

### Pulses from Very Distant Objects

Thorne and Braginskii<sup>32)</sup> have recently considered a different type of gravitational wave source. They point out that it is likely that supermassive black holes ( $M \sim 10^6$  to  $10^{10} M_\odot$ ) exist at the centre of quasars and galaxies. They then calculate the gravitational wave flux that would be expected on earth from the formation of the superheavy black holes and the collision between them.

Results of such an analysis yield that, assuming a distance of  $10^{10}$  light years (Hubble distance) the gravitational wave amplitude is  $2 \times 10^{-17} \left( \frac{M}{10^6 M_\odot} \right)$ , the duration of the pulse being  $\tau = 90 \text{ sec} \left( \frac{M}{10^6 M_\odot} \right)$ . The number of such events that would occur range from 50 times per year to 1 per 300 years depending on the model chosen to estimate the number of such black hole systems.

### Astrophysical Generators of Continuous Gravitational Radiation

#### Binary Star Systems

It has been estimated that as many as  $\frac{1}{5}$ <sup>33)</sup> of all stars are binary structures. The system is two stars of mass  $M_1$  and  $M_2$  rotating at a frequency  $\omega$ , and an analysis of this type of system yields

$$\frac{dE}{dt} = \left( \frac{32}{5} \right) \frac{G}{c^5} \left( \frac{M_1 \times M_2}{M_1 + M_2} \right) r^4 \omega^6 \quad -(1.16.)$$

This equation may be applied to both observed binaries and postulated ones. The results are summarised in Fig. 1.2.

Name	Period	Spiral time	distance (pc)	Flux $\text{W. m}^{-2}$	h
i Boo	.268 d	$2 \times 10^9 \text{ y}$	12	$1.8 \times 10^{-13}$	$1.2 \times 10^{-20}$
YY Eri	.321 d	$6.6 \times 10^9 \text{ y}$	42	$.2 \times 10^{-14}$	$1.6 \times 10^{-21}$
WZ Sge	81 min	$1.1 \times 10^9 \text{ y}$	100	$.04 \times 10^{-14}$	$1.2 \times 10^{-22}$
Hypothetical Binaries (Characterised by separation 'r')					
$\frac{r}{10^4 \text{ km}}$	12.2 sec	3.2 y	1000	$2.7 \times 10^{-6}$	$2.5 \times 10^{-20}$
$10^3 \text{ km}$	.39sec	2.8 hr.	1000	$2.7 \times 10^{-1}$	$2.5 \times 10^{-19}$
$10^2 \text{ km}$	12.2 ms	1.0 sec	1000	$2.7 \times 10^4$	$2.5 \times 10^{-18}$
10 km	.39 ms	.1 ms	1000	$2.7 \times 10^9$	$2.5 \times 10^{-17}$

(Based on Ref.23 page 990)

#### A SUMMARY OF BINARY SYSTEMS

From the figure it should be noted that some postulated fast binary systems are relevant to a search for continuous radiation described in this thesis.

Mironovski (1965)<sup>39)</sup> has estimated the integrated flux from all binary systems in the Galaxy with periods greater than or equal to 1 hour. He predicts an incident flux of  $10^{-9}$  erg cm<sup>-2</sup> s<sup>-1</sup>, the spectrum being peaked at a period of four hours. This corresponds to a gravitational wave amplitude of  $1.8 \times 10^{-20}$ .

#### Gravitational Waves from Rotating and Vibrating Neutron Stars

The amount of gravitational radiation from a star collapsing, causing maybe a neutron star, has been dealt with. This section deals with the continuous gravitational radiation expected from a neutron star after it has been formed.

The neutron star is able to emit gravitational waves by both rotation and vibration.

In order to obtain gravitational radiation from a rotating body there has to be a deviation from perfect rotational symmetry. Such an asymmetry could be produced by the presence of strong magnetic fields, if the magnetic axis does not coincide with the rotational axis.

This would mean that the star would tend to flatten at the magnetic poles and thus produce a time varying quadrupole moment. The power radiation (L) from a slightly deformed, homogeneous sphere with moment of inertia I and eccentricity e is:-

$$L = \frac{32}{5} \frac{G}{c^5} I^2 e^2 \omega^6 \quad -(1.17.)$$

The value of  $e$  may be limited by various processes.

As a lower limit for  $e$  one could take that due to the magnetic field<sup>74)</sup>

$$e = \frac{B^2 a^8}{2 G I^2} \quad e \sim 10^{-11}$$

The value of  $e$  could not be so great as to predict that the star would slow down at a rate greater than the observed value; this gives  $e \sim 10^{-3}$ . An analysis of the strength of star crusts and theoretical interpretation of the glitches of neutron stars indicate a value for  $e$  of  $10^{-5} - 10^{-7}$ . The Crab pulsar (NP 0532) is the fastest pulsar known at present, and the values predicted for this<sup>34)</sup> are as follows

$$\begin{aligned} h &\leq .7 \times 10^{-24} & \text{for } e &= 10^{-3} \\ &\sim 10^{-26} \text{ to } 10^{-28} & \text{for } e &= 10^{-5} - 10^{-7} \\ h &\geq .7 \times 10^{-32} & \text{for } e &= 10^{-11} \end{aligned}$$

The fact that the luminosity is proportional to the sixth power of the rotational frequency means that if fast pulsars exist, they will of course radiate much more. After the star is newly formed, it will spin fast and will start to slow down.

The progress of such a star has been analysed by various authors. Sejnowski<sup>35)</sup> estimates that a neutron star in our own galaxy rapidly rotating during the first few days of its life has a frequency of about  $10^3$  Hz with a

gravitational wave amplitude of  $10^{-22}$  at the earth.

Vibrations of a Neutron Star. A vibrating neutron star can also emit gravitational radiation and Misner, Thorne and Wheeler<sup>23)</sup> predict oscillations of the order of 1 kHz with a damping time of a few seconds.

The power output for a typical mode, of frequency 5 kHz and damping time 11 secs, is  $1 \times 10^{43} \left(\frac{\delta R}{R}\right)^2 W$ .  $\frac{\delta R}{R}$  is the fractional change in the star's radius, and values for this figure are not known. The predicted wave amplitude at the earth for a star in our galaxy would be  $4 \times 10^{-21} \left(\frac{\delta R}{R}\right)$  and even for unlikely large  $\frac{\delta R}{R}$  the effect is too small to be detected in the near future.

#### Incoherent Continuous Gravitational Radiation

Gravitational radiation of an incoherent nature could be found by mass transferring from one system to another, perhaps even falling into a black hole.

Background radiation of the type similar to the 3° K microwave background is thought to exist at a lower temperature ( $\leq 1.6$  K). However it has been shown that it is too small to be detected by present methods.<sup>34)</sup>

A summary of the various sources is presented in Fig. 1.3.

#### The Detection of Gravitational Radiation

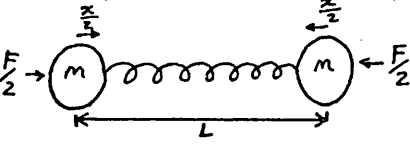
As stated previously, for two free masses changes in the Riemann curvature tensor will produce a tidal force between them of  $F = m c^2 L R_{\alpha\beta\gamma\delta}$  (Eqn. 1.5.).

A gravitational radiation detector could therefore

Source	Timescale	Gravitational wave amplitude measured at the earth (h)
<u>Pulses</u>		
Birth of neutron stars and black holes		
a) Own galaxy (1 per 300 years)	$10^{-3}$ sec.	$10^{-17}$
b) Galaxy at 30 Mpc (20 per year)		$5 \times 10^{-21}$
Particles falling into a black hole	$10^{-3}$ sec.	$5 \times 10^{-18}$
Fly-by at the galactic centre	$\frac{1}{20}$ sec.	$6 \times 10^{-20}$
Supermassive events	$\sim 100$ secs.	$2 \times 10^{-17}$
<u>Continuous</u>		
Binary systems		
a) i Boo	.28 days	$10^{-20}$
b) Integrated sources	1 hour	$10^{-20}$
c) Hypothetical fast binary	12.2 ms	$2.5 \times 10^{-18}$
Crab pulsar	$\frac{1}{50}$ sec.	$< 10^{-24}$
Hypothetical fast pulsar	1 msec.	$10^{-22}$
Vibration of neutron star ( in our own galaxy )	.2 msec.	$10^{-27}$

A SUMMARY OF POSSIBLE GRAVITATIONAL WAVE SOURCES

consist of two 'free'<sup>1</sup> masses and the separation between them monitored. However a more common approach is to construct a resonant system with an equivalent spring between the masses; this only alters the equation of motion of the masses to



$$m \frac{d^2 x}{dt^2} + \frac{\omega_m}{Q_m} \frac{dx}{dt} + \omega_m^2 x = mc^2 LR_{1010} \quad -(1.18.)$$

The harmonic system in its simplest form, just consists of an aluminium cylinder. Applying it to the above situation the two masses  $m$  would be equal to the mass of  $\frac{1}{2}$  the cylinder and the spring constant such that the resonant angular frequency is equal to  $\sqrt{\frac{k}{m}}$ .

Analysis of the interaction of a cylinder (rather than two point masses) to gravitational waves shows that no great error is introduced by considering it as a system of two masses with a spring. (Chapter 5, Eqn.5.3.) gives the numerical difference).

Therefore gravitational radiation interacting with the system induces a motion in the detector and this motion is converted into an electrical signal by various transducers. The sensitivity of the measurements of distance is limited however due to the thermal motion of the detector and the noise of the sensing system. These factors are discussed

<sup>1</sup> By 'free', in connection with this usage, one means that the frequency of the exciting force is much higher than the resonant frequency of the masses plus supports.



in Chapter 3.

### A Summary of Gravitational Radiation Detectors

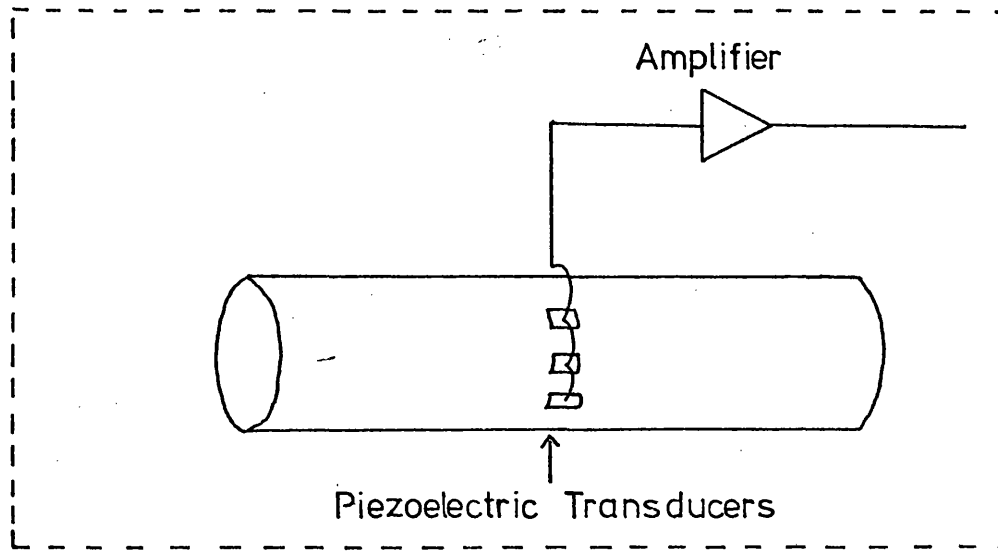
The type of gravitational detector designed by Weber has been discussed and a diagram is presented in Fig. 1.4. Other detectors similar to Weber's have been constructed by Tyson, Garwin, Douglass and Bonazzola. The detector designed by Billing<sup>8</sup> et al. although very similar to Weber's uses a different method of affixing the transducers to a single aluminium cylinder.

Braginski et al used a single cylinder with a capacitive transducer at the centre of the bar, the motion being transferred to this point by metal horns.( Fig. 1.5.A.). The separation between the plates was maintained at a distance of a few microns by a servo system, and the change in the capacitance was measured by a radio frequency technique.

The design used by Drever, Aplin and Allen is that of a split bar detector.(Fig.1.4.B.). The aluminium cylinder is cut across the centre and the piezoelectric transducers are inserted into the gap, rather than onto the surface of the aluminium. This type of detector gives a much higher coupling between the mechanical and electrical systems. As the signal voltage is higher due to this increase in coupling a wider bandwidth may be used, thus giving the experiment greater time resolution.

A different type of detector has been used by Hirakawa et al.<sup>13</sup> It consists of a 'square' of aluminium (Fig.1.5.B) and used a capacitive transducer.

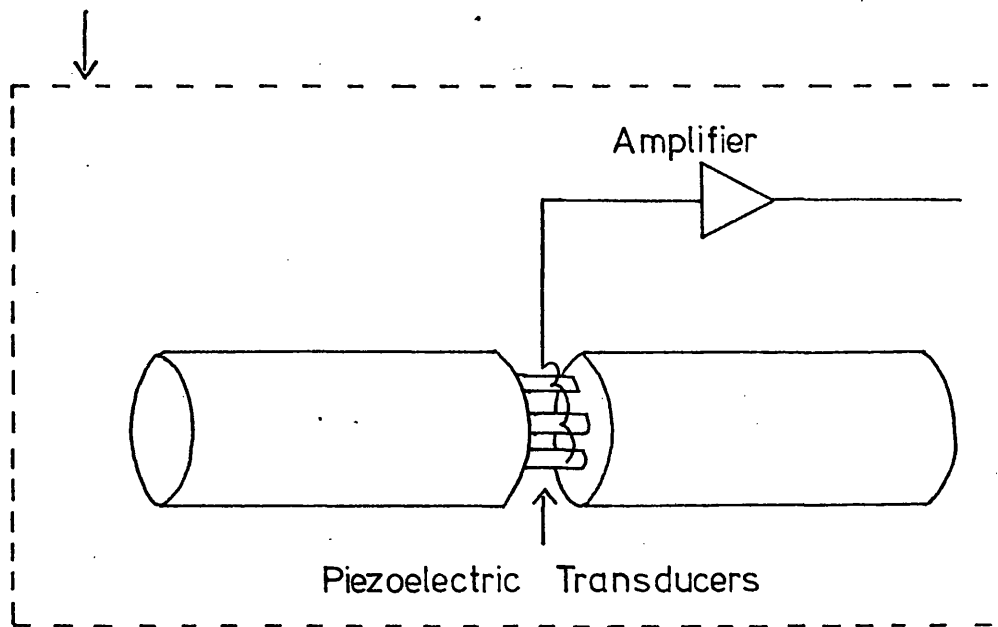
A 'free' mass detector has been used by Forward<sup>36)</sup> et al at the Hughes Research Laboratories. This type of detector



↑  
Vacuum  
Tank

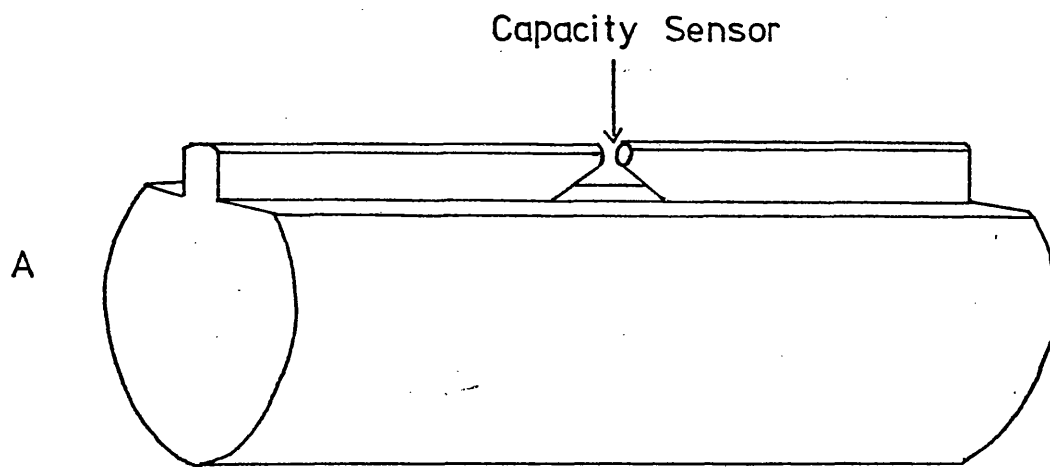
A

THE TYPE OF DETECTOR USED BY WEBER

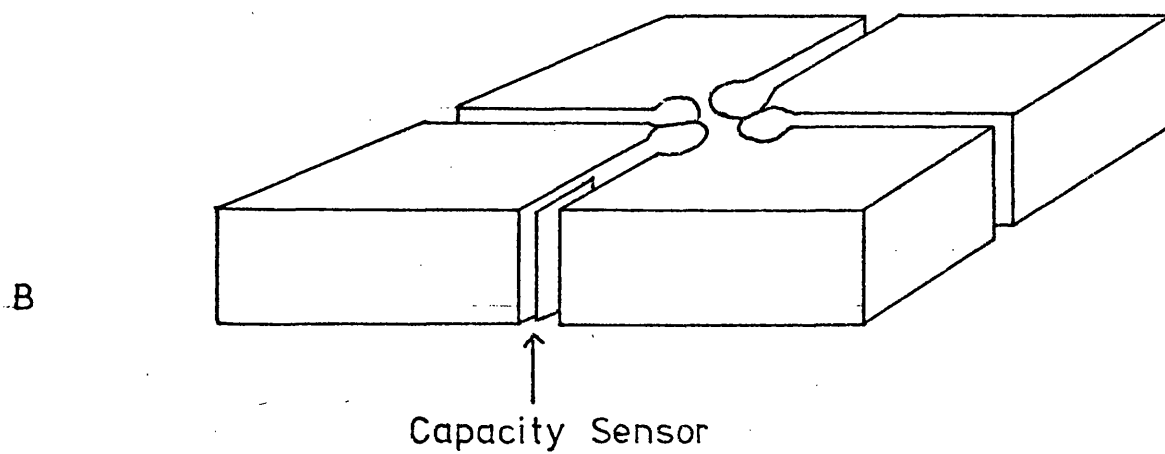


B

THE TYPE OF DETECTOR USED BY DREVER, APLIN and ALLEN



THE TYPE OF DETECTOR USED BY BRAGINSKII *et al*



THE TYPE OF DETECTOR USED BY HIRAKAWA *et al*

uses a laser to monitor the separation between two independent masses. An extension of this type of system is shown in Figure 1.6.

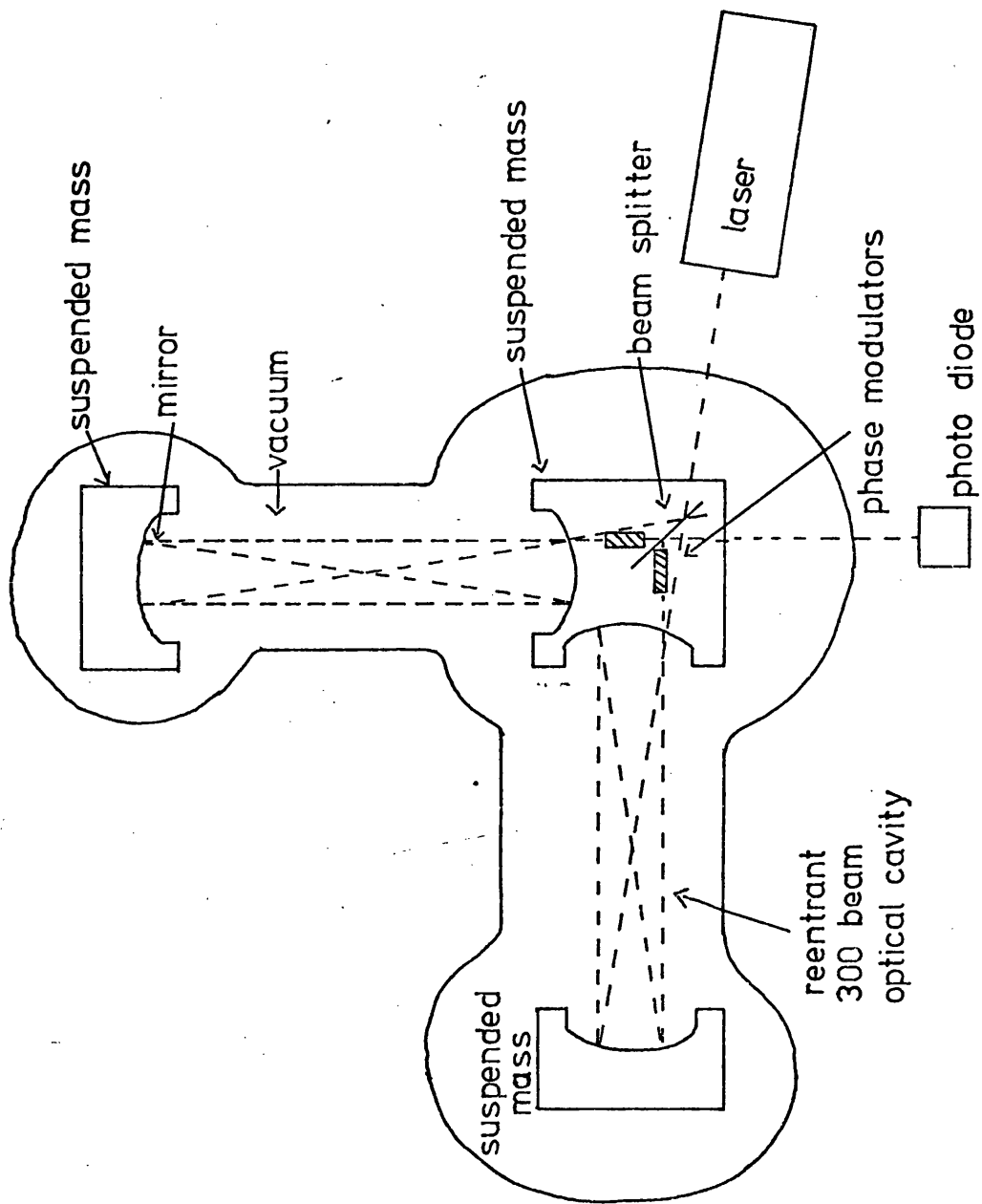
The sensitivity of various experiments has been analysed by Paik,<sup>80)</sup> and his results are presented in Figure 1.7.

### Conclusion

On comparing the sensitivity of present detectors (Fig. 1.7.) with the magnitude of the effect expected from various gravitational wave sources it is found that, at present, one might expect to detect very infrequent bursts from supernovae in our own galaxy. This means that improvement has to be made in the sensitivity of detectors before a reasonable rate of detection may be achieved, due to the inclusion of supernovae from other galaxies. Much of the work in this thesis is an investigation into possible improvements of detector sensitivity.

The low noise amplification of signals from gravitational radiation detectors is a major problem. This problem has been approached firstly by considering the possibility of reducing the noise in Field Effect Transistor amplifiers, which are used at present, by cooling the transistor. Secondly, new types of amplifier have been considered and in particular measurements have been made on the noise performance of a Superconducting QUantum Interference Device (SQUID).

Using the knowledge gained from this work the sensitivity of many different types of detector has been evaluated in order to form conclusions on the best type of



A LASER INTERFEROMETER TYPE OF DETECTOR

The experiment	Sensitivity ( $\frac{\Delta L}{L}$ )
Weber 69-70	$3.6 \times 10^{-16}$
Weber 72-73	$1.2 \times 10^{-16}$
Tyson 72-73	$9 \times 10^{-17}$
Braginskii 72	$2.1 \times 10^{-16}$
Drever 72-73	$1.8 \times 10^{-16}$
Bramanti 73	$4.7 \times 10^{-17}$
Garwin 73	$4.4 \times 10^{-16}$

A SUMMARY OF DETECTOR SENSITIVITY (PAIK)

detector to construct. The possible use of sapphire, as well as aluminium, has been investigated and some of these calculations are presented in Chapter 3.

Pulses of gravitational radiation, including the low frequency type, seem the best candidate for detection; however, continuous radiation should not be neglected. As mentioned previously a few experiments have been performed in this field, including the experiment described in Chapter 5. In carrying out this experiment, and anticipating new experiments, various techniques of extracting continuous signals from noise are necessary and the implementation of these techniques is described in this thesis.

## Chapter 2

### Investigation into the Low Noise Amplification of Signals

The need for low noise amplification of signals from gravitational wave detectors has been emphasised previously, and the object of this chapter is to consider some possible improvements.

Field Effect Transistor (F.E.T.) amplifiers are used at present, in the 1 kHz frequency region, to amplify the signals from the transducers.( Fig.1.4.). The possibility of cooling this amplifier was considered and also the noise performance of a new type of low noise amplifier was measured.

### Investigation into Field Effect Transistor (F.E.T.)

#### Amplifiers

Up to the present, in connection with the amplification of signals from gravitational radiation detectors, F.E.T. amplifiers have been used in the frequency region around 1 kHz.

Investigation therefore has been performed into the improvement of noise figures by cooling F.E.T.s working in this frequency range.

In any amplifier the first stage produces most noise, as the noise of subsequent stages is amplified less. It was therefore the first stage F.E.T. that was studied and cooled.

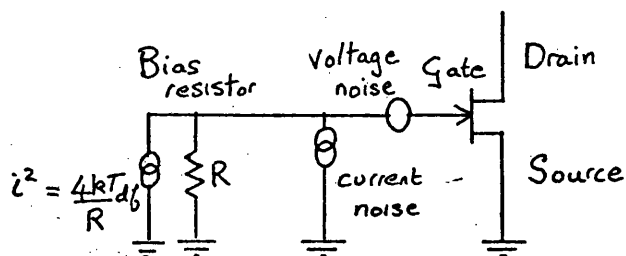
Firstly the methods of measuring the noise in F.E.T. amplifiers will be discussed followed by a description of



experiments on the reduction of noise by cooling.

### Measurement of F.E.T. Noise

In the frequency region of interest the noise in a F.E.T. may be represented by two noise generators connected as shown below.



The voltage noise component is thought to be due to the thermal noise from the resistance of the semiconductor channel. The current noise component, in this frequency region, may be attributed to shot noise in the gate leakage current. The biasing resistor, required to keep the gate at zero potential, will also produce thermal current noise; however, by increasing the size of the resistance, the noise can be reduced.

The method of measuring the two noise components is to construct a circuit as shown in Fig. 2.1.. This is essentially a high gain, low noise, amplifier (Fig. 2.2) followed by a bandpass filter set from 500 Hz to 1.5 kHz. The output from the bandpass filter is measured by an RMS voltmeter.

The two contributions were separated, in the first place, by connecting a large capacitance, from the gate of the F.E.T. to earth, to short out the current noise and leave the voltage noise component. Secondly, a small capacity was then connected between the gate and earth, and the total

## THE SYSTEM USED TO MEASURE AMPLIFIER NOISE

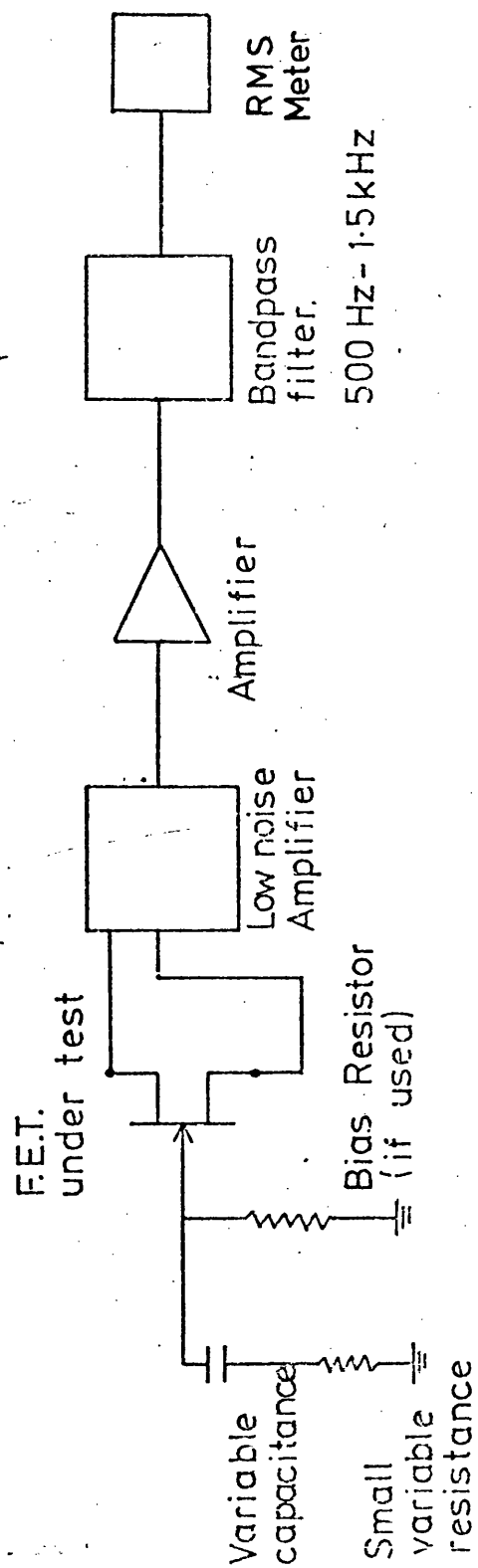
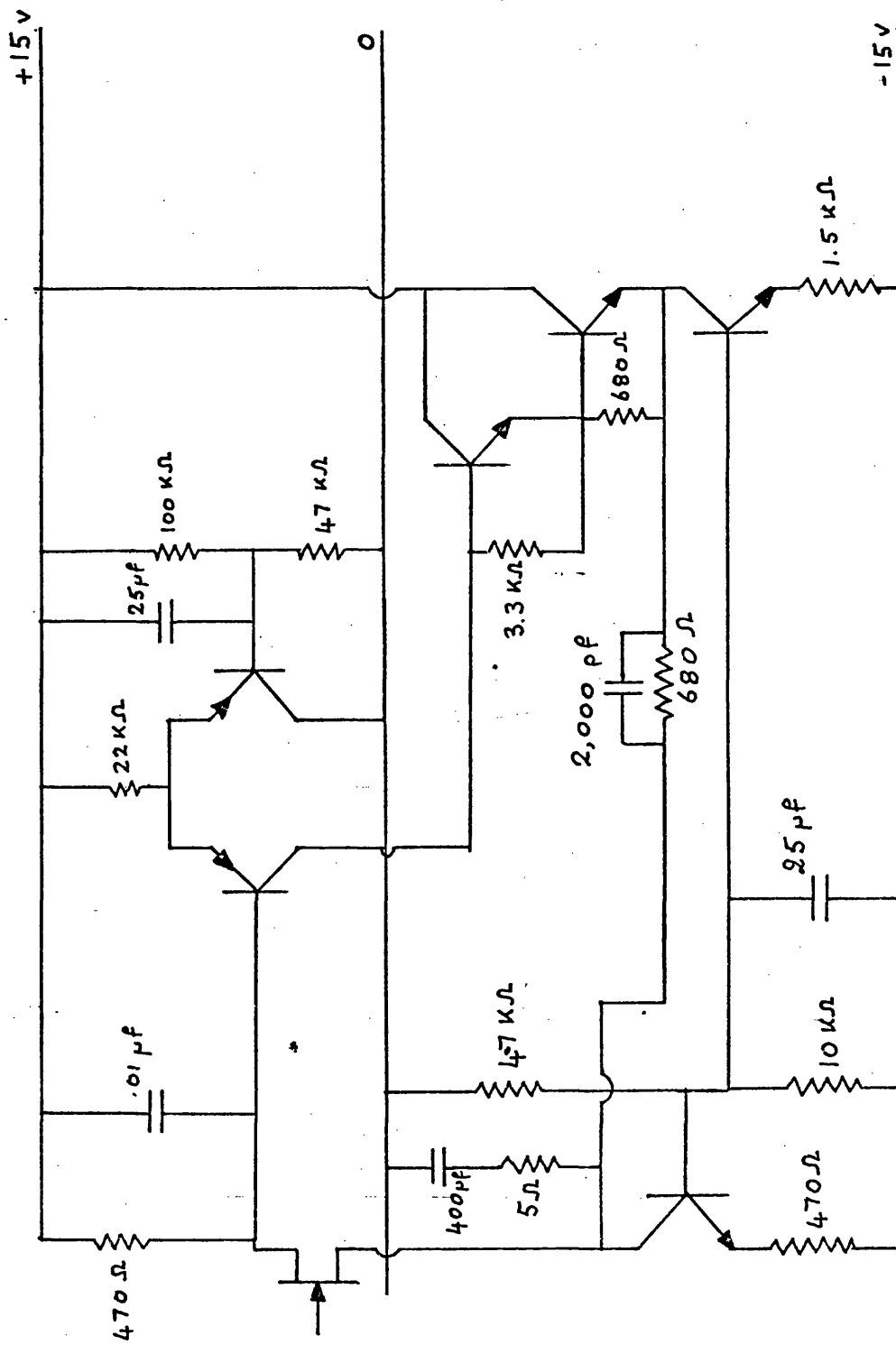


Fig. 2.2.



THE LOW NOISE AMPLIFIER

noise voltage was measured. The voltage noise was then subtracted in quadrature leaving the current noise voltage developed across this capacitance, and the absolute value of the current noise was then calculated.

The value of the large capacitance was chosen to be 10,000 pF and it was found to be adequate in shorting out the current noise component, for frequencies around 1 kHz.

The output level was then measured for a range of smaller capacitors, and it was found that the noise began to increase because the current noise became important. This method of using many capacitors ensured that a false reading was not made due to a dirty capacitor. The capacitors had to be kept very clean to ensure that there was no current leakage introduced across its surface, which would produce noise. A typical graph of output noise as a function of capacitance is shown in Fig. 2.3., the type of F.E.T. being a Texas Instruments BF 818.

In order to relate a measurement at the output with an equivalent noise power per unit bandwidth at the input both the gain and the bandwidth have to be known. A method of providing an absolute calibration without necessarily knowing these parameters is to use the thermal noise from a resistor. Several wirewound small value resistors ( $10\Omega$  -  $100\Omega$ ) were used in turn to obtain the voltage produced by them at the output. The result of such a procedure is presented in Fig. 2.4.; the optimum capacity of the amplifier was obtained from Fig. 2.3. The standard Nyquist formula was then used to calculate the noise at the input and the gain  $\sqrt{\text{bandwidth}}$  product

Fig. 2.3.

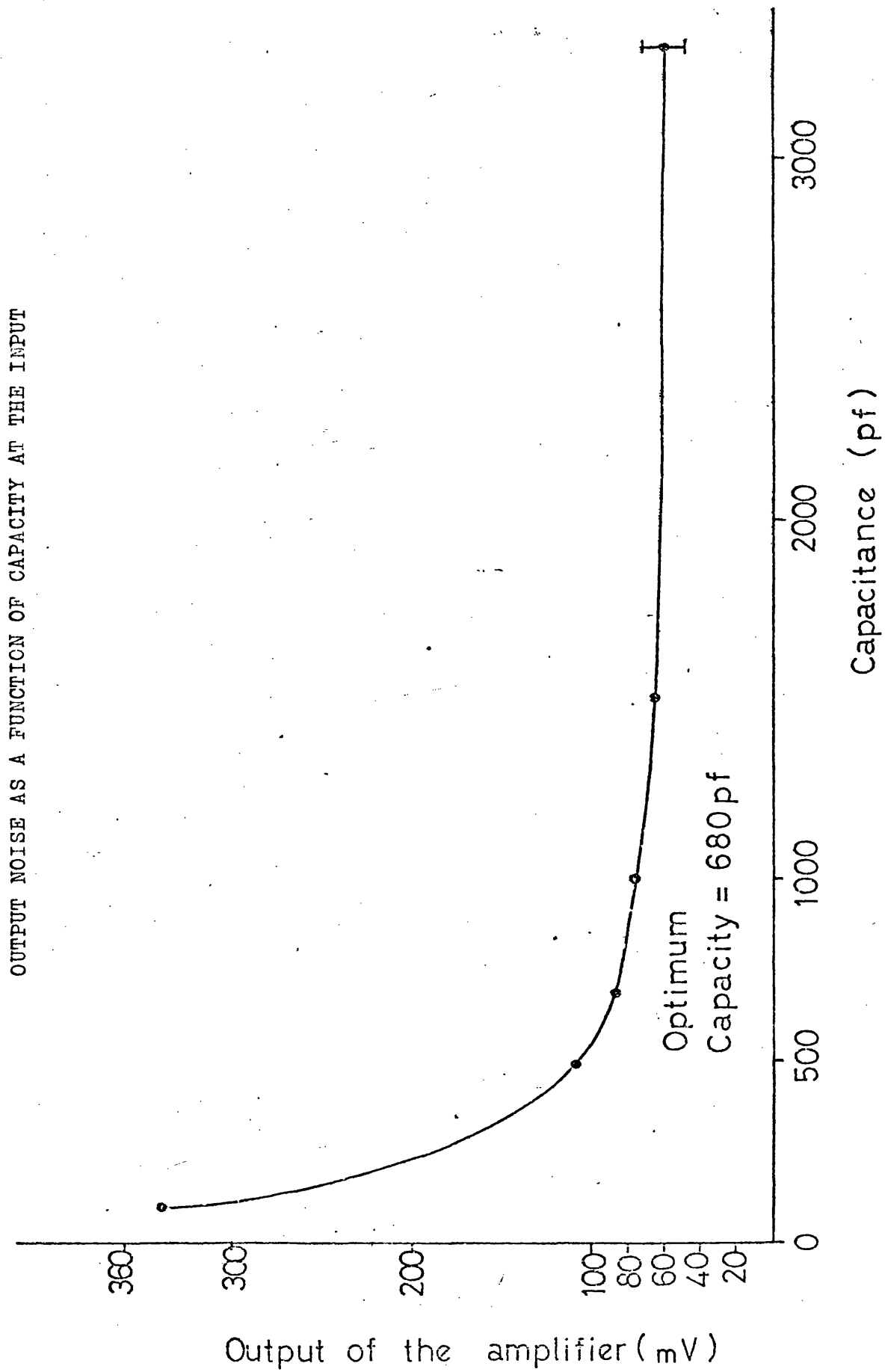
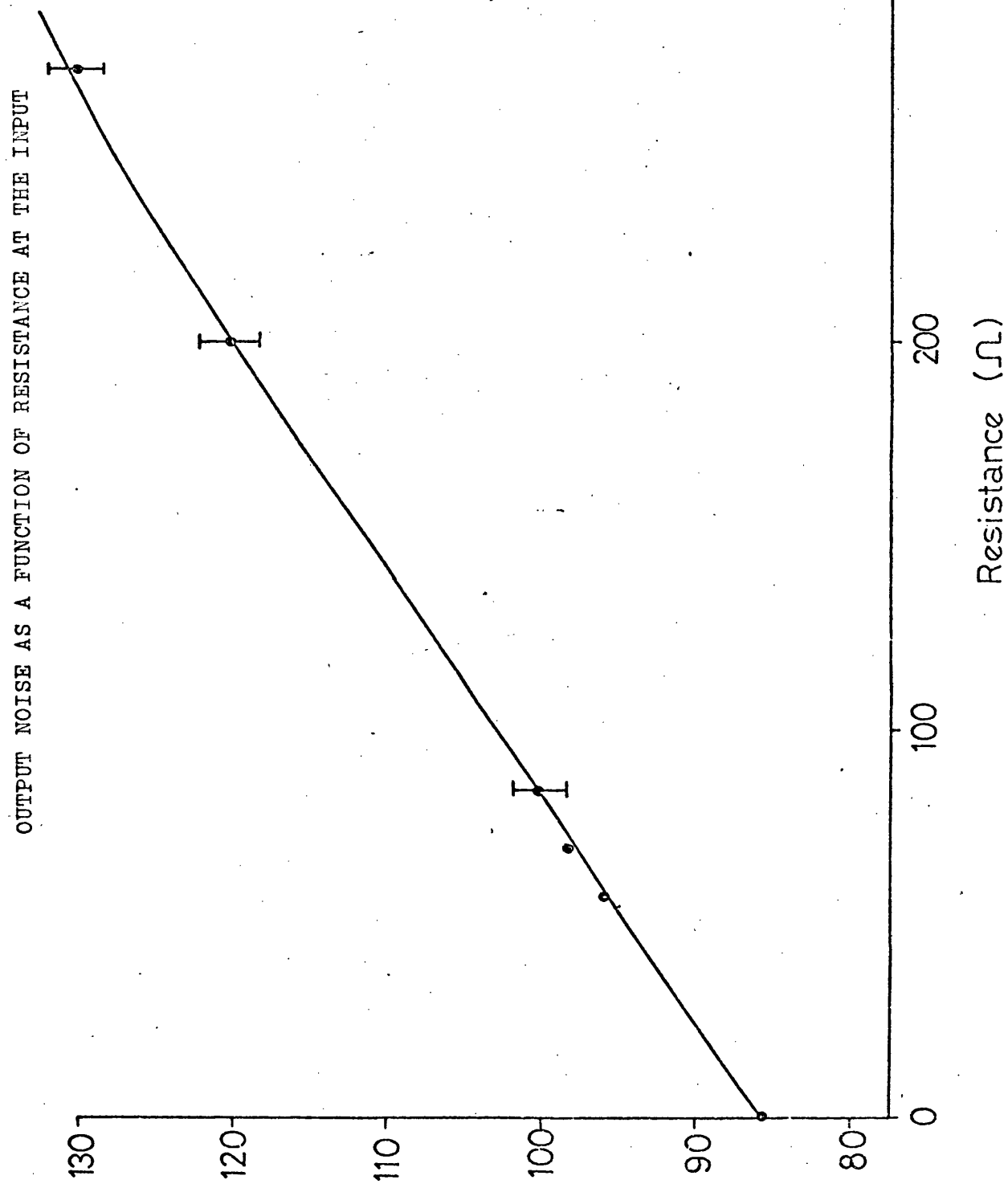


Fig. 2.4.



Output of the amplifier (mV).

(With 680pf capacitance on the input)

was deduced. A cross check was made between these values with an actual measurement of gain and bandwidth and agreement was found.

Measurements were made on a preamplifier with a Texas Instruments BF 818 (E8000) F.E.T installed in the circuit as shown in Fig. 2.2.

These results show that for this F.E.T. the optimum capacity\* ( $C_{opt}$ ) is 680 pF and a total noise resistance ( $R_{noise}$ ) of 226  $\Omega$ . (The noise resistance is that resistance whose thermal noise, at room temperature, is the same as the total amplifier noise).

The noise temperature is taken in this case to be the temperature a resistance of value  $\frac{1}{\omega C_{opt}}$  would have to be in order to produce the amplifier noise.

$$\text{i.e.} \quad T = 290 \omega C_{opt} R_{noise}$$

The noise figure in this case may be calculated by the following formula.

$$F = 10 \log_{10} (1 + \omega C_{opt} R_{noise})$$

Applying these formulae to the amplifier above, the noise temperature was found to be .28°K with a noise figure of  $4.19 \times 10^{-3}$  dB.

- \* The optimum capacity means the capacity at which the voltage noise is equal to the current noise. It is the optimum situation when a charge signal is developed across a capacitance, such as that from Piezoelectric transducers.

### Noise Improvements by the Cooling of F.E.T.S.

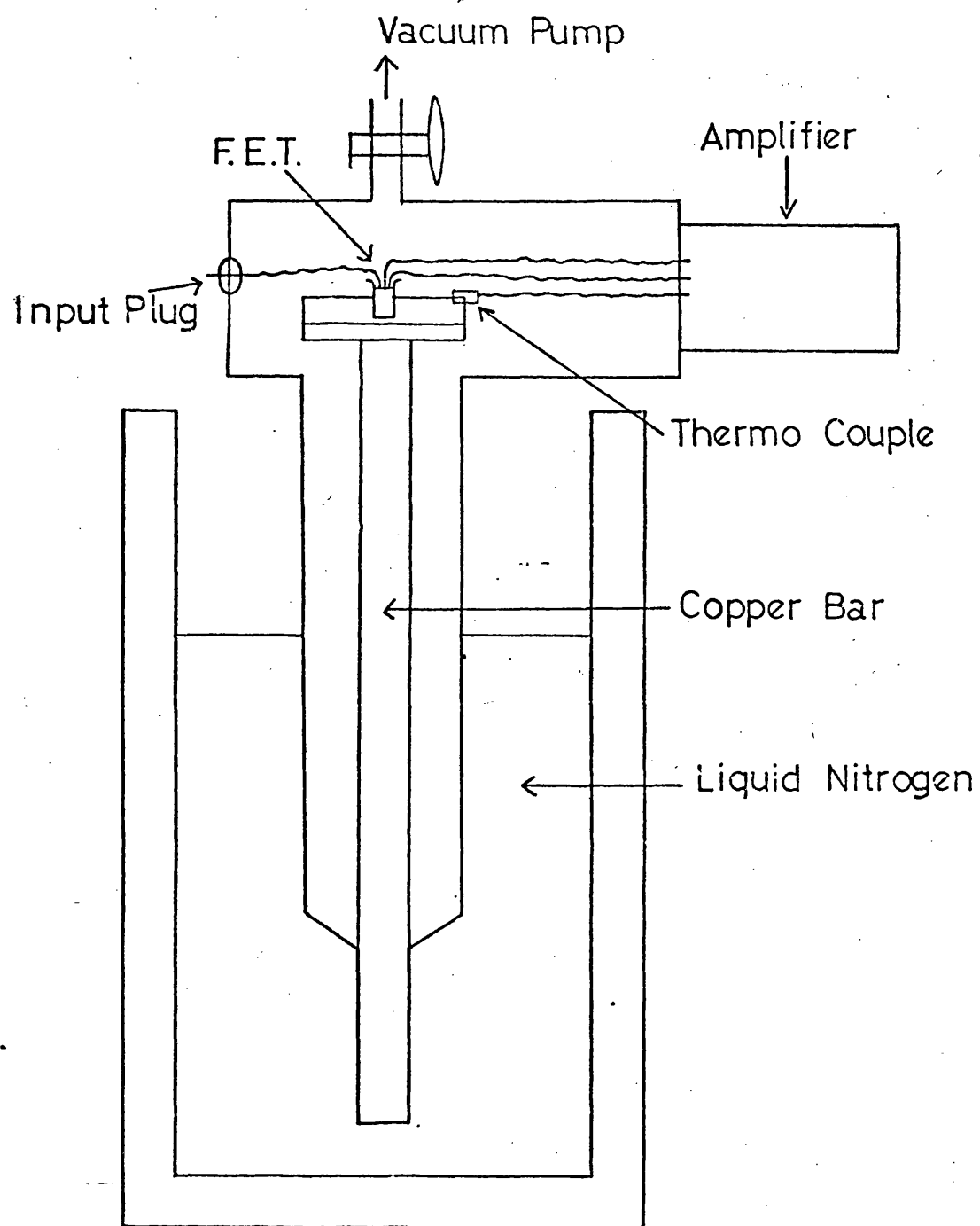
It was thought that the noise of the F.E.T. would reduce on cooling. For example, the voltage noise of a F.E.T. is attributed to the thermal noise of the channel resistance. The thermal noise from a resistance is governed by the 'Johnson noise' formula ( $v^2 = 4kTRdf$ ), and so would be expected to decrease on cooling. It was also expected that gate leakage current would decrease when the semi-conductor was cooled.

To cool the F.E.T. it was embodied in the end of a copper bar as shown in Fig. 2.5., the copper bar then being immersed in liquid nitrogen (77°K). The chamber where the F.E.T. was installed was evacuated with a rotary pump: this was done to prevent water condensing in the region of the F.E.T. when it was cooled. In order to measure the temperature of the copper bar a thermocouple was fixed to the copper but was electrically insulated by two very thin sheets of mica. This insulation did not seem to impair the temperature measurement.

### Tests on the (BF 818) F.E.T.

This selected low noise field effect transistor was used as the input of the amplifier as shown in Fig. 2.2., and the DC current through the device was set to be about 10 mA. As the noise was measured at the output of the amplifier it was important that the gain did not change, as a function of temperature, hence producing an error in the evaluation of the noise. Measurement of the gain from room temperature to that of liquid nitrogen was made experimentally and no significant change was observed.





THE METHOD OF COOLING THE F.E.T.

(The amplifier shown has negative feedback, so not much change in the gain of the amplifier as a function of temperature was envisaged).

Voltage Noise. The F.E.T. was biased with a 600 K Meg resistor onto the gate and a capacitor of 5,600 pF was used on the gate to short out the current noise component. The circuit was set up as shown previously in Fig. 2.1., and the noise voltage was measured out of the system.

Measurements of voltage noise were performed while the F.E.T. was heating up from the liquid nitrogen temperature. The reason for this was that noise was introduced by a microphonic mechanism from the nitrogen boiling on cool down. The whole cold finger apparatus containing the F.E.T. was suspended by a rope to attenuate any microphonics from the room. Results for the voltage noise of the BF 818 F.E.T. are shown in Fig. 2.6.

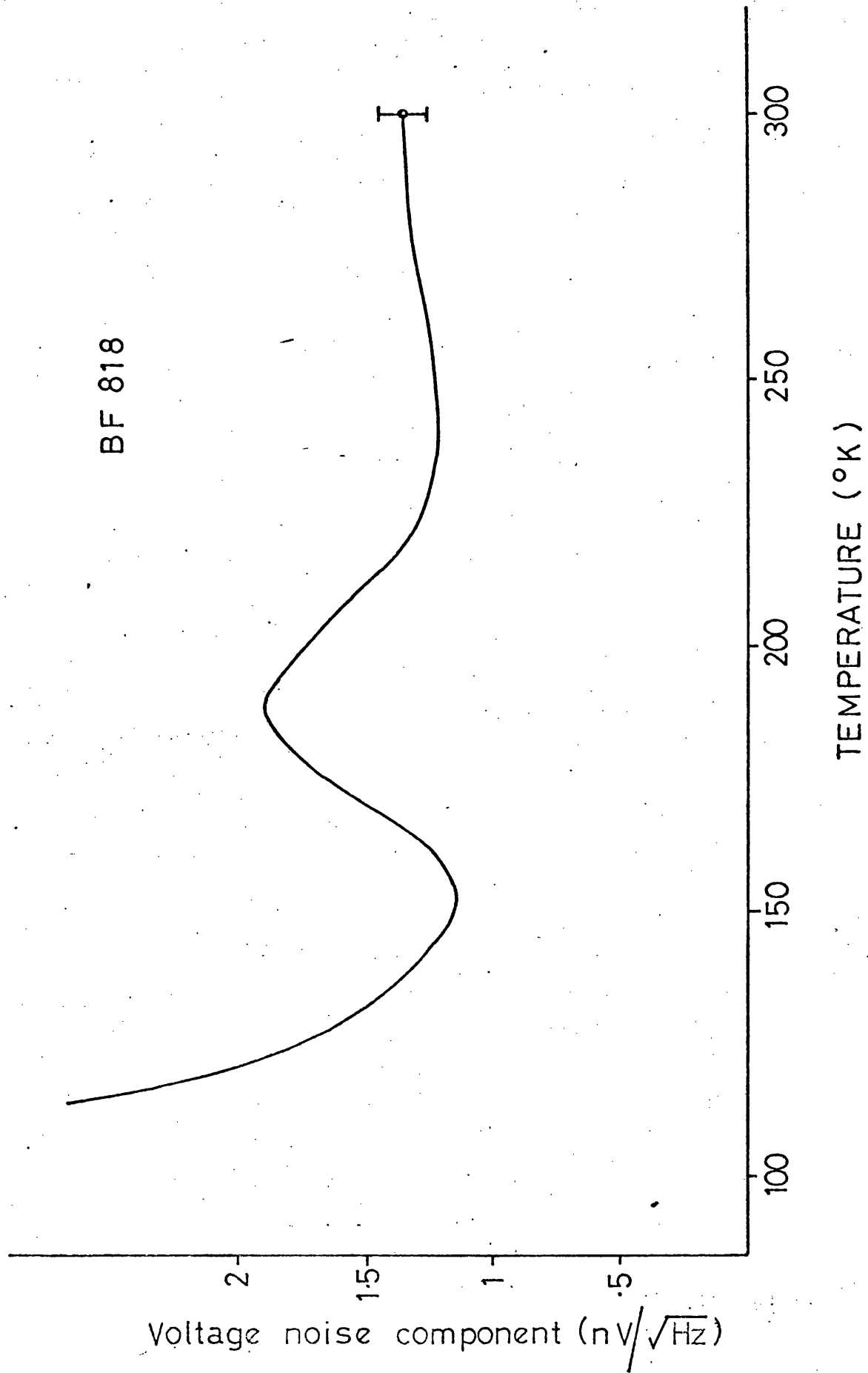
From these results it is seen that, in the range from room temperature to 77°K, there is an optimum temperature as far as voltage noise is concerned, and for this F.E.T. is 150°K. The voltage noise at this temperature was .8 times that of the room temperature value, and was  $1.1 \text{ nV} / \sqrt{\text{Hz}}$ .

The Current Noise Component. The noise current was measured by connecting a smaller capacitor to the gate of the F.E.T. The size of the capacitor necessary of course depended on the current noise. However, 100 pF was a suitable value, as it gave an easily measurable effect due to the current noise and still remained much larger than the stray capacitances in the system.

Fig. 2.6.

VOLTAGE NOISE AS A FUNCTION OF TEMPERATURE

BF 818



With a 100 pF capacitor onto the input the noise was measured, as before, while the F.E.T. heated up from liquid nitrogen temperature, the F.E.T. being biased by 625 K $\Omega$  resistor. The current noise was then calculated as previously described and the results of this are shown in Fig. 2.7.

It was also decided to test the amount of current noise introduced by the resistor. The function of the resistor is to provide a path for any leakage current from the gate, thus holding it near zero voltage. With the F.E.T. cold it was found that the leakage current was small enough to enable the F.E.T. to remain biased with only the capacitor connected. The improvement obtained by exclusion of the 625 K $\Omega$  resistor is also shown in Fig. 2.7. The noise contribution is more than calculated and this is probably due to surface leakage or excess noise in the resistor.

The noise due to surface current leakage is quite an important factor and it was noted that it was possible that the plug also connected to the input was causing current noise. It was therefore not used and the capacitor was soldered directly onto the input lead. The improvement due to this change on the BF 818 F.E.T. is also shown in Fig. 2.7.

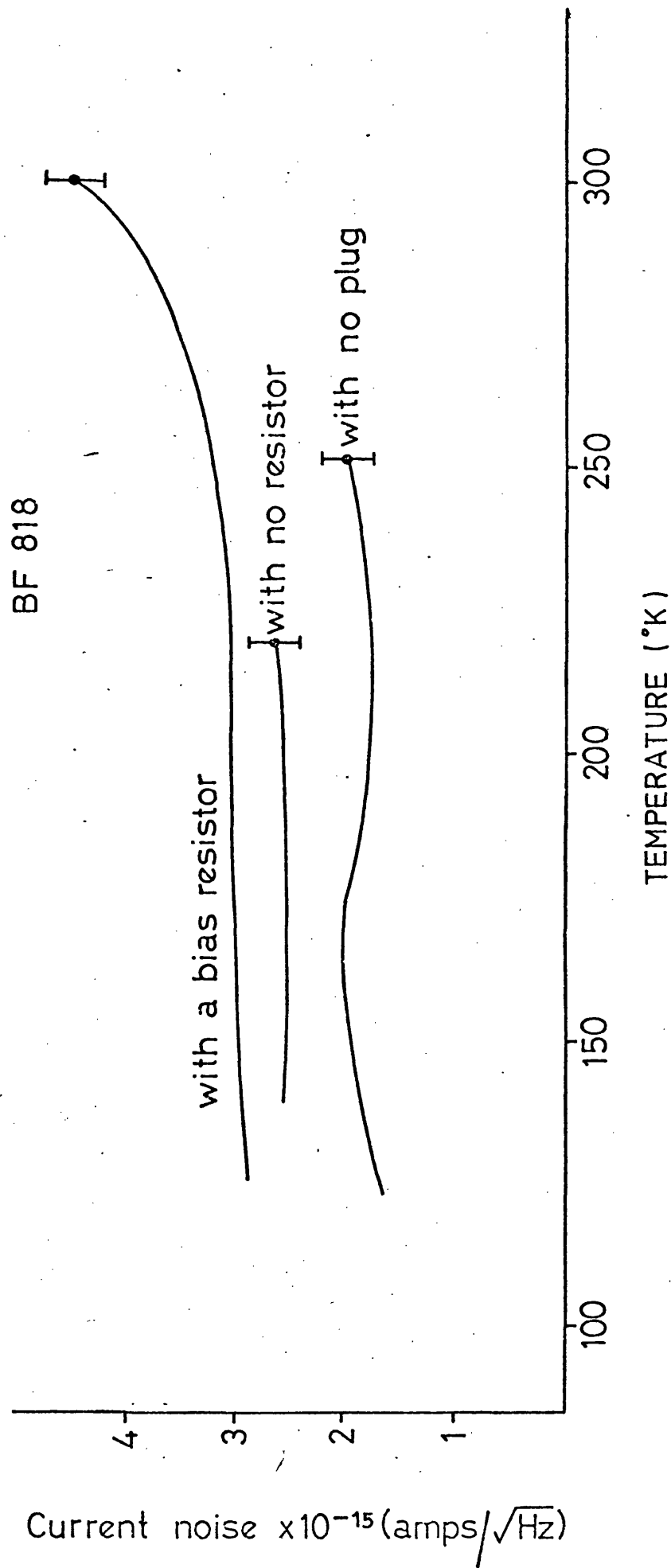
#### Other F.E.T.s Tried

The noise components of a VX 9286 F.E.T. were measured. As this F.E.T. has a very high transconductance the voltage noise component could be expected to be quite small. The relationship between the voltage noise

Fig. 2.7.

CURRENT NOISE AS A FUNCTION OF TEMPERATURE

BF 818



and the temperature was very similar to that obtained for the BF 818. However in this case the voltage noise did not fall below the room temperature value of  $2.3 \text{ nV} / \sqrt{\text{Hz}}$ .

The noise measurements on a Texas Instrument BF 817 low noise F.E.T. proved to be much more fruitful, and the results are presented in Fig. 2.8. The current noise component was measured with no bias resistor or input plug connected. This F.E.T. had the best noise performance measured, with a minimum voltage noise of  $.9 \text{ nV} / \sqrt{\text{Hz}}$  at a temperature of  $145^\circ \text{K}$ , and a current noise of about  $1.2 \times 10^{-15} \text{ A} / \sqrt{\text{Hz}}$ .

#### An Investigation into another Method of Reducing the Current Noise

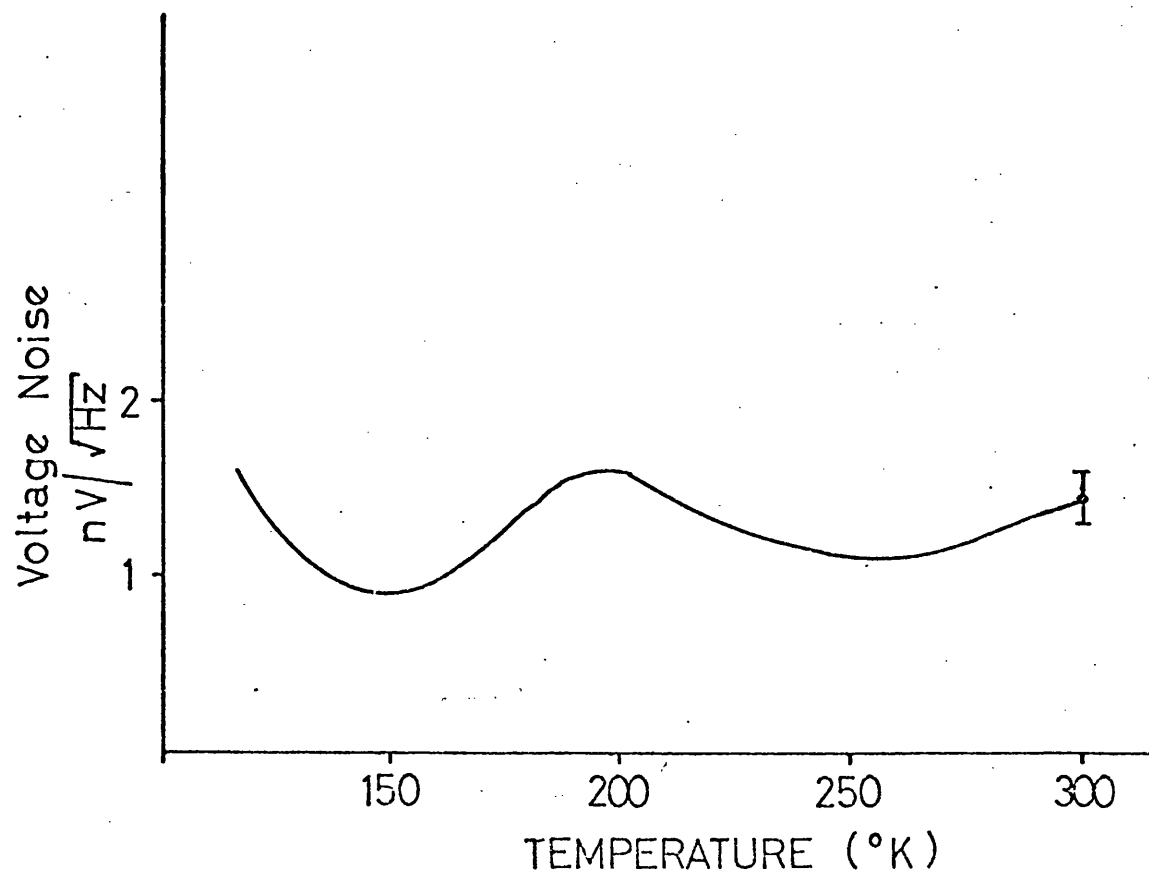
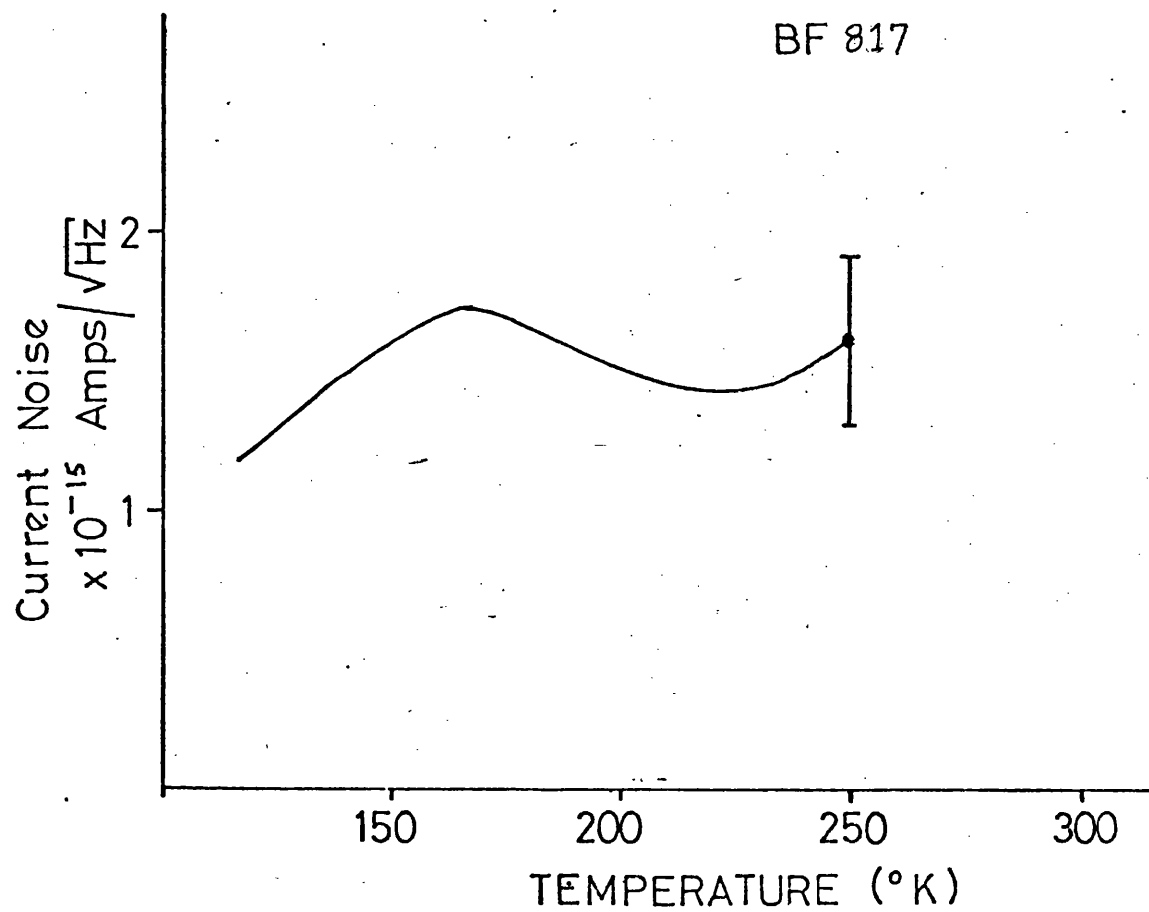
It was thought that the leakage current could depend very much on the Drain - Gate voltage and indeed perhaps an avalanche effect could occur. The Drain - Gate voltage was therefore reduced for both the BF 818 and BF 817 F.E.T.s.

For the BF 818 F.E.T. the voltage was at 3 volts and was reduced to 2.4 volts but no reduction in the current noise was noticed. The BF 817 F.E.T. voltage was reduced from 4.75 volts to 3 volts again with no reduction in the current noise. The voltage was not reduced below these values as this would bring the voltage near to the 'pinch off' region.

#### Conclusions

The Voltage Noise The curves as shown in Figs. 2.6. and 2.8. have the same form as the curves obtained by others

## THE NOISE COMPONENTS AS A FUNCTION OF TEMPERATURE



during work on different F.E.T.s .

Haslett and Kendall<sup>3,)</sup> report an optimum temperature of 140°K, with an improvement over room temperature by a factor of 2; however, the F.E.T.s described have a higher noise level ( $\sim 3 \text{ nV} / \sqrt{\text{Hz}}$ ).

The frequency of 1 kHz is just in the low frequency excess noise region. It is generally thought that this excess low temperature noise is caused by a generation-recombination mechanism, and the resonance due to inter-gap trapping levels. These levels are thought to be due to either gold or oxygen impurities in the semiconductor.<sup>39,40)</sup>

The Current Noise Component The main source of the current noise at the frequency of 1 kHz is shot noise in the gate leakage current. At higher frequencies induced grid noise is caused by the channel noise inducing a current in the gate, due to the capacitance.

The results have shown the noise contribution of the bias resistor and the electrical plug. The effect of leakage due to the ceramic base of the F.E.T. may also be a contributing factor to the current noise. It is thought that these added contributions, to the current noise, are responsible for the current noise not reaching a smaller value on cooling.

### Summary

In this work the lowest values measured for the F.E.T. noise have been  $.9 \text{ nV} / \sqrt{\text{Hz}}$  for the voltage noise and  $1.2 \times 10^{-15} \text{ amp} / \sqrt{\text{Hz}}$  for the current noise at an optimum temperature of 145°K. By connecting F.E.T.s in parallel



the voltage noise can be reduced at the expense of increased current noise, and this does give a method of optimising the amplifier for a particular application. An amplifier using one cooled F.E.T. would have the following parameters

Optimum capacity	210 pF
Total noise resistance	98 $\Omega$
Noise temperature	.038 °K
Noise figure	$5.6 \times 10^{-4}$ dB

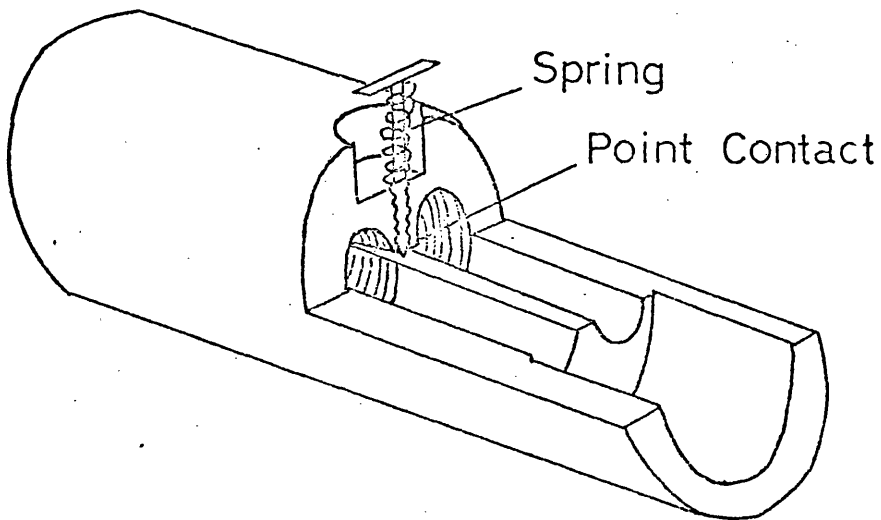
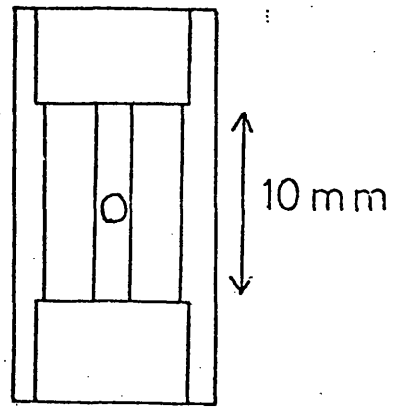
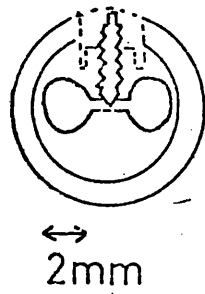
Several other low noise amplifiers were considered and an extremely promising one was a Superconducting Quantum Interference Device (SQUID)<sup>41-43)</sup>, which had only recently been developed. It was thought that as the device was operating at a very low temperature (4°K) the thermal noise contribution would be small. Initial measurements described in the literature seemed promising; however, the noise contribution of the SQUID was not clear, and this had to be investigated.

#### An Experimental Investigation into the Noise of a Commercial SQUID

A commercial SQUID was acquired for the purpose of investigating its possible use in the low noise amplification of signals from gravitational wave detectors. The type investigated was a symmetric SQUID operating at a bias frequency of 19 MHz.

The SQUID used is shown in Fig. 2.9.. It is constructed from niobium which is a superconductor at liquid Helium temperatures. It may be considered as a superconducting loop with a 'weak link' introduced into

Fig. 2.9.



A TYPICAL SQUID

the loop. The weak link in this case was that of a niobium screw tip onto the niobium surface.

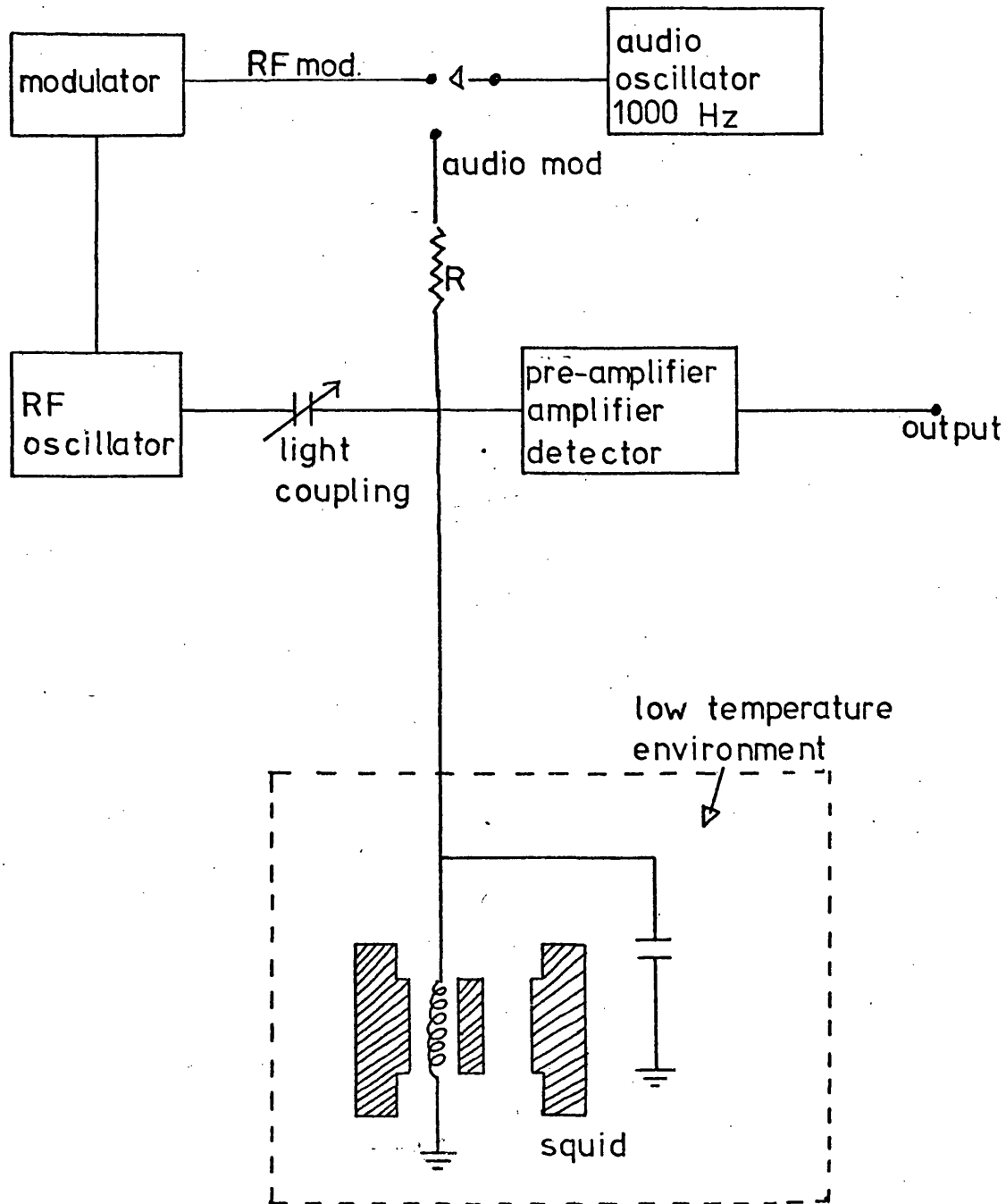
The SQUID is a device which reacts to external magnetic flux in such a way that it will exclude the applied flux until the current flowing in the SQUID, necessary to oppose the flux, reaches a critical value. At this point the SQUID will allow 1 magnetic flux quantum ( $\frac{h}{2e}$ ) to enter and this value will not again change until the conditions for 2 quanta are reached.

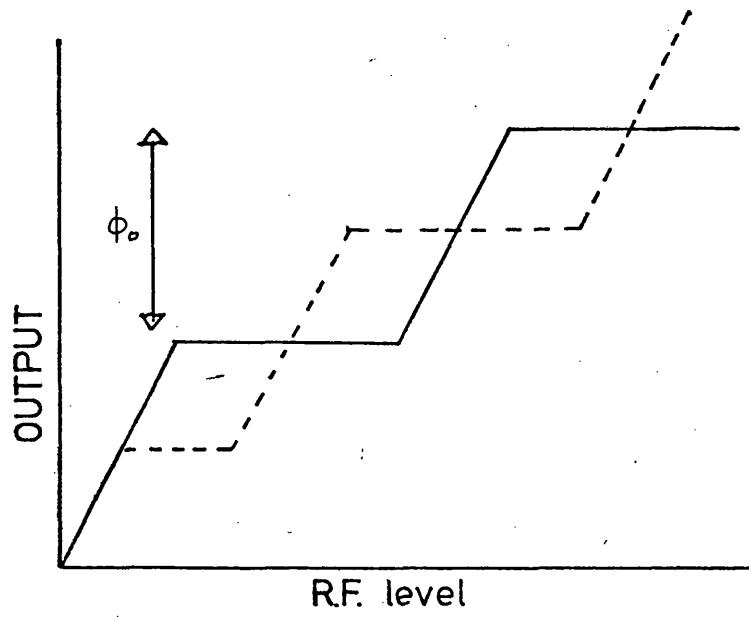
If the SQUID is biased with a high frequency external flux, the flux level allowed into the SQUID will be changing its quantum number. This changing of quantum levels affects the RF driving circuit in a way that depends on both amplitude of the flux change and the DC component of the flux.

The electronic system for the SQUID obtained is shown in Fig. 2.10. It consists of a 19 MHz RF oscillator, which can be amplitude modulated, weakly coupled to the driving circuit and this provides the RF bias. The driving circuit is monitored by use of a preamplifier - amplifier combination, connected to a diode detector. The driving coil is tuned to resonance at 19 MHz by an external capacitor.

If the level of the RF biasing signal is monitored as a function of RF drive applied, a step pattern is obtained as shown in Fig. 2.11A. However if the level is monitored as a function of the DC flux introduced by the biasing coil, with a constant driving signal amplitude a triangular pattern is obtained as shown in Fig. 2.11B.

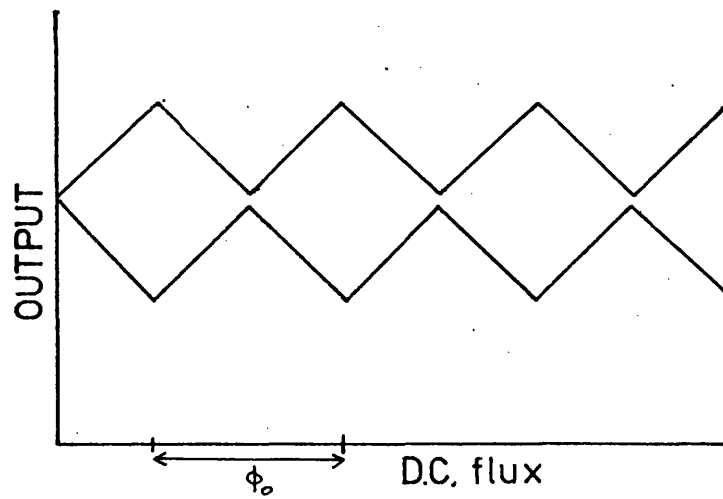
## THE ELECTRONIC SYSTEM FOR THE SQUID





A

THE 'STEP' PATTERN



B

THE 'TRIANGLE' PATTERN

The SQUID was cooled down to liquid Helium temperatures and by modulating the amplitude of the RF level the step pattern was obtained. With a constant RF amplitude a low frequency current was added to the bias signal, and this produces the triangular pattern when the low frequency signal was used as the horizontal axis of an oscilloscope.

#### Noise Measurements on the SQUID

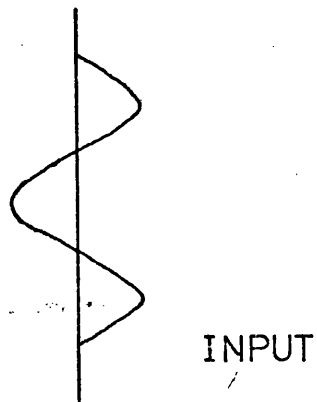
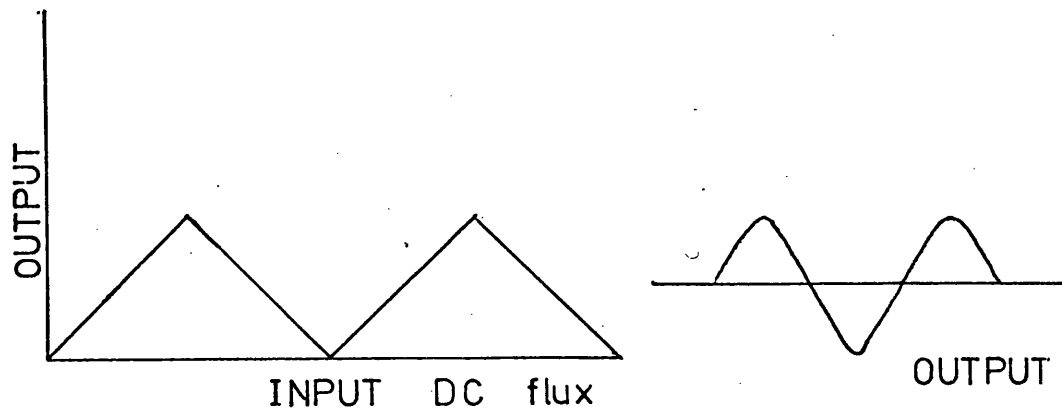
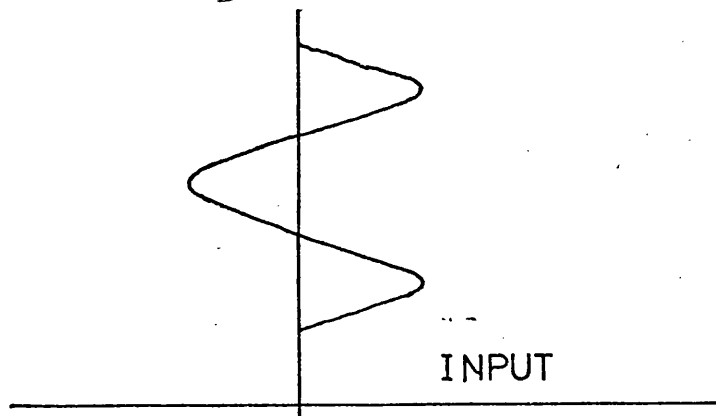
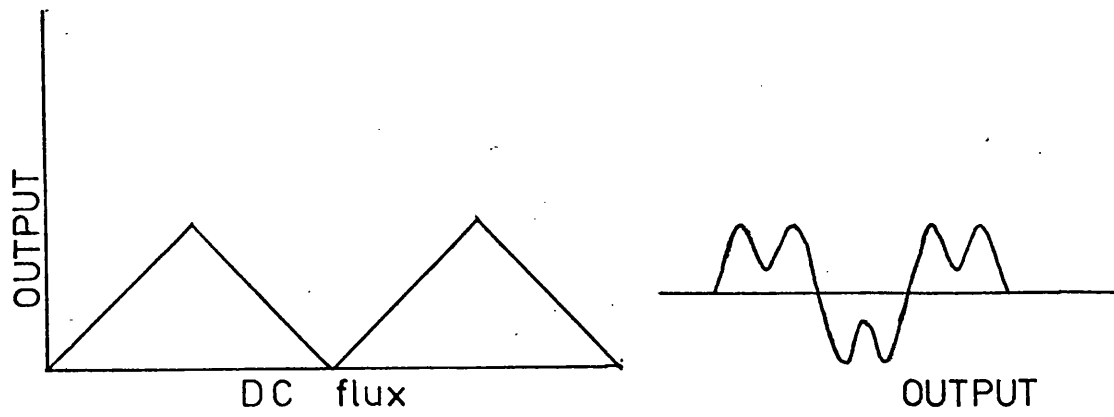
A constant RF amplitude was applied to the SQUID, and the output of the detector was observed as a function of time. For a sinusoidal low frequency signal applied to the coil the output was, for low amplitude, sinusoidal (this corresponds to operation on the side of a triangle). If the amplitude was increased the sine wave became distorted due to the fact that it was being driven beyond the extent of the triangle. (Fig. 2.12.). To ensure that the sine wave was limited for both positive and negative amplitude equally a DC bias current was introduced to set the zero level half way along the triangle.

By measuring the sinusoidal voltage from the detector just before the signal limited a measure was obtained of the voltage output that corresponded to a flux change of  $\phi/2$  in the SQUID. This was essential to calibrate the noise in terms of flux units.

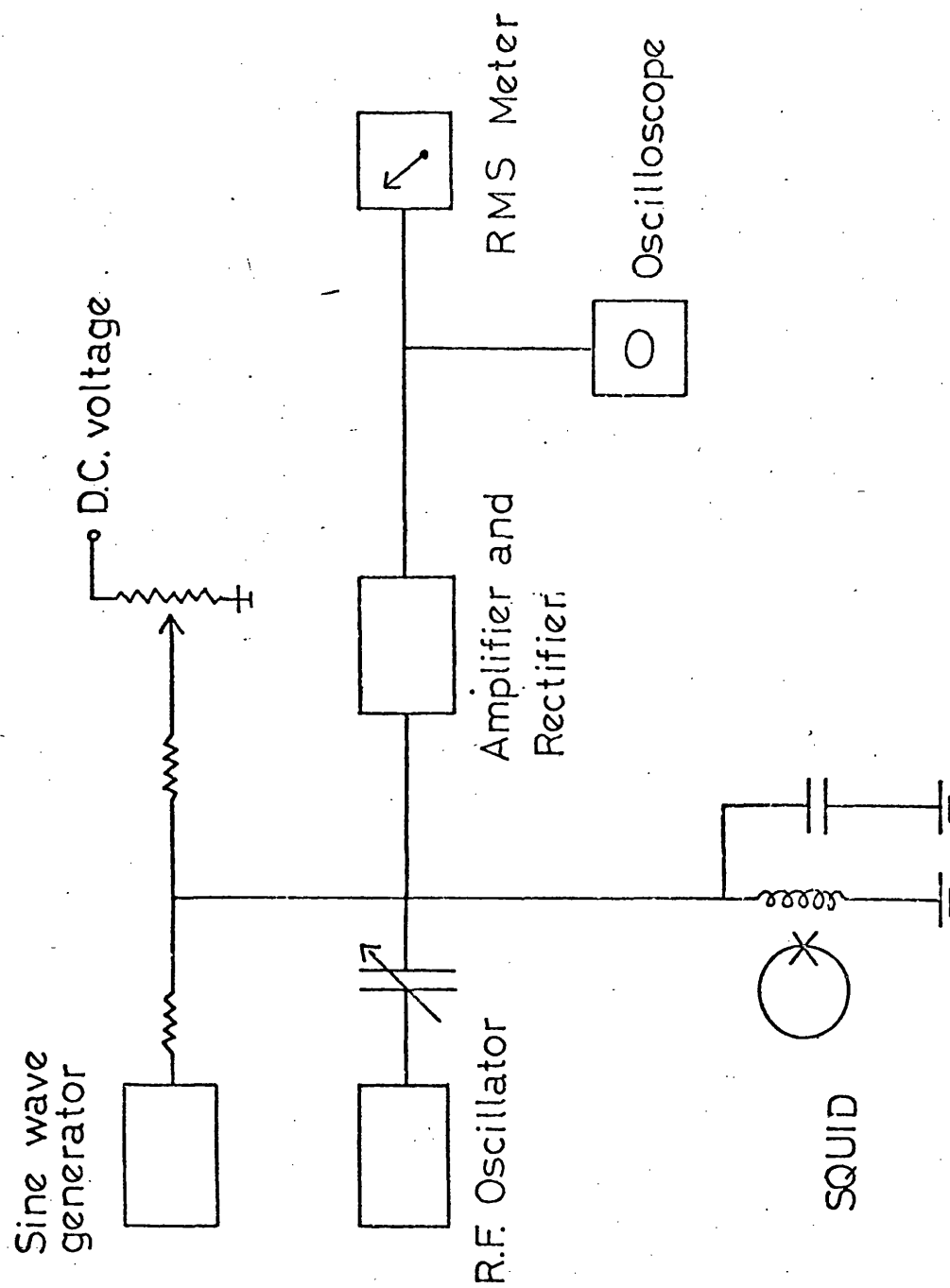
A circuit was constructed as shown in Figure 2.13., the bandwidth of the filter being set from 500 to 1500 Hz and the RMS level was measured by a meter.

With the SQUID working under a constant RF bias and with no external field applied the RMS signal level from the detector was measured. This voltage was related to

Fig. 2.12.



DRIVING THE SQUID WITH A LOW FREQUENCY SIGNAL



SYSTEM TO MEASURE THE SQUID NOISE



flux noise at the input and it was found to be  $2.9 \times 10^{-4} \phi_0 / \sqrt{\text{Hz}}$ .

With the SQUID not working but with the inductance cooled to liquid Helium temperature there was no measurable difference in the value obtained with the SQUID working. This indicated that the dominant noise was produced by the biasing system and amplifying circuit. Zimmerman<sup>42)</sup> also points out that the intrinsic noise of the SQUID is about  $10^{-7} \phi_0 / \sqrt{\text{Hz}}$  in the frequency range discussed in the paper. A result of  $10^{-4} \phi_0$  has been used in the calculations as this should be attainable with better electronics and indeed has now been measured by others<sup>43) 83)</sup>.

### General Conclusion

The work done on the cooling of F.E.T.s does offer a method of reducing the noise by a significant, but not large, factor. The noise performance of field effect transistors, as a function of cooling, does improve at higher frequencies, and an argument could be made for transferring the signal to higher frequency, if a suitable low noise mixer could be found.

The noise performance of the SQUID was found to be in excess of the theoretical noise, and the investigation showed that this excess noise was produced by the RF biasing system. This noise is an important factor used in the calculations on the sensitivity of detectors using SQUID sensors, and is of concern when the effect of the sensing system on the detector is considered.

## Chapter 3

### An Investigation into the Sensitivity of Various Gravitational Wave Detectors

The sensitivity of various gravitational wave detectors to pulses of radiation has been considered, and in this chapter the analysis is performed in detail, for two detection systems. The Brownian motion of the detector is considered along with the noise introduced by the sensing system. However, unlike the majority of previous calculations, performed by others, the effect of the measuring system on the detector is considered, and indeed is found to be an important factor.

Firstly a detector using a capacitive sensor coupled to a F.E.T. amplifier is considered for both aluminium and sapphire bars. The information gained in Chapter 2 on the noise components of a F.E.T. are used as possible limits on the present attainable minimum noise contributions. Secondly the use of a SQUID sensor, coupled onto both aluminium and sapphire bars, is considered and the information gained in the last chapter about the source of noise proves to be an important feature of the calculations. The use of sapphire as a detector material is considered because although the attainable mass is not large ( 40 kgm) the  $Q$  is much larger than that of aluminium, and this more than compensates for the increased thermal motion corresponding to the reduced mass.

#### Method

The method of performing the calculations is to consider

the following general system

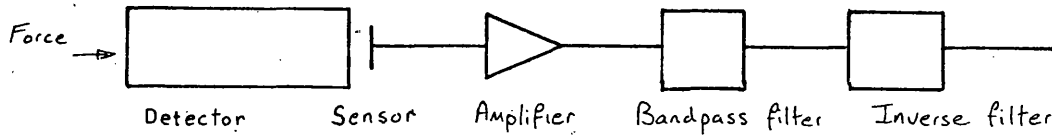


fig. 3.a.

The inverse filter is a circuit which changes the signal from the amplifier (corresponding to the detector motion) into a signal which represents the force that would have to be applied to the detector to produce the motion observed. It may also be considered in the frequency domain as a filter which nulls out the resonant response of the detector to applied force. The circuit of such a filter is discussed in Chapter 5.

The bandpass filter defines the bandwidth of the experiment to a value of  $\Delta f$ . As the output of the experiment is a measure of force applied to the detector, the various noise sources were considered in terms of force noise acting on the detector. The noise components were then combined to find the total noise from the system.

The gravitational wave force signal was assumed to be a sinusoidal pulse of a frequency close to the resonance of the bar, and the pulse could consist of several cycles. The force measured at the output was then related to the input force signal in terms of the experimental bandwidth. The signal to noise ratio was then investigated as a function of the bandwidth and the coupling between the detector and the sensor. The optimum bandwidth was then chosen for a particular gravita-

tional wave pulse.

A result that is used in all the following calculations is the relationship between a sinusoidal force pulse and the amplitude of motion induced in a gravitational wave detector.

The Relationship between a Sinusoidal force Pulse and the Motion induced: A gravitational wave detector may be considered as follows

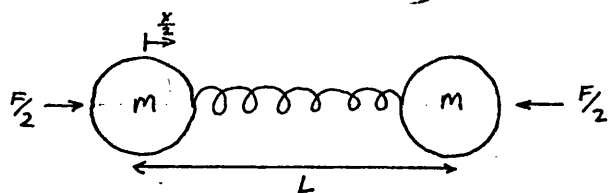


Fig. 3.b.

where  $m = \frac{1}{2}$  of the total mass

$L = \frac{1}{2}$  of the total length

The amount of error introduced by this approximation is small (Chapter 5 Eqn.5.3.).

The equation of motion is, (ignoring damping)

$$\frac{d^2 x}{dt^2} + \omega_m^2 x = \begin{cases} \frac{F_0}{m} \sin \omega t & ; 0 < t < T \\ 0 & ; t > T \end{cases} \quad -(3.1.)$$

Applying Laplace Transforms to the equation and assuming  $x(0) = 0$  and  $x'(0) = 0$

$$(p^2 + \omega_m^2) \bar{x}(p) = \frac{F_0 \omega (1 - e^{-pT})}{m (p^2 + \omega^2)} \quad -(3.2.)$$

$$\text{where } \bar{x}(p) = \mathcal{L}(x(t)) = \int_0^\infty x(t) e^{-pt} dt$$

From Equation 3.2.

$$\bar{x}(p) = \frac{1}{p} (1 - e^{-pT}) \frac{F_0 p \omega}{m (p^2 + \omega_m^2)(p^2 + \omega^2)} \quad -(3.3.)$$

To obtain  $x(t) = \mathcal{L}^{-1}(\bar{x}(p))$  use the convolution theorem

i.e.  $\mathcal{L}^{-1}[\bar{a}(p) \bar{b}(p)] = \int_0^t a(u) b(t-u) du$   
 and noting that  $f(t) = \begin{cases} 1 & 0 \leq t \leq T \\ 0 & t > T \end{cases}$

has the Laplace Transform

$$\bar{f}(p) = \frac{1}{p} (1 - e^{-pT})$$

therefore  $\mathcal{L}^{-1}\left[\frac{1}{p} (1 - e^{-pT})\right] = \begin{cases} 1 & ; 0 \leq t \leq T \\ 0 & ; t > T \end{cases}$

and therefore using partial fractions

$$\bar{g}(p) = \frac{F_0 p \omega}{m (p^2 + \omega_n^2)(p^2 + \omega^2)} = \frac{F_0 \omega}{m (\omega^2 - \omega_n^2)} \left[ \frac{p}{(p^2 + \omega_n^2)} - \frac{p}{(p^2 + \omega^2)} \right]$$

This has an inverse transform

$$g(t) = \frac{F_0 \omega}{m (\omega^2 - \omega_n^2)} [\cos \omega_n t - \cos \omega t]$$

Using the convolution theorem on Equation 3.3.

$$\begin{aligned} x(t) &= \int_0^t \frac{F_0 \omega}{m (\omega^2 - \omega_n^2)} [\cos \omega_n(t-u) - \cos \omega(t-u)] du && \text{for } t \leq T \\ &= \int_0^T \frac{F_0 \omega}{m (\omega^2 - \omega_n^2)} [\cos \omega_n(t-u) - \cos \omega(t-u)] du && \text{for } t > T \end{aligned}$$

-(3.4.)

On integrating and letting the force pulse be an integral number of cycles

$$\begin{aligned} x(t) &= \frac{F_0}{m \omega_n (\omega^2 - \omega_n^2)} \left\{ \omega \sin \omega_n t - \omega_n \sin \omega t \right\} && \text{for } t < T \\ x(t) &= \frac{2 F_0 \omega}{m \omega_n (\omega^2 - \omega_n^2)} \left\{ \sin \left( \frac{\omega_n T}{2} \right) \cos \omega_n \left( t - \frac{T}{2} \right) \right\} && \text{for } t > T \end{aligned}$$

-(3.5.)

If the pulse satisfies the condition that  $\omega_n - \omega \ll \frac{2}{T}$  (i.e. the power spectrum of the pulse includes the system resonance) the above formula for  $t > T$  indicates that the amplitude of

the induced oscillation is

$$\Delta x = \frac{F \cdot T}{2 m \omega_m} \quad -(3.6.)$$

### A Gravitational Wave Detector using a Capacitive Transducer

The method of sensing the motion of a detector by means of the change in capacitance has been used in<sup>a</sup> previous gravitational wave experiment<sup>4</sup>. The variable capacitance may be used either as part of a DC circuit or in a resonant circuit, and both systems have been considered. The following analysis is for the capacitor installed in a resonant circuit as this system seems better than the DC case.

The proposed system is as follows

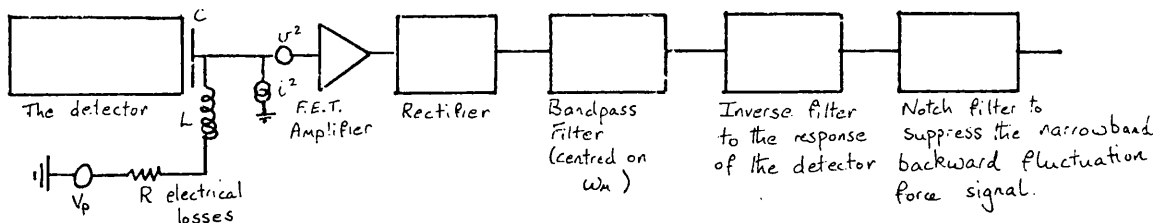


Fig. 3.c.

### The Relationship between the Voltage Signal and a Force Pulse Applied to the Detector.

The frequency of motion at the end of the detector is in the region around 1 kHz, (the detector resonant frequency). The capacitance will therefore have the following value as a function of time.

$$C = C_0 + C_1 e^{j\omega_m t} \quad -(3.7.)$$

The equation for the circuit of Fig. 3.c. is

$$\frac{L d^2 q}{dt^2} + R \frac{dq}{dt} + \frac{1}{C} q = V_p e^{j\omega_p t} \quad -(3.8.)$$

and applying the equation for C and relating R to the electrical  $Q_e$

$$\frac{d^2 q}{dt^2} + \frac{\omega_e}{Q_e} \frac{dq}{dt} + \omega_e^2 q = \frac{V_p}{L} e^{j\omega_p t} + \frac{C_1 q}{LC_0^2} e^{j\omega_m t} \quad -(3.9.)$$

A perturbation approach is used to solve this equation.

The following equation is solved and the value for q obtained is then used to solve the main equation 3.9.

$$\frac{d^2 q}{dt^2} + \frac{\omega_e}{Q_e} \frac{dq}{dt} + \omega_e^2 q = \frac{V_p}{L} e^{j\omega_p t} ;$$

this has the solution

$$q = \frac{V_p e^{j\omega_p t}}{L \left\{ \omega_e^2 - \omega_p^2 + j \frac{\omega_e \omega_p}{Q_e} \right\}} \quad -(3.10.)$$

One common approach is to choose the pump frequency to be less than the electrical resonance by the mechanical resonant frequency i.e.  $\omega_e = \omega_p + \omega_m$ .

$$\therefore q = \frac{V_p e^{j\omega_p t}}{L \left\{ 2\omega_e \omega_m + j \frac{\omega_e \omega_p}{Q_e} \right\}} \quad -(3.11.)$$

It is possible with superconducting techniques that the electrical Q ( $Q_e$ ) could reach  $10^6$  and for this case, where  $\omega_m \sim 6.28 \times 10^3$  and  $\omega_e \sim 6.28 \times 10^7$ , equation 3.11. becomes

$$q = \frac{V_p e^{j\omega_p t}}{2 L \omega_e \omega_m} \quad -(3.12.)$$

and this produces a voltage across the capacitor of

$$V_v = \frac{V_p \omega_e e^{j\omega_p t}}{2 \omega_m}$$

using Equation 3.12. back in Equation 3.9. yields

$$q' = \frac{V_p C_1 e^{j\omega_e t} Q_e}{L^2 C_o^2 2 \omega_e \omega_m \omega_e^2}$$

Hence

$$V_{out} = \frac{V_{\omega} Q_e C_1}{C_o} \quad -(3.13.)$$

As this is a narrowband signal it will take a time  $\tau_e (= \frac{2Q_e}{\omega_e})$  to build up to the value indicated. Therefore, in an observation time  $\tau$  the output signal will be

$$V_{out} = \frac{C_1}{C_o} V_{\omega} Q_e \frac{\tau}{\tau_e} \quad -(3.14.)$$

The time  $\tau_e$  can be related to the  $Q_e$  of the circuit by

$$\tau_e = \frac{2Q_e}{\omega_e} \text{ and so } V_{out} = \frac{C_1}{C_o} V_{\omega} \frac{\omega_e}{2} \tau \quad -(3.15.)$$

and in terms of  $\Delta x$  as  $\frac{\Delta x}{d} = \frac{C_1}{C_o}$ ; where  $d$  is the plate separation

$$V_{out} = \left( \frac{V_{\omega}}{d} \right) \frac{\omega_e}{2} \tau \Delta x \quad -(3.16.)$$

the displacement  $\Delta x$  may now be related to a sinusoidal force pulse (of amplitude  $F_o$ ) which has the same length as the experimental observation time  $\tau$ .

$\therefore$  From Equation 3.6.

$$\Delta x = \frac{F_o \tau}{2m \omega_m}$$

$$\therefore V_{out} = \left( \frac{V_{\omega}}{d} \right) \frac{\omega_e \tau^2 F_o}{4m \omega_m}$$



$$\therefore F_o^2 = \left(\frac{d}{V_m}\right)^2 16 m^2 \left(\frac{\omega_m}{\omega_c}\right)^2 \frac{1}{\gamma^4} V^2 : \quad -(3.17.)$$

and relating this to the experimental bandwidth,

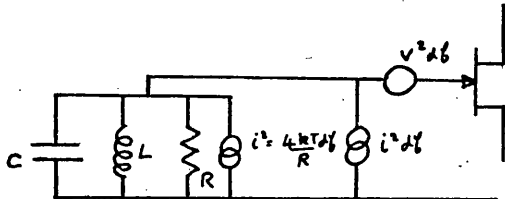
$$\Delta f = \frac{1}{2\gamma}$$

$$F_o^2 = \left(\frac{d}{V}\right)^2 16 m^2 \left(\frac{\omega_m}{\omega_c}\right)^2 16 \Delta f^4 V^2 \quad -(3.18.)$$

## A Consideration of the Noise Components

### The Backward Fluctuation Force

The electrical system is as follows



and as before  $v^2 = (\text{amplifier voltage noise})^2 / \text{Hz}$

$i^2 = (\text{amplifier current noise})^2 / \text{Hz}$

$R$  - represents the electrical damping of the circuit and this is related to the quality factor  $Q_e$  by  $R = (\omega_c C)^{-1} Q_e$ .

The energy in the circuit, due to the resistance thermal noise current, ( $i^2 = 4kT/R$ ) is equal to  $kT$  and this is related to a broadband noise current ( $i^2 \Delta f$ ) by the following relation

$$\mathcal{E} = \alpha \langle i^2 \rangle \text{ and in fact } \alpha = \frac{Q_e}{4 \omega_c C}$$

Therefore the energy in the circuit from both the resistor and the amplifier current noise is given by

$$\mathcal{E} = \left\{ kT + \frac{i^2 Q_e}{4 C \omega_c} \right\} \quad -(3.19.)$$

where  $i^2 = (\text{amplifier noise current})^2 / \text{Hz}$ .

This corresponds to an RMS voltage of

$$V_{RMS}^2 = \frac{1}{C} \left\{ kT + \frac{i^2 Q_e}{4 C \omega_e} \right\}$$

The force produced by a voltage on a capacitor plate is

given by:- 
$$F(t) = - \frac{V^2(t) C}{2 d}$$

where  $V(t)$  is the voltage on the capacitor

$d$  is the plate separation

$C$  is the capacity

However the voltage consists of the following components:-

$$V(t) = V_{\omega} \sin \omega_p t + V_s \sin \omega_e t$$

where  $V_{\omega}$  is the biasing voltage at a frequency of  $\omega_p$

$V_s$  is the noise signal at  $\omega_e$  with a bandwidth of  $\omega_e / Q_e$ .

Therefore the force becomes

$$F(t) = - \frac{C}{2 d} \left\{ V_{\omega}^2 \sin^2 \omega_p t + V_{\omega} V_s \{ \cos(\omega_e - \omega_p) t - \cos(\omega_p + \omega_e) t \} + V_s^2 \sin^2 \omega_e t \right\}$$

As the system detects forces in the region of 1 kHz the dominant term is:-

$$F(t) = - \frac{C V_{\omega} V_s \cos \omega_e t}{2 d} \Rightarrow F_{RMS} = \left( \frac{V_{\omega}}{d} \right) \frac{C}{2} V_{s(RMS)} \quad (3.21)$$

Substituting for  $V_s$  (Eqn. 3.20)

$$F^2 = \left( \frac{V_{\omega}}{d} \right)^2 \frac{C}{4} \left\{ kT + \frac{i^2 Q_e}{4 \omega_e C} \right\}$$

This backward fluctuation force has a narrow bandwidth equal to  $\frac{\omega_e}{Q_e}$  and a decay time of  $\tau_e = 2 Q_e / \omega_e$ .

If an additional filter is added to the output in order to suppress this narrowband signal (i.e. a notch filter) the noise transmitted in an observation time  $\tau$  is equivalent to :-

$$F^2 = \left( \frac{V_{\omega}}{d} \right)^2 \frac{C}{4} \left\{ kT + \frac{i^2 Q_e}{4 \omega_e C} \right\} \frac{\tau}{\tau_e}$$

$$\therefore F^2 = \left(\frac{V}{d}\right)^2 \frac{C}{16} \left\{ kT + \frac{i^2 Q_e}{4 \omega_e C} \right\} \frac{\omega_e}{Q_e df} \quad -(3.23.)$$

### The Amplifier Noise

from Equation 3.20. the (voltage noise)<sup>2</sup> from resonant circuit and noise current =  $\frac{1}{C} \left\{ kT + \frac{i^2 Q_e}{4 \omega_e C} \right\} \frac{\gamma}{\gamma_e}$

and for the amplifier voltage noise =  $v^2 df$

and these components combine to give

$$V^2 = v^2 df + \frac{1}{C} \left\{ kT + \frac{i^2 Q_e}{4 \omega_e C} \right\} \frac{\omega_e}{2 Q_e} \quad -(3.24.)$$

This noise may be related to an equivalent force pulse by Equation 3.18.

$$F_o^2 = \left(\frac{d}{V_o}\right)^2 16 m^2 \omega_m^2 \frac{16 df^4}{\omega_e^2} \left\{ v^2 df + \frac{1}{C} \left\{ kT + \frac{i^2 Q_e}{4 \omega_e C} \right\} \frac{\omega_e}{2 Q_e} \frac{1}{2 df} \right\} \quad -(3.25.)$$

$$\therefore F_o^2 = 16 m^2 \left(\frac{\omega_m}{\omega_e}\right)^2 \left(\frac{d}{V_o}\right)^2 \left\{ v^2 16 df^5 + \frac{1}{C} \left\{ kT + \frac{i^2 Q_e}{4 \omega_e C} \right\} \frac{\omega_e}{Q_e} 4 df^3 \right\} \quad -(3.26.)$$

### The Noise Due to the Brownian Motion of the Detector

The harmonic oscillator of Fig. 3.b. has a mean thermal energy of  $kT_m$  (where  $k$  is Boltzmann's constant and  $T_m$  - the temperature of the detector). It may be shown that the white noise force signal required to excite the detector to an energy of  $kT$  is

$$F_{per Hz}^2 = \frac{8 m \omega_m k T_m}{Q_m} \quad -(3.27.)$$

On combining the noise terms

$$\begin{aligned}
F_N^2 &= \frac{8m\omega_k T_m}{Q_m} df + (16)^2 m^2 \left( \frac{\omega_m}{\omega_e} \right)^2 \left( \frac{d}{V} \right)^2 v^2 df^5 \\
&+ (8)^2 m^2 \left( \frac{\omega_m}{\omega_e} \right)^2 \left( \frac{d}{V} \right)^2 \frac{1}{C} \left\{ kT_e + \frac{i^2 Q_e}{4\omega_e C} \right\} \frac{\omega_e}{Q_e} df^3 \\
&+ \left( \frac{V}{d} \right)^2 \frac{C \omega_e}{4 \times 4 Q_e} \left\{ kT_e + \frac{i^2 Q_e}{4\omega_e C} \right\} \frac{1}{df}
\end{aligned} \tag{3.28.}$$

#### To Minimise the Total Noise

The above formula has the following form

$$\begin{aligned}
F_N^2 &= AT_m df + B y df^5 + C y df^3 \\
&+ \frac{D}{y df}
\end{aligned} \tag{3.29.}$$

where y represents the coupling  $= \left( \frac{d}{V} \right)^2$

and A, B, C, D have the appropriate values.

The optimum value of  $\left( \frac{d}{V} \right)^2$  (as a function of df), to minimise

the noise, is now found.

$$\text{From above } F_N^2 = AT_m df + (B df^5 + C df^3) y + \frac{D}{y df}$$

$$\frac{\partial F_N^2}{\partial y} = B df^5 + C df^3 - \frac{D}{df y^2}$$

We require gradient = 0

$$\text{i.e. } y^2 = \frac{D}{(B df^5 + C df^3) df}$$

$$\therefore y = \frac{D^{1/2}}{(B df^5 + C df^3)^{1/2} df^{1/2}} \tag{3.30.}$$

and if this optimum value is substituted back into the equation, the formula for the noise becomes

$$\begin{aligned} F_N^2 &= AT_m df + 2(B df^4 + C df^2)^{1/2} D^{1/2} \\ F_N^2 &= (AT_m + 2(B df^2 + C)^{1/2} D^{1/2}) df \end{aligned} \quad -(3.31.)$$

This formula suggests that the optimum bandwidth (to reduce the noise) is zero. However the signal pulse has to be considered at this stage.

If the power spectrum of the signal pulse is enclosed within the bandwidth of the experiment, the pulse will not be attenuated. If however the experimental bandwidth is narrower than the pulse power spectrum the output will be attenuated, and the attenuation is described by

$$F_{sig\ out}^2 = F_{sig\ in}^2 \left( \frac{\Delta f}{\Delta F} \right)^2 \quad -(3.32.)$$

where  $F_{sig\ out}$  - Force signal amplitude at output  
 $F_{sig\ in}$  - Force signal amplitude at input  
 $\Delta f$  - Experimental bandwidth  
 $\Delta F$  - Bandwidth of pulse

Note: This would not be true for white noise passing through a frequency band (where  $F_N^2 \propto df$ ).

Therefore consider a specific pulse length  $T$  and hence bandwidth  $\Delta F = \frac{1}{T}$ .

On considering an experimental bandwidth ( $df$ ) wider than the pulse bandwidth ( $\Delta F$ ), Equation 3.29. indicates that the signal to noise ratio  $\left( \frac{F_{sig}^2}{F_N^2} \right)$  will increase on reducing the bandwidth. (The signal is staying the same and the noise reduces with decreasing  $df$ ). Eventually the

bandwidth will become smaller than the bandwidth of the pulse and the signal will start to be attenuated.

Equation 3.29. indicates that the noise ( $F_n^2$ ) will eventually reduce proportional to  $df$  (the point where this commences depends on the constants which are evaluated later). However the signal ( $F_s^2$ ) is reduced as  $(df^2)$  and therefore the signal to noise ratio will decrease. Due to the two opposing effects, the signal to noise ratio is maximum when the experimental bandwidth is approximately equal to the pulse bandwidth. This argument is illustrated numerically in the aluminium detector case.

The optimum experimental bandwidth is taken therefore equal to the bandwidth of the pulse. This means that if the pulse is long and of constant amplitude a narrower experimental bandwidth should be used and hence the signal to noise ratio will be higher. However more energy has been presented to the detector (Energy  $\propto T^2 F_s^2$ , where  $T$  is the length of the pulse). It is interesting to minimise the energy that is detectable and find the length of pulse that is best for the detector.

Now  $df = \frac{1}{T}$  ( $T$  = the length of the pulse)

the minimum energy is proportional to  $F_s^2 T^2$

From Equation 3.31.

$$F_s^2 T^2 = (AT_n + 2(B df^2 + C)^{1/2} D^{1/2}) T$$

$$\text{Energy} \propto AT_n T + 2(BD + CDT^2)^{1/2} \quad \text{---(3.33.)}$$

For ease of calculation this equation will be studied after the constants have been evaluated in the particular

case of aluminium.

This type of detection scheme is analysed for both aluminium and sapphire bars.

### The Aluminium Detector

The parameters of the system are defined as follows

#### The Aluminium

$m = 2.5 \times 10^3$  Kgm (a 5 tonne aluminium cylinder,  
as this mass of detector is under  
construction<sup>63</sup>).

$$Q_m = 5 \times 10^5$$

$$\omega_m = 6.28 \times 10^3 \text{ rad s}^{-1}$$

$$L_o = 1.3\text{m} \text{ (The length of the cylinder} = 2.6\text{m)}$$

$$T_m = \text{to be investigated}$$

#### The Electrical Circuit

$$\omega_e = 6.28 \times 10^7 \text{ rad s}^{-1}$$

$$Q_e = 10^6$$

$$C = 2 \times 10^{-10} \text{ F}$$

$$T_e = 4 \text{ K (Due to the fact that the electrical components have to be superconducting).}$$

#### The Amplifier

$$v = 10^{-9} v / \sqrt{\text{Hz}}$$

$$i = 2 \times 10^{-15} \text{ Amps} / \sqrt{\text{Hz}}$$

The parameters as described in Eqn. 3.26 are now calculated.

Note: All units are in the MKS system.

$$A = \frac{8 m \omega_m k T_m}{Q_m} = 3.5 \times 10^{-21} \times T_m$$

(Brownian Noise)

(Amplifier voltage noise)

$$B = (16)^2 m^2 \left( \frac{\omega_m}{\omega_e} \right)^2 v^2 = 1.6 \times 10^{-17}$$

(Amplifier current and circuit noise)

$$\begin{aligned} C &= (8)^2 m^2 \left( \frac{\omega_m}{\omega_e} \right)^2 \frac{1}{C} \left\{ kT_e + \frac{i^2 Q_e}{4 \omega_e C} \right\} \frac{\omega_e}{Q_e} \\ &= 1.3 \times 10^{12} \{ 5.5 \times 10^{-23} + 8 \times 10^{-23} \} \\ &= 1.7 \times 10^{-10} \end{aligned} \quad -(3.34.)$$

(Backward fluctuation)

$$\begin{aligned} D &= \frac{C \omega_e}{4.04} \left\{ kT_e + \frac{i^2 Q_e}{4 \omega_e C} \right\} \\ &= 7.9 \times 10^{-10} \{ 5.5 \times 10^{-23} + 8 \times 10^{-23} \} \\ &= 1.1 \times 10^{-31} \end{aligned} \quad -(3.35.)$$

### A Numerical Evaluation of the Signal to Noise Ratio as a Function of df

An argument has been presented to justify the choice of using a bandwidth of 1 kHz for the best detection of 1 ms pulses. However for the particular case of aluminium this assumption is shown to be true.

Using the values of A, B, C, D (with  $T_m = 1^\circ K$ ) pulses of length 1 ms and 2 ms have been considered and a graph of signal to noise ratio  $\left( \frac{F_s^2}{F_n^2} \right)$  as a function of df for the two pulses has been constructed (Fig.3.1.). The graph does confirm what was previously thought to be the result, and the bandwidth should be chosen to equal the pulse length.

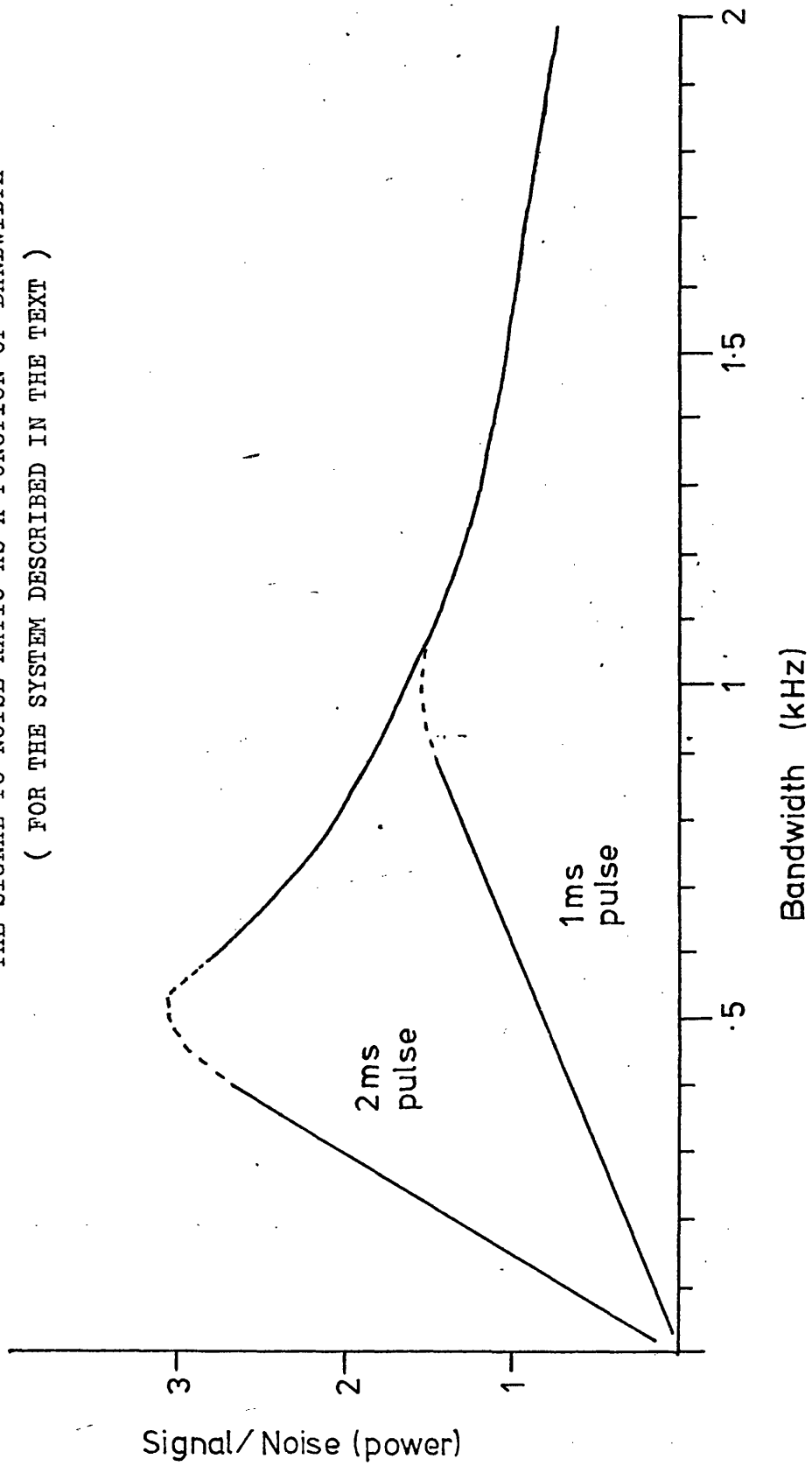
### The Sensitivity of the Detector to 1 ms Force Pulses

$$df = 1 \text{ kHz} \left\{ \text{this implies } \left( \frac{v}{d} \right) = 2.0 \times 10^8 \right\}$$



Fig. 3.1.

THE SIGNAL TO NOISE RATIO AS A FUNCTION OF BANDWIDTH  
( FOR THE SYSTEM DESCRIBED IN THE TEXT )



From Equation 3.31

$$\begin{aligned}
 F_N^2 &= \{A T_M + 2(B df^2 + C)^{1/2} D^{1/2}\} df \quad (3.36) \\
 &= \{3.5 \times 10^{-21} T_M + 2(1.6 \times 10^{-11} + 1.7 \times 10^{-10})^{1/2} (1.1 \times 10^{31})^{1/2}\} 10^3 \\
 &= \{3.5 \times 10^{-21} T_M + 9 \times 10^{-21}\} 10^3
 \end{aligned}$$

Choosing  $T_M$  such that the thermal noise component is equal to the sum of the other components

$$F_N^2 = 1.8 \times 10^{-17} \Rightarrow F_N = 4.2 \times 10^{-9}$$

This may now be related to the amplitude of the Riemann tensor and hence to gravitational wave amplitude.

$$F = m c^2 L_p R_{\dots} \quad \text{from Eqn. 1.5}$$

$$\text{and } R_{\dots} c^2 = \frac{1}{2} \ddot{h}$$

$$\therefore h = \frac{4 \pi F}{m \omega^2 L_p} \quad (3.37)$$

$$\Rightarrow h = 4.1 \times 10^{-19}$$

Briefly, the situation corresponding to the minimum energy detectable is considered. It is only done for this case but it may be extended to other systems if desired.

$$\begin{aligned}
 \text{Energy} &\propto A T_M T + 2(BD + CDT^2)^{1/2} \quad (3.38) \\
 &3.5 \times 10^{-21} T_M T + 2(1.68 \times 10^{-48} + 1.78 \times 10^{-41} T^2)^{1/2}
 \end{aligned}$$

$$\text{Therefore reduce } T \text{ until } BD \sim CDT^2 \text{ i.e. } T^2 = \frac{B}{C}$$

$$\Rightarrow T \sim \sqrt{\frac{B}{C}} = 3 \times 10^{-4} \text{ secs}$$

This indicates that 0.3 ms pulses correspond to the minimum detectable signal energy. However, in order to standardise the situation the sensitivity of the detectors will be compared for a 1 ms pulse.

#### Conclusion about $T_M$

From Equation 3.36 it is noticed that under the conditions of optimum coupling the thermal noise component becomes

dominant above a temperature of 3 K.

### The Sapphire Detector

It has been proposed by Braginskii<sup>36)</sup> that sapphire should be a good detector material. The mass of sapphire available is not large but, as stated previously, the high  $Q_m$  more than compensates and reduces the thermal noise. However due to the smaller mass it is possible that the backward fluctuation force has more effect and this is considered in the following calculations.

The parameters are as follows

#### The Bar

$$\begin{aligned} m &= 20 \text{ kgm} \\ Q_m &= 10^8 \\ \omega_m &= 6.28 \times 10^3 \text{ rad s}^{-1} \\ L &= 2.5 \text{ m} \end{aligned}$$

#### The Sensor

$$\begin{aligned} \omega_e &= 6.28 \times 10^7 \text{ rad s}^{-1} \\ Q_e &= 10^6 \\ C &= 2 \times 10^{-10} \text{ F} \\ T_e &= 4^\circ\text{K} \quad (\text{Electronics cooled}) \end{aligned}$$

#### The Amplifier

$$\begin{aligned} i &= 2 \times 10^{-15} \text{ A} / \sqrt{H_z} \\ v &= 10^{-9} \text{ nV} / \sqrt{H_z} \end{aligned}$$

The parameters as described in Eqn. 3.26. are calculated

(Brownian Noise)

$$A = 1.4 \times 10^{-25} \times T_m$$

(Amplifier voltage noise)

$$B = 1.0 \times 10^{-21}$$

(Amplifier current noise and Bias circuit noise)

$$C = 8 \times 10^7 \{ 5.5 \times 10^{-23} + 8 \times 10^{-23} \} = 1 \times 10^{-14}$$

(Backward Fluctuation)

$$D = 7.9 \times 10^{-10} \{ 5.5 \times 10^{-23} + 8 \times 10^{-23} \} = 1.1 \times 10^{-31}$$

For 1 ms pulses

$$df = 1 \text{ kHz and using Eqn. 3.30. } \left( \frac{V}{d} \right) = 1.7 \times 10^7$$

using Equation 3.31.

$$\begin{aligned} F_w^2 &= \left\{ (1.4 \times 10^{-25} T_m + 2(10^{-15} + 10^{-14})^{1/2} (1.1 \times 10^{-31})^{1/2}) \right\} 10^3 \\ &= \{ 1.4 \times 10^{-15} T_m + 7 \times 10^{-23} \} 10^3 \end{aligned} \quad - (3.39)$$

Assuming that  $T_m$  is not greater than room temperature

$$F_w^1 \sim 7 \times 10^{-20} \text{ and using Eqn. 3.37.}$$

$$h = 1.7 \times 10^{-18} \quad - (3.40)$$

#### The Value of $T_m$

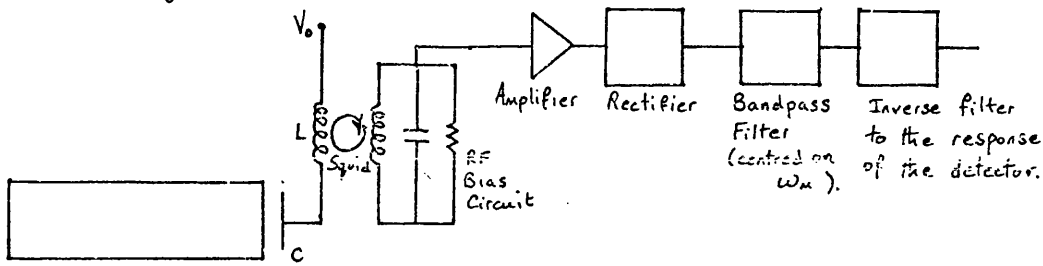
From Equation 3.39., which assumes optimum coupling, the thermal noise is not dominant at room temperature. The fact that the mass is lower means that the backward reaction has more effect.

### A Gravitational Wave Detector Combined with a SQUID

#### Sensing System

The coupling system considered was that of a DC voltage producing the bias for the capacitive sensing circuit, the signal current was then coupled into the SQUID by an inductance. This DC method is similar to other systems even though the details of the coupling differ.

The system is as follows



To Find the Relationship between the Motion of the Cylinder and Signal Flux Coupled into the SQUID

$$\text{Circuit equation} = \frac{d^2 q}{dt^2} + \frac{1}{L C_0} q = \frac{V_0}{L} + \frac{C_1}{L C_0^2} q e^{j\omega_m t}$$

-(3.41.)

Solving by a perturbation method

$$q = V_0 C_0$$

and apply this to the equation

$$\frac{d^2 q}{dt^2} + \frac{1}{L C_0} q = \frac{C_1}{L C_0^2} V_0 C_0 e^{j\omega_m t}$$

$$q = \frac{C_1 V_0 e^{j\omega_m t}}{L C_0 (\omega_c^2 - \omega_m^2)}$$

$$i = \frac{C_1 \omega_m V_0 e^{j\omega_m t}}{L C_0 (\omega_c^2 - \omega_m^2)}$$

$$\omega_c \gg \omega_m$$

$$i = C_1 \omega_m V_0 e^{j\omega_m t}$$

$$i = \omega_m C_0 \left( \frac{V}{d} \right) \Delta x \quad \text{-(3.42.)}$$

$\therefore$  flux into the SQUID =  $\mathcal{M} i$

$\mathcal{M}$  = mutual inductance

$$\Phi_s = \mathcal{M} \omega_m C_0 \left( \frac{V}{d} \right) \Delta x \quad \text{-(3.43.)}$$

and as before this is related to a force pulse of

$$\text{length} = \gamma$$

$$\Phi_s = \mathcal{M} \omega_m C_o \left( \frac{V_o}{d} \right) \frac{F_o \gamma}{2 m \omega_m} \quad -(3.44.)$$

$$F_o = \left( \frac{d}{V_o} \right) \frac{2 m \Phi_s}{C_o \mathcal{M}} \frac{1}{\gamma}$$

$$\Rightarrow F_o = \left( \frac{d}{V_o} \right) \frac{4 m \Phi_s}{C_o \mathcal{M}} df \quad -(3.45.)$$

### The Amplifier Noise Term

The noise from the SQUID operating at a frequency of about 10 MHz is taken to be  $10^{-4} \Phi_o / \sqrt{\text{Hz}}$ . This source of noise is related to a force pulse on the detector.

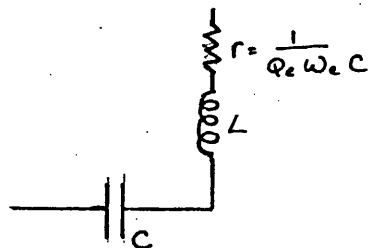
The noise is related to a force using Equation 3.45.

and

$$F_o^2 = \left( \frac{d}{V_o} \right)^2 \frac{(4)^2 m^2 \Phi_N^2 df^3}{\mathcal{M}^2 C^2} \quad \Phi_N^2 - \text{Squid noise.} \quad -(3.46.)$$

This is not the only source of noise however; there is a component introduced by the DC biasing circuit for the variable capacitor.

i.e.



$Q_e$  - quality factor of circuit

$\omega_e$  - electrical resonant frequency

The flux noise coupled to the SQUID (in a frequency region around 1 kHz) is

$$\Phi_s^2 = \frac{\mathcal{M}^2 4 k T_e \omega_m^2 C df}{Q_e \omega_e} \quad -(3.47.)$$

∴ The total amplifier noise is

$$F_o^2 = \left( \frac{d}{v_o} \right)^2 \frac{(4)^2 m^2}{C_o^2 M^2} \left( \Phi_N^2 df + \frac{M^4 4 k T_e \omega_e^2 C}{Q_e \omega_e} df \right) df^2 \quad -(3.48.)$$

### The Brownian Noise Term

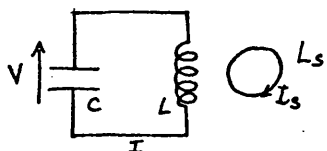
As before from Equation 3.27.

$$F^2 = \frac{8 m \omega_e k T_m df}{Q_m} \quad -(3.49.)$$

### The Backward Fluctuation force

Assume a flux noise  $\Phi_B^2 df$  is available to be fed back into the circuit, the value of  $\Phi_B$  will be discussed later.

The situation is as follows



one requires to calculate \$V\$.  
Applying the circuit equations and  
eliminating \$I\$

$$\frac{V_s}{I_s} = \left\{ j\omega L_s + \frac{\omega^2 M^2}{\frac{1}{j\omega C} + j\omega L} \right\}$$

Eliminating \$I\_s\$

$$- \frac{M}{L_s} \frac{V_s}{I} = \frac{1}{j\omega C}$$

$$\therefore I = - j\omega C \frac{M}{L_s} \left\{ j\omega L_s + \frac{\omega^2 M^2}{\frac{1}{j\omega C} + j\omega L} \right\} I_s$$

$$V = \frac{M}{L_s} \left\{ j\omega L_s + \frac{\omega^2 M^2}{\frac{1}{j\omega C} + j\omega L} \right\} I_s$$

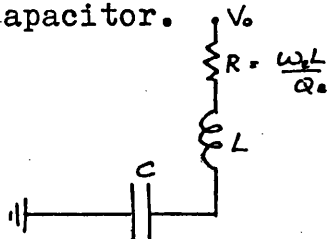
$$\therefore V = j \omega_m \sqrt{\frac{L}{L_s}} \Phi_B \left( 1 - \frac{1}{(1 - \frac{\omega_e^2}{\omega_s^2})} \right)$$

Now as  $\omega_e \gg \omega_m$

$$V^2 = \omega_m^2 \frac{\Phi_B^2}{L_s} L \, df \quad -(3.50.)$$

where  $\Phi_B^2$  - (flux noise)<sup>2</sup> / Hz that is available to be fed onto the input circuit.

Another source of backward force is the noise introduced by the thermal noise in the biasing circuit for the variable capacitor.



and from the resistance  $v^2 = 4 kT_e R \, df$

$$\therefore v^2 = \frac{4 kT_e}{Q_e \omega_e C} \, df$$

total  $v^2$  across the capacitor is

$$v^2 = \left( \omega_m^2 \frac{\Phi_B^2}{L_s} L + \frac{4 kT_e}{Q_e \omega_e C} \right) df$$

The force produced by the voltage on the capacitor is

$$F = \left( \frac{V_0}{d} \right) C v$$

$$\therefore F_N^2 = \left\{ \omega_m^2 \frac{\Phi_B^2}{L_s} L + \frac{4 kT_e}{Q_e \omega_e C} \right\} \left( \frac{V_0}{d} \right)^2 C^2 \, df \quad -(3.51.)$$

On combining the noise terms

$$F_N^2 = \frac{8 m \omega_m k T_m}{Q_m} \, df + \left( \frac{d}{V_0} \right)^2 \frac{16 m^2}{C^2} \left\{ \frac{\phi_N^2}{M^2} + \frac{4 kT_e \omega_m^2 C}{Q_e \omega_e} \right\} df^3 + \dots$$



$$\dots + \left( \frac{V}{d} \right)^2 \left\{ \frac{C^2 \omega_n^2 \Phi_s^2 L}{L_s} + \frac{4 k T_e C}{Q_e \omega_e} \right\} df \quad -(3.52.)$$

This equation has the form

$$F_N^2 = A T_m df + y B df^3 + \frac{C df}{y} \quad -(3.53.)$$

where  $y = \left( \frac{d}{V} \right)^2$  and A, B, C have the appropriate values.

$$\frac{\partial F_N^2}{\partial y} = B df^3 - \frac{C df}{y^2}$$

$$\text{and a minimum} \Rightarrow y^2 = \frac{C}{B} \frac{1}{df^2}$$

$$\text{This value } y = \sqrt{\frac{C}{B}} \frac{1}{df} \quad -(3.54.)$$

is substituted (into 5.53.)

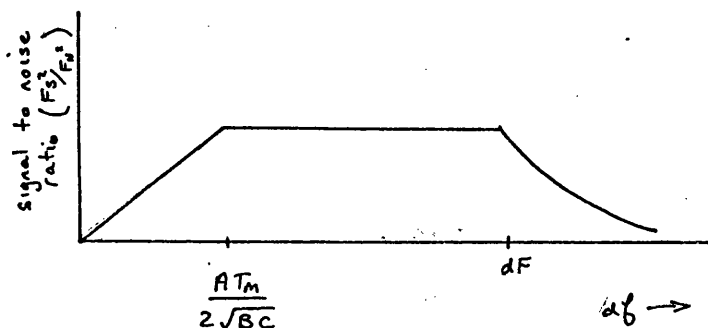
$$\Rightarrow F_N^2 = A T_m df + 2\sqrt{BC} df^2$$

$$F_N^2 = (A T_m + 2\sqrt{BC} df) df \quad -(3.55.)$$

The fall off of the noise is proportional to  $df^2$  until  $df$  falls to  $df < \frac{A T_m}{2\sqrt{BC}}$  when the noise reduces proportional to  $df$ .

The signal  $F_s^2$  (of bandwidth  $df$ ) will start to fall off as  $df^2$  when  $df < df$ . If at this stage the noise is falling off as  $df^2$  the signal to noise ratio will stay constant until the noise reduces as  $df$ .

i.e.



This offers a range of  $df$  to use from  $df$  to  $\frac{AT_m}{2\sqrt{BC}}$

if  $\frac{AT_m}{2\sqrt{BC}} < df$ , and it is best to use  $df = df$  if  $\frac{AT_m}{2\sqrt{BC}} > df$ .

The optimum value of coupling  $\left(\frac{V}{d}\right)$  is dependent on  $df$ , so if  $\left(\frac{F_s^2}{F_N^2}\right)$  was constant it might be best to go to smaller  $df$ , but if not a bandwidth of  $df = df$  is chosen.

As before the analysis is done for 1 ms pulses.

To evaluate Equation 3.44. the SQUID parameters are first determined.

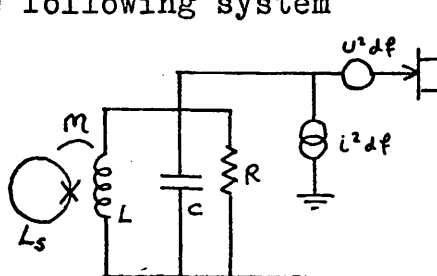
$\Phi_N^2$  - This is the flux noise of the SQUID and it was measured to be  $2.9 \times 10^{-4} \Phi_0 / \sqrt{\text{Hz}}$ . In the calculation a value of  $10^{-4} \Phi_0 / \sqrt{\text{Hz}}$  has been used, as with a better SQUID this figure should be attained.

$\Phi_B^2$  - This is the flux noise that is available at the SQUID to couple back into the input circuit. The measurements, made in the previous chapter, indicated that the majority of the noise was produced in the SQUID RF biasing circuit, with perhaps a small intrinsic noise ( $\sim 10^{-7} \Phi_0 / \sqrt{\text{Hz}}$ ) produced in the SQUID.

One might expect that the noise produced in the RF biasing circuit does not get coupled back, through the SQUID, onto the input circuit, or even if it did the frequency of the noise would be too high to affect the low frequency signals at the input. However the action of the SQUID will be to 'beat down' the RF noise with the RF pump signal thus reducing the flux noise to low frequency and this noise is available to be coupled into the input circuit. This means that the expected backward

flux noise will be higher than  $10^{-7} \phi_0 / \sqrt{\text{Hz}}$ . By assuming all the noise flux at high frequency is beaten down to low frequency, the amount of flux available for back reaction is estimated in the following way:

Consider the following system



The value of  $R$  is such that  $R = \omega_c L Q_e$  where  $Q$  is the quality factor of the resonant circuit (isolated from the SQUID).

The equivalent temperature, at which  $R$  is considered to be, is above the ambient temperature due to the current noise from the amplifier. However from an analysis of the situation in a typical commercial SQUID the biasing circuit can probably be considered as producing the dominant noise for a low noise r.f.t. connected to the device.

When the SQUID is in operation, coupled to the device, it has the effect of damping the  $Q$  of the circuit to  $Q_{eff}$ ; however, the value of  $R$  remains approximately the same. (This situation is similar to an active circuit damping the  $Q$  of a resonant circuit without increasing the noise, and this operation can be considered as cooling the effective resistance).

The noise current through the inductance is

$$i^2 = \frac{Q_{eff}^2}{R} 4 k T_e df \quad R = Q_e L \omega_c \quad (3.56)$$

$$i^2 = Q_{eff}^2 \frac{4 k T_c df}{Q_c L \omega_c'}$$

$$\therefore \bar{\Phi}_S^2 = K^2 L L_s \frac{4 k T_c Q_{eff}^2}{Q_c L \omega_c'} df \quad (3.57)$$

where K - coupling coefficient

The value of  $Q_{eff}$  has been calculated by Kurkijärvi<sup>46)</sup> to be

$$Q_{eff} \sim \frac{1}{K^2} \left( \frac{k T_s}{\frac{2\sqrt{2}}{3\pi} i_c \Phi_0 \left(\frac{1}{2\pi}\right)^{3/2}} \right)^{2/3} \quad T_s - \text{temperature of SQUID}$$

$$Q_{eff} \sim \frac{14}{K^2} \left( \frac{k T_s}{i_c \Phi_0} \right)^{2/3} \quad (3.58)$$

and substituting into Equation 3.57

$$\bar{\Phi}_S^2 = \frac{K^2 L_s}{Q_c \omega_c'} \frac{4 k T_c (14)^2}{K^4} \left( \frac{k T_s}{i_c \Phi_0} \right)^{4/3} \quad (3.59)$$

and assuming optimum coupling of

$$K^2 Q_c \sim 1$$

$$\bar{\Phi}_S^2 = \frac{4 k T_c L_s}{\omega_c'} (14)^2 \left( \frac{k T_s}{i_c \Phi_0} \right)^{4/3} \quad (3.60)$$

and evaluating this for a typical SQUID inductance of  $4 \times 10^{-10}$  H and mF bias frequency of 20 MHz. ( $T_c = T_s = 4$  K)

$$\bar{\Phi}_S = 6 \times 10^{-6} \Phi_0 / \sqrt{\text{Hz}}$$

Firstly an aluminium system with the following parameters is considered

Mass	=	$2.5 \times 10^3$ Kgm	(Total mass = 5 tonnes)
$\omega_M$	=	$6.28 \times 10^3$ rad s <sup>-1</sup>	
$Q_M$	=	$5 \times 10^5$	
$T_M$	=	under investigation	
$L_0$	=	1.3 m	
C	=	$2 \times 10^{-10}$ F	

$$\begin{aligned}
L &= 10^{-4} \\
Q_e &= 10^6 \\
T_e &= 4^\circ\text{K} \\
\omega_e &= 7 \times 10^6 \text{ rad s}^{-1}
\end{aligned}$$

$$\begin{aligned}
\Phi_N &= 10^{-4} \Phi_0 / \sqrt{\text{Hz}} = 2 \times 10^{-19} \text{ Wb} / \sqrt{\text{Hz}} \\
&= 6.0 \times 10^{-6} \Phi_0 / \sqrt{\text{Hz}} = 1.2 \times 10^{-20} \text{ Wb} / \sqrt{\text{Hz}} \\
L_s &= 4 \times 10^{-10} \text{ H}
\end{aligned}$$

$$k = 1.38 \times 10^{-23} \text{ J/}^\circ\text{K}$$

The coupling constant between the signal coil and the SQUID is about unity and this means

$$\begin{aligned}
\text{that } \mathcal{M} &= \sqrt{L L_s} \\
\mathcal{M} &= 2 \times 10^{-7} \text{ H}
\end{aligned}$$

The constants as specified by Eqn. 3.52. are now evaluated.

(Brownian Motion)

$$A = \frac{8 \pi \omega_n k}{Q_n} = 3.5 \times 10^{-21} \quad -(3.61.)$$

(Amplifier Noise)

$$\begin{aligned}
B &= \frac{16 \pi^2}{C^2} \left\{ \frac{\Phi_N^2}{\mathcal{M}^2} + \frac{4 k T_e \omega_n^2 C}{Q_e \omega_e} \right\} \\
&= 2.5 \times 10^{17} \{ 10^{-24} + 24 \times 10^{-38} \} = 2500
\end{aligned}$$

(Backward Fluctuation)

$$\begin{aligned}
C &= \left\{ \frac{C^2 \omega_n^2 \Phi_s^2 L}{L_s} + \frac{4 k T_e C}{Q_e \omega_e} \right\} \\
&= 5.7 \times 10^{-47} + 6.4 \times 10^{-45}
\end{aligned}$$

The backward fluctuation term is dominated by noise in the biasing circuit rather than the SQUID. To investigate the limiting properties of the SQUID this electronic circuit is assumed to be cooled enough to let the SQUID

noise dominate.

Equation 3.55. therefore becomes with  $df = 10^3 \left( \frac{V}{d} \right) = 8 \times 10^{13}$

$$F_N^2 = (3.5 \times 10^{-11} T_m + 7.6 \times 10^{-21} \times 10^3) \times 10^3 \quad (3.62)$$

Choosing  $T_m$  such that the thermal noise component is equal to the sum of the other components

$$F_N^2 = 1.5 \times 10^{-15} \text{ and using Eqn. 3.37}$$

$$h = 3.8 \times 10^{-18}$$

Equation 3.62 shows that under the conditions of optimum coupling the thermal noise dominates above a temperature of 220 K.

#### A Sapphire Bar Coupled to a SQUID

A sapphire (40 kgm) detector is now considered with the following parameters.

$$m = 20 \text{ kgm}$$

$$\omega_m = 6.28 \times 10^3 \text{ rad s}^{-1}$$

$$Q = 10^8$$

$$L = 2.5 \text{ m}$$

$$C = 2 \times 10^{-10} \text{ F}$$

$$L = 10^{-4} \text{ H}$$

$$Q_e = 10^6$$

$$T_e = 4 \text{ K}$$

$$\omega_e = 7 \times 10^6 \text{ rad. s}^{-1}$$

$$\Phi_N = 2 \times 10^{-19} \text{ Wb} / \sqrt{\text{Hz}}$$

$$\Phi_B = 1.2 \times 10^{-20} \text{ Wb} / \sqrt{\text{Hz}}$$

$$L_S = 4 \times 10^{-10} \text{ H}$$

$$k = 1.38 \times 10^{-23} \text{ J / } ^\circ\text{K}$$

$$\mathcal{M} = 2 \times 10^{-7} \text{ H}$$

The constants as specified by Eqn. 3.52. are now evaluated.

$$A = \frac{8 m \omega_n k}{Q_n} = 1.4 \times 10^{-25}$$

$$B = \frac{16 m^2}{C^2} \left\{ \frac{\Phi_n^2}{M^2} + \frac{4 k T_e \omega_n^2 C}{Q_e \omega_e} \right\}$$

$$1.6 \times 10^{23} \{ 10^{-24} + 24 \times 10^{-38} \} = .16$$

$$C = \{ 5.7 \times 10^{-47} + 6.4 \times 10^{-45} \} = 5.7 \times 10^{-47}$$

As before the contribution of the capacitor sensing circuit to the backward fluctuation term is neglected.

Equation 3.55. becomes (using  $df = 10^3 \Rightarrow \left(\frac{V}{d}\right) \sim 7.2 \times 10^{12}$ )

$$\begin{aligned} F_n^2 &= (A T_n + 2 \sqrt{BC} \times 10^3) 10^3 \\ &= (1.4 \times 10^{-25} T_n + 6.0 \times 10^{-24}) 10^3 \end{aligned}$$

Assuming that  $T_n$  is not greater than room temperature

$$F_n^2 = 6 \times 10^{-18} \quad \text{and using Eqn. 3.37}$$

$$h = 7.8 \times 10^{-18}$$

Note: 1) The very high  $\left(\frac{V}{d}\right)$  required to achieve the optimum coupling indicates that a different system should perhaps be employed. For instance the type planned by Fairbank et al, although similar in principle to the system analysed might be technically more easily achieved.

2) The analysis has been performed for a SQUID operating at an RF bias frequency of 20 MHz, however from the equations it seems likely that with a high pump frequency the sensitivity will increase, (assuming that the amplifier noise does not increase excessively at

higher frequency). The use of high frequency SQUIDS coupled to perhaps a Maser amplifier have been proposed and it seems a possible system to achieve an improvement in detector performance.

### Conclusions

The results may be summarised as follows:-

#### The Sensitivity of the Preceding Detectors in Terms of the Gravitational Wave Amplitude

	The 5 tonne Aluminium Bar	The 40 kg Sapphire Crystal
Parametric system with r.e.t. amplifier	$4.1 \times 10^{-19}$ Thermal noise dominates above 3 K	$1.7 \times 10^{-18}$ Thermal noise not dominant at room temperature
SQUID sensor	$3.8 \times 10^{-18}$ Thermal noise dominates above 220 K	$7.8 \times 10^{-18}$ Thermal noise not dominant at room temperature

For the systems considered here the SQUID sensor does not appear to be as good as the r.e.t. amplifier. The high  $(\frac{V}{d})$  required for optimum coupling of the SQUID could probably be reduced by using a parametric system similar to that described for the r.e.t. amplifier.

It should be pointed out that in some of the cases considered the optimum coupling cannot be achieved in practice\*, because of limitations in field strength. For this situation some of the equations and conclusions presented above do not apply. In these cases the loss in sensitivity may be minimised by reducing the bandwidth and decreasing the detector temperature.

In the calculations it was assumed that the noise due to the capacitor bias circuit was neglected in order to find the noise introduced by the SQUID. The backward fluctuation

\* This is almost certainly the situation for the two detectors using the SQUID sensor.



term was a limiting factor and the value of it has not previously been considered in the literature. However, recent work by others seems to agree with the model presented for the backward flux.

A Maser system was also considered by an analysis similar to that presented above. Results of such an analysis indicated that it was an extremely promising system with a sensitivity of about  $5 \times 10^{-20}$  with the detector cooled to a few degrees kelvin.

Due to the importance of backward fluctuation it was thought to be worthwhile to analyse the Glasgow split bar detectors. The backward fluctuation is produced by the amplifier current noise component being fed onto the transducers and causing a force on the detector. The increase in the mean energy of the detector, caused by the backward force, was estimated not to be in excess of about 30% in one detector and to be less than 10% in the other.

The assumption, used in Chapter 5, that the detector energy was equal to  $kT$  was not changed, but this result should be borne in mind.

## Chapter 4

### The Consideration and Implementation of Various Techniques to extract Continuous Signals from Gravitational Radiation Detectors

A characteristic of all searches for gravitational radiation is that the expected signals may be buried deep in the detector noise. In this chapter various aspects of the problem of detecting continuous signals from gravitational radiational detectors are studied. The methods of cross correlation and spectrum analysis have been implemented using an on-line digital computer, and details of the systems are presented.

The type of analysis employed is very dependent on the expected form of the signal. If the signal is expected to be sinusoidal of unknown frequency, Fourier transform analysis is a good method of detection, and for two detectors this may be extended to cross spectrum analysis. If the period of the expected repetitive signal is known the method of cyclic averaging is a good method to employ, as in general it may be more easily implemented than the full spectrum analysis and also the time of computation will be less.

The method of cross correlation is useful in detecting signals in noise both as an intermediate stage in computing the power spectrum and as an analysis technique in its own right.

### The Cross Correlation Method of Detection and its Implementation

Cross correlation is a useful technique for extracting any common signal which may be present in two independent noise sources. By comparing the two signals in the way prescribed by the method of cross correlation any common signal is enhanced, whereas independent signals tend to average to zero. The cross correlation function is defined as:-

$$R(\tau) = \frac{1}{T} \int_0^T x(t) y(t-\tau) dt \quad -(4.1.)$$

where

$\tau$  - delay

$T$  - length of experimental run

$x(t), y(t)$  are the two signals

However as the cross correlation was performed by digital computer the discrete function is more relevant.

$$R(k \Delta\tau) = \frac{1}{N} \sum_{n=0}^{N-1} y(n\tau) x((n-k)\tau) \quad \text{for } N \gg k \quad -(4.2)$$

In the search for continuous gravitational radiation the most important feature was that of the improvement in signal to noise ratio. Other properties such as the shape of the function were not as important in this case.

A theoretical study of the sensitivity of the cross correlation technique has been performed by several people.<sup>44,47,50</sup> The result of such an analysis is that

$$\frac{R}{\sigma} = \sqrt{\pi B T} \left( \frac{S_1}{N_1} \right)^{1/2} \left( \frac{S_2}{N_2} \right)^{1/2} \quad -(4.3.)$$

where

$B$  - Bandwidth

$T$  - Integration time

$\left( \frac{S}{N} \right)$  - Power signal/noise ratio

$\sigma$  - Standard deviation of  $R$ .

Note: The factor  $\pi$  is for a 'tuned circuit' bandwidth shape. A factor of 2 should be used for a square bandwidth.

To compute the discrete cross correlation function the two signals have to be sampled at regular intervals and the rate of sampling is dictated by the following theorem:- Any signal which is band-limited to an upper frequency limit  $F$  Hz is completely specified by stating its values at a rate of  $2F$  per second or faster. (Nyquist's Theorem). In fact once these values have been obtained the original signal may be reproduced by the superposition of many sinc ( $t$ ) functions related to the sampled values. (Shannon's Theorem).

As discussed in the next chapter the cross correlation technique has been used to search for continuous gravitational radiation in a frequency range from 910 Hz to 1070 Hz. To sample this data one has to use a sampling rate of about 2 kHz. As the data of interest is from 910 - 1070 Hz. one could multiply the signal by a sine wave at a frequency of 910 Hz and then low pass filter to a frequency of 170 Hz (equal to the bandwidth) thus passing the difference frequencies and attenuating the sum. This would mean that the sampling frequency would only then need to be  $2 \times 170$  Hz

However in the search for continuous gravitational radiation no pre-multiplication was performed and this meant that the sampling rate had to be high. It was desirable that the cross correlation was performed in real time thus demanding that the programme was able to compute

the cross correlation function within one sample interval. The speed required posed a problem, and even by programming in machine code the computing time would have been too long. However if the cross correlation is performed on the polarity of the two signals, only comparison is required compared to full multiplication, and this means that the programme takes less time.

In conditions of low signal to noise ratio the loss in sensitivity is quite small and indeed may be shown to be equal to  $\left(\frac{2}{\pi}\right)^{44}$ . In fact the normalised correlation function  $R'(\tau)$  obtained by using the polarity of the signals alone is related to the full normalised correlation function  $R(\tau)$  by the following relation.<sup>48,49)</sup>

$$R'(\tau) = \frac{2}{\pi} \sin^{-1} R(\tau) \quad -(4.4.)$$

It was decided that the loss in signal to noise ratio was justified by the speed increase; in the search for continuous gravitational radiation the speed increase obtained by using the one bit technique proved vital.

#### The Method of Implementation

A digital computer system combined with a small interface was used to perform the cross correlation of signals.

The type of computer used was a Data General Corps. Nova 1220 with 24K words of memory. This machine uses 16 bit words and has four accumulators to perform arithmetic and logical instructions in a time of  $1.35 \mu s$ .

The interface into the computer consisted of circuitry to determine the polarity of the signal and then

to store this data in a D type flip flop. This data was then entered into the computer using a 10 bit A.D.C. An A.D.C. was not essential as it was only used to sample a logic level, however it offered the easiest implemented choice. The details and circuitry of the interface are discussed later.

#### The Cross Correlation Programme

The value of the one bit cross correlation function at any one delay point is computed by comparing the sign of the signal from one source with the sign of the other signal measured  $\gamma$  seconds previously. The number +1 is added to this delay point if the two signals have the same polarity and -1 if they differ.

To produce this delay ranging from 0 secs to  $m\gamma$  secs (where  $m$  is the number of points in the delay curve and  $\gamma$  the time between samples)  $m$  past values for one signal have to be stored. On sampling the two signals A and B the store of signal A is updated and all the values in the store are compared to the one newly obtained for signal B.

The store of past values had to be updated and compared to the other channel in the fastest possible time. The method chosen for this was to store the polarity data as single bits in one of the computer accumulators thus avoiding time wasted in using the computer memory. This meant that 17 delay points could be computed (present value + 16 bits stored in accumulator). The operation of examining and updating the store was to shift the accumulator right putting the right most bit into the carry

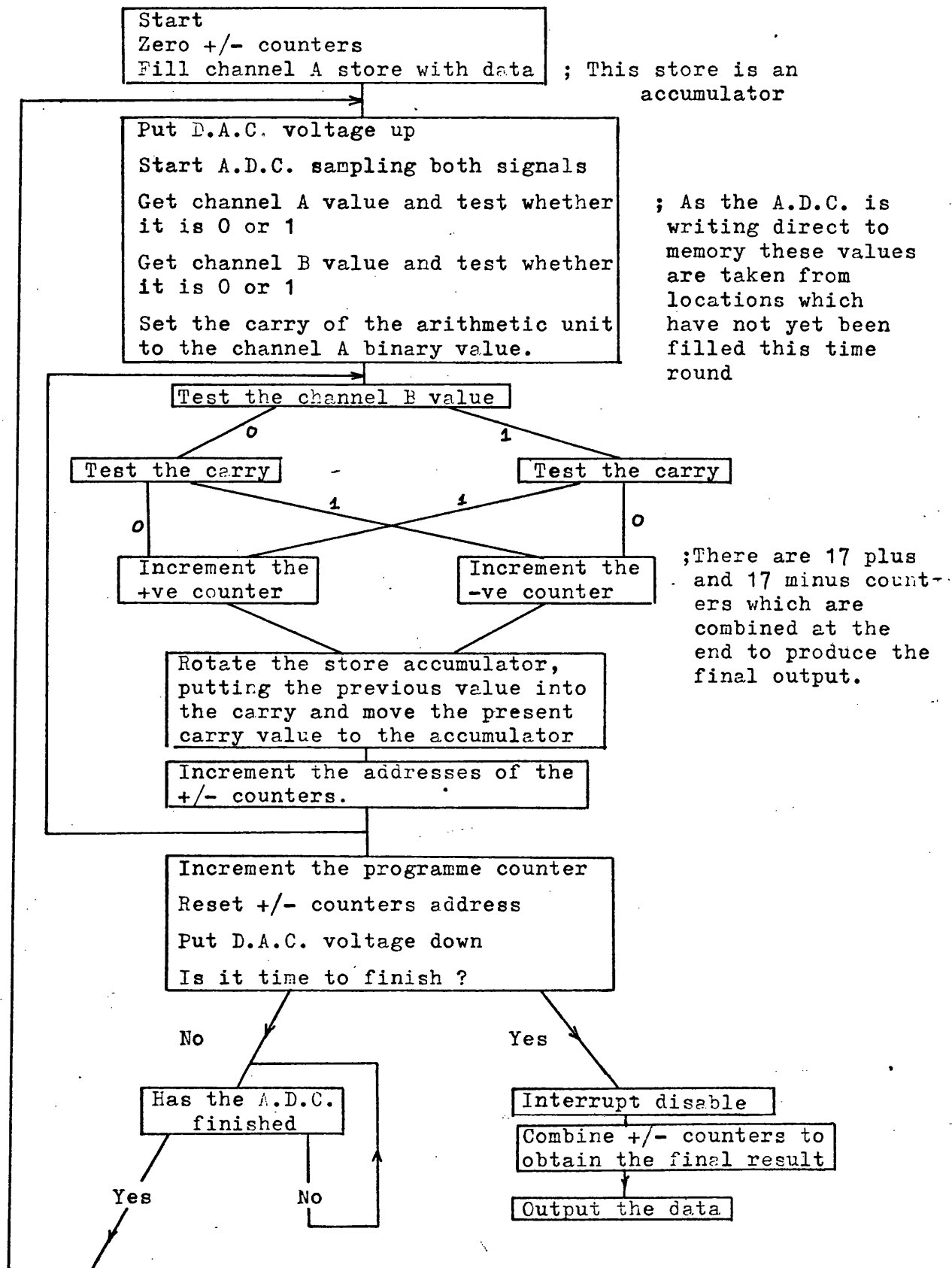
and examining or setting it to the desired value. The operation of the programme is easiest explained by studying Fig. 4.1

The A.D.C. is designed to work in such a way that the data is transferred directly to memory without having to be passed through intermediate accumulators. This method of transfer is called the data channel mode. The sampling rate of the A.D.C. was controlled by a temperature regulated crystal oscillator. To operate the programme in real time one had to ensure that all the computation was completed before new values were read. However the delay between completion of the programme and reading new values should be as short as possible.

To determine this timing as accurately as possible the D.A.C. was used to indicate when the programme was running and then the sampling rate was set in accordance with this information. It was then found by using this technique that the maximum clock rate allowable was 2 kHz, which incidentally was barely high enough to perform the search for continuous gravitational radiation.

#### The Interface

As the computer A.D.C. equipment consists of a multiplexer connected to a single A.D.C., problems in using this for cross correlation analysis are encountered. Firstly for the cross correlation function both signals should be sampled together, but as the input channels are multiplexed this is not possible. Secondly cross-talk between channels was present and hence undesirable cross correlation. The best method to eliminate these problems



THE CROSS CORRELATION PROGRAMME

Fig. 4.1.



was to construct a simple interface. The interface consisted of two discriminators with their thresholds set at 0 volts; this system produces logic levels depending on the polarity of the incoming signals. The binary signals are then fed onto the inputs of two D type flip flops and on the positive edge of a clock pulse the data at the input is passed to the output and stored. The computer was then able to read in the binary levels stored in the flip flops sequentially and as this was now a relatively large binary level, cross-talk was no longer a problem. The clock for the flip flops was the D.A.C. signal used to determine the programme speed and has been previously mentioned. It was ideal for this purpose as the D.A.C. level was put to 5 volts on the start of the programme and down to 0 volts when the programme had finished.

The programme was tested in many ways. For the same signal in both channels the value at the zero delay was indeed equal to the number of samples taken, and for a sinusoidal input on both channels (after the renormalisation) a sine wave was obtained for the cross correlation function.

With uncorrelated noise fed into both channels the cross correlation function was checked for any effect, and with due regard to the elimination of mains hum no correlation was apparent. The signal to noise ratio at the output was compared to that of the input and using the formula for expected improvement (Eqn. 4.3.) an agreement between theory and experiment was obtained.

This cross correlation system has already been used

in an experiment on the detection of gravitational radiation and this is discussed in detail in Chapter 5.

### The Fourier Transform

The Fourier transform of a signal is given by the following transformation

$$X(f) = \int_{-\infty}^{\infty} x(t) e^{-i2\pi ft} dt \quad -(4.5)$$

and

$$x(t) = \int_{-\infty}^{\infty} X(f) e^{i2\pi ft} df \quad -(4.6.)$$

However as the Fourier transform was carried out by a digital computer the discrete Fourier transform (as an estimate to the Fourier transform) is more relevant.

$$X(j) = \frac{1}{N} \sum_{k=0}^{N-1} x(k) e^{-i2\pi jk/N} \quad -(4.7.)$$

and

$$x(k) = \sum_{j=0}^{N-1} X(j) e^{i2\pi jk/N} \quad -(4.8.)$$

The algorithm used to calculate the  $X(j)$ 's, both real and imaginary parts, from the  $x(k)$ 's was the one described by Cooley and Tukey<sup>51-54)</sup> and it is called a fast Fourier transform (FFT). The algorithm is particularly efficient as it reduces the number of operations, for an  $N$  point transform, from  $N^2$  to approximately  $N \log_2 N$ . The operation of the algorithm is as follows:-

Using Cooley's notation the FFT algorithm involves evaluating the expression

$$\hat{X}(j) = \sum_{k=0}^{N-1} A(k) W^{jk} \quad -(4.9.)$$

$$\text{where } W = e^{\frac{2\pi}{N}i} \quad (i = \sqrt{-1})$$

From Equation 4.7.

If the forward transform is required

$$\hat{X}(j) = X^*(j) \quad \text{and} \quad A(k) = \frac{1}{N} x^*(k)$$

The algorithm is used when the number of points (N) in the transform equals an integral power of 2 (i.e.  $N = 2^m$ ), and for this example the number of points is set equal to eight.

$$j = 0, 1, \dots, 7 \quad k = 0, 1, \dots, 7$$

and may be represented as follows

$$j = j_2 \cdot 4 + j_1 \cdot 2 + j_0 \quad k = k_2 \cdot 4 + k_1 \cdot 2 + k_0$$

where  $j_2, j_1, j_0, k_2, k_1, k_0$  are binary numbers.

Equation 4.9. now becomes

$$\hat{X}(j_2, j_1, j_0) = \sum_{k_2=0}^1 \sum_{k_1=0}^1 \sum_{k_0=0}^1 A(k_2, k_1, k_0) W^{(j_2 \cdot 4 + j_1 \cdot 2 + j_0)(k_2 \cdot 4 + \dots + k_1 \cdot 2 + k_0)}$$

$$\text{Now noting} \quad W^{m \cdot n} = W^m W^n$$

$$\begin{aligned} & W^{(j_2 \cdot 4 + j_1 \cdot 2 + j_0)(k_2 \cdot 4 + k_1 \cdot 2 + k_0)} \\ &= W^{(j_2 \cdot 4 + j_1 \cdot 2 + j_0)k_2 \cdot 4} W^{(j_2 \cdot 4 + j_1 \cdot 2 + j_0)k_1 \cdot 2} W^{(j_2 \cdot 4 + j_1 \cdot 2 + j_0)k_0} \end{aligned}$$

Now looking at the individual terms and rearranging

$$W^{(j_2 \cdot 4 + j_1 \cdot 2 + j_0)k_2 \cdot 4} = \left[ W^{8(j_2 \cdot 2 + j_1)k_2} \right] W^{j_0 k_2 \cdot 4}$$

$$W^{(j_2 \cdot 4 + j_1 \cdot 2 + j_0)k_1 \cdot 2} = \left[ W^{8j_2 k_1} \right] W^{(j_1 \cdot 2 + j_0)k_1 \cdot 2}$$

Note that  $W^{8M} = 1$  for any integer

$$\hat{X}(j_2, j_1, j_0) = \sum_{k_0=0}^1 \underbrace{\sum_{k_1=0}^1 \sum_{k_2=0}^1 A(k_2, k_1, k_0)}_{A_1} \underbrace{W^{j_0 k_2 \cdot 4}}_{A_2} \underbrace{W^{(j_1 \cdot 2 + j_0)k_1 \cdot 2}}_{A_3}$$

Thus the equation may be evaluated by the following steps:

$$A_1(j_0, k_1, k_0) = \sum_{k_2=0}^1 A(k_2, k_1, k_0) W^{j_0 k_2 4}$$

$$A_2(j_0, j_1, k_0) = \sum_{k_1=0}^1 A(j_0, k_1, k_0) W^{(j_1 2 + j_0) k_1 2}$$

$$A_3(j_0, j_1, j_2) = \sum_{k_0=0}^1 A(j_0, j_1, k_0) W^{(j_2 4 + j_1 2 + j_0) k_0}$$

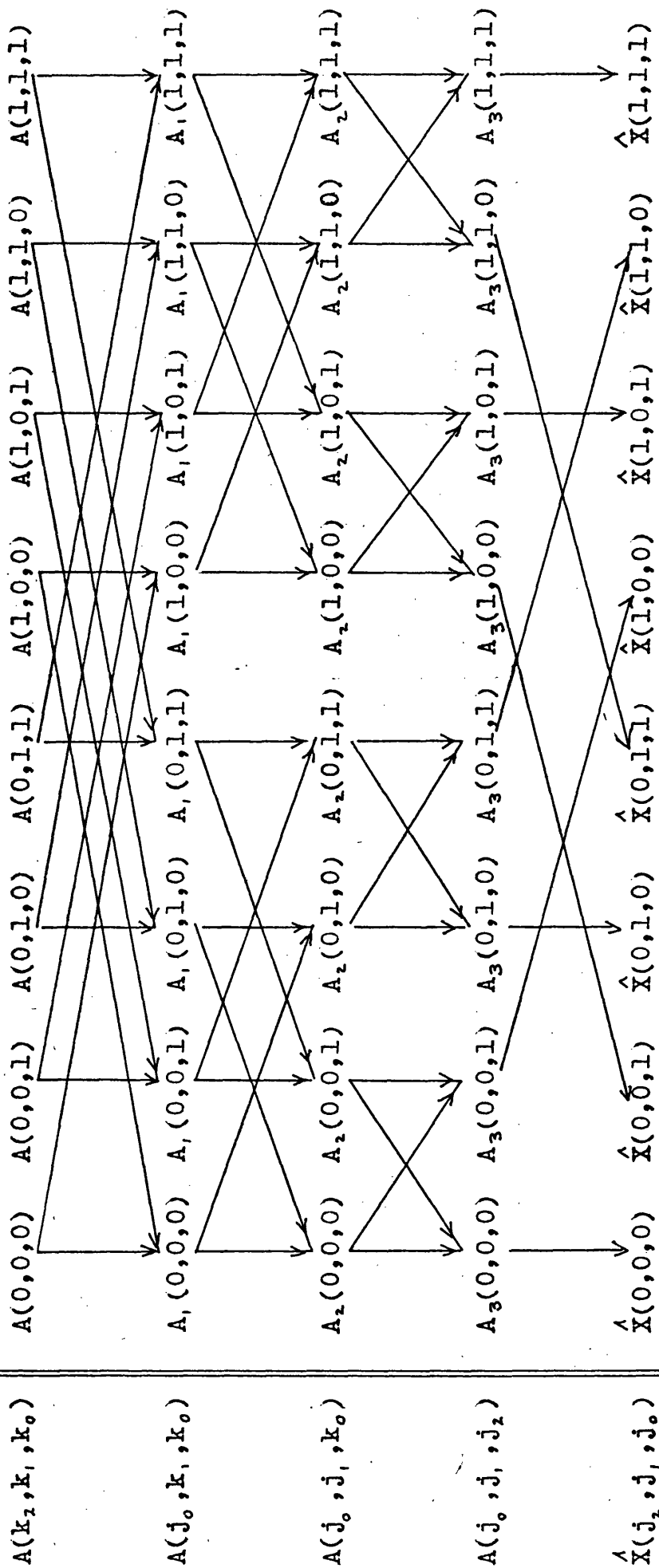
and

$$\hat{X}(j_2, j_1, j_0) = A_3(j_0, j_1, j_2)$$

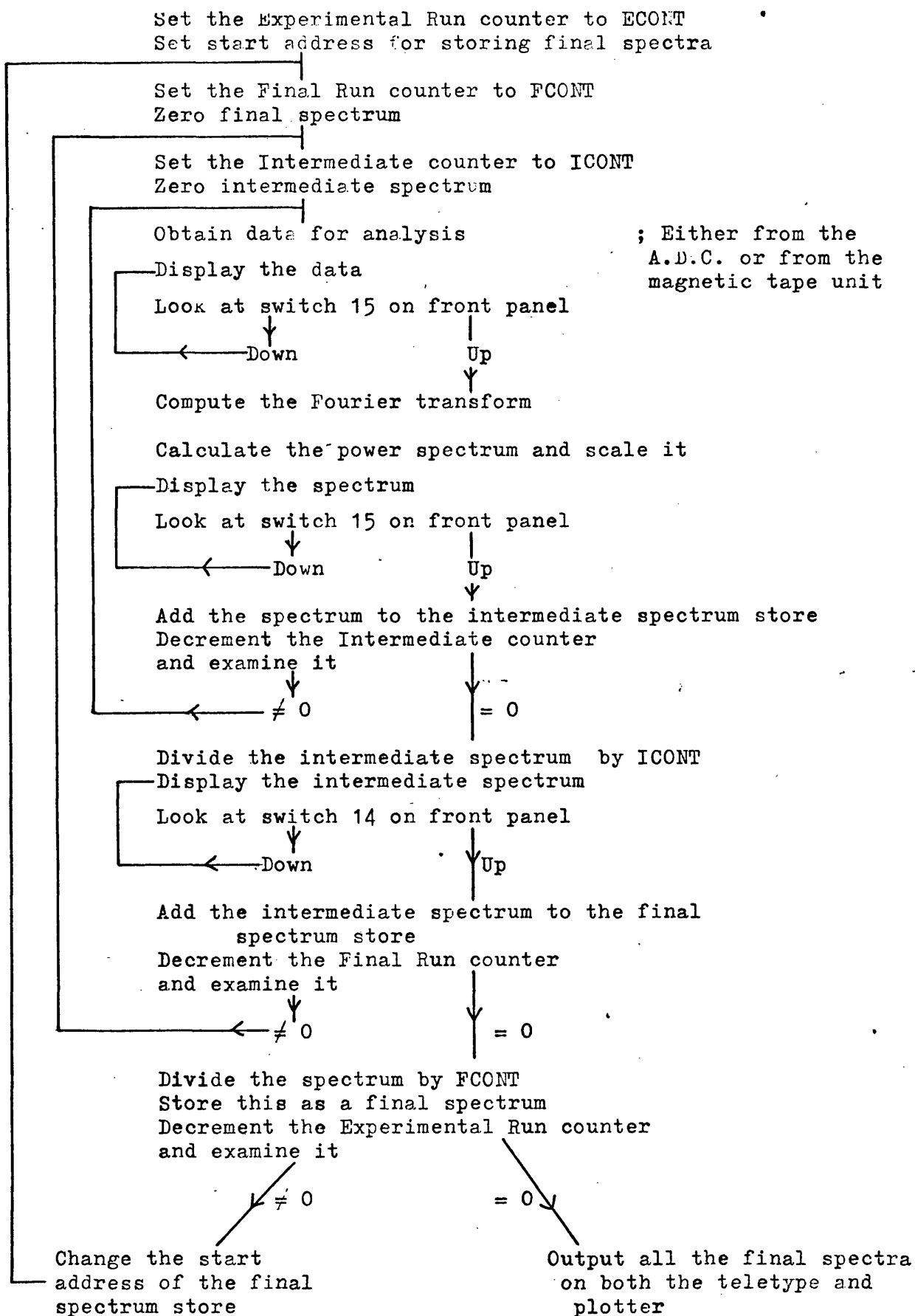
A summary showing the terms contributing to each sum is shown in Figure 4.2.

The programme used to compute the components of the transform was a standard one (D.G.C. User Group Programme 001 by S. Cox and R. Stutheit). This subprogramme was incorporated into a main programme designed to sample the A.D.C.'s and after the Fourier transform, compute the power spectrum, rescale the data, and integrate many power spectra.

The flow diagram of this programme is shown in Figure 4.3. An important feature of this programme was the method of scaling the data to avoid overflow and the subsequent integration of the spectra. The timing of the programme will be discussed later. The method of integrating the data was simply to add together  $m$  spectra and divide by the number  $m$ . Another method considered was that of the 'scale as necessary' method, where if the addition of subsequent data (to the store) would cause an overflow the incoming data and stored data were then scaled. This method has the advantage that overflow cannot occur but carries the disadvantage that the incoming data sets



A SUMMARY OF THE FAST FOURIER TRANSFORM ALGORITHM



THE PROGRAMME TO COMPUTE THE POWER SPECTRUM

are not all scaled equally. The basic danger of the chosen method was that overflow could occur, but this danger was averted in the following way.

On returning from the Fourier transform subroutine the output has been scaled so no overflow occurs, the scale factor being returned in an accumulator. As it is the squares of the numbers that are required, the data are made positive to ease the operation of squaring. The maximum number therefore is  $2^{15} - 1$  and this is then squared giving a maximum number of less than  $2^{30}$ , and this may be contained without overflow in a double precision computer word. The other component is also squared and added to this and nevertheless no overflow can occur.

The scaling factor returned from the subroutine is combined with a numerical factor specified by the operator. Therefore in addition to the scaling in the subroutine being cancelled, the spectrum may also be multiplied by a constant factor. This means that all the data sets are scaled equally in any one run. The output spectrum is then displayed using the D.A.C. onto an oscilloscope. The constant scale factor was then adjusted to ensure that the D.A.C. did not overflow. The factor could have been set at a 'worst case value' so as not to overflow the D.A.C. but this usually resulted in the spectrum being too small. This was due to the fact that for the worst case, one would assume all the power going into one frequency bin, however this was not the case. With the factor adjusted so as not to overflow the D.A.C. and as the D.A.C. is 10 bit, one is allowed 64 additions before any risk of

overflow. In fact a maximum number of 50 was allowed.

This was the basis of the method of integration.

Less than 50 spectra were added to give an intermediate spectrum. This spectrum was then divided by the number of additions and a number (less than 50) of these intermediate results were added to give a final spectrum. Memory was available in the computer to store 7 of these final spectra.

The method of output was to plot the spectrum on an x-y plotter by using a D.A.C. also a numerical output of the spectrum was obtained on a Teletype.

The Fourier transform was implemented and it was found that for a transform of 2048<sub>0</sub> points the time taken was about 3 seconds. Two spectral analysis programmes were in fact written and differed only in the way the data was obtained. One programme used the A.D.C. to obtain the data. One sample of 2048<sub>0</sub> points was read and the Fourier transform was then calculated and then another sample taken. If the sampling rate was allowed to be lower than 680 Hz the process of double buffering (filling one buffer with new data while operating on the other buffer) could have been used, however this restriction on operation was not imposed.

The other programme read the data from digital magnetic tape. The data had been written onto tape by a double buffering technique in order to preserve phase from one record to the next. The Fourier transform programme did not use the fact that phase was not lost between records but for the method of cyclic averaging this property is very important. In order to store the maximum amount of



data on a tape the data amplitude resolution was reduced to 8 bit, and with 9 track tape this leads to efficient storage.

#### Various Problems Encountered and their Solutions

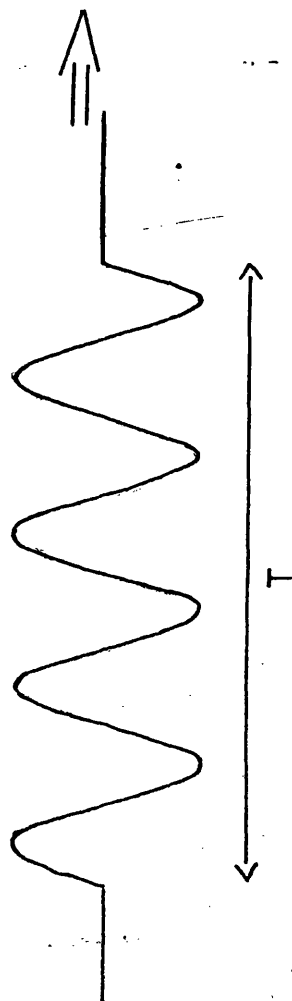
In sampling any signal the Nyquist criterion has to be followed. If this is not done and the signal frequency is allowed to be greater than half the clock frequency the effect of aliasing is introduced. This means that signals (and noise) greater than the Nyquist frequency are 'folded' back down into the power spectrum (from 0 to  $\frac{f_c}{2}$  Hz,  $f_c$  = clock frequency), thus giving a false power spectrum.

As only a finite length of data is used for the Fourier transform, the effect of leakage is introduced. This may be explained by considering a sine wave, which ideally would produce a delta function in the frequency domain. However, as the data is truncated after a time  $T$  the Fourier transform of the waveform in Figure 4.4. has to be considered and the resulting transform is a sinc ( $f$ ) function centred on the frequency of the sine wave.

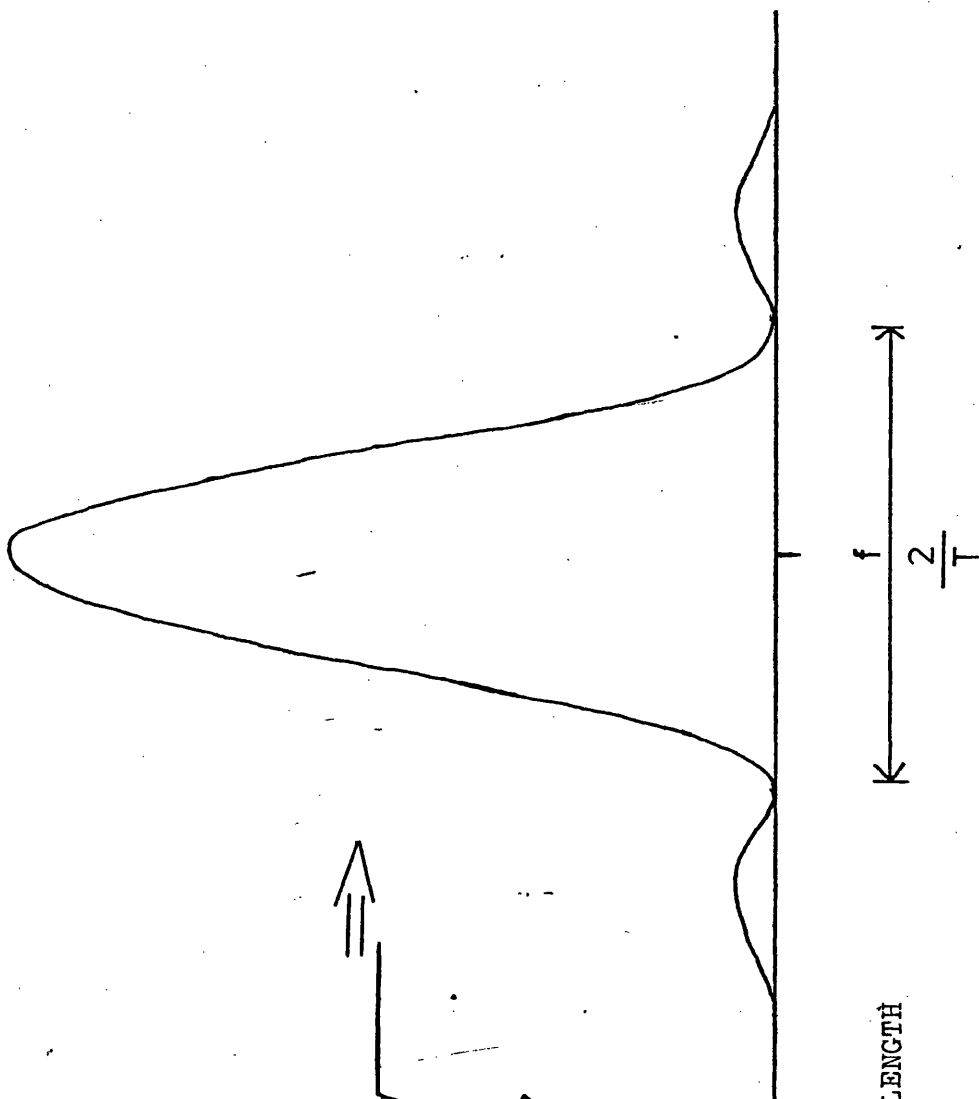
This leakage may be reduced by multiplying the data by a time shaping function such as a cosine bell or those described by Hanning<sup>55)</sup>. This time filtering was not done at present as it was felt that signal-noise ratio was important and not necessarily the spectrum shape.

The 'picket-fence' effect is caused by the fact that each spectral component may be considered as a bandpass filter and it is found that the power frequency response of the components is as follows, where the minimum amplitude is approximately  $\frac{1}{2}$  the maximum in terms of power.

A sinewave of frequency  $f$   
sampled for a time  $T$

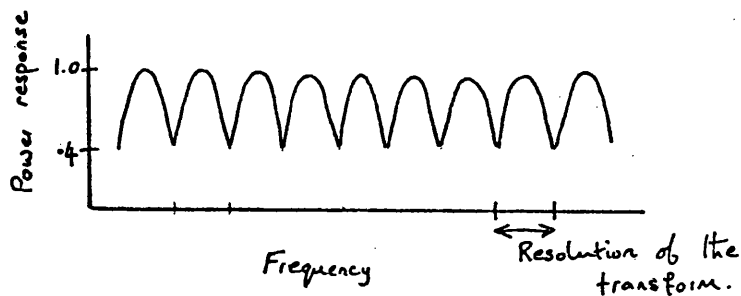


The power spectrum



THE POWER SPECTRUM OF A SINEWAVE OF FINITE LENGTH

Fig. 4.4.



It is shown in the literature<sup>52)</sup> that this effect may be reduced by padding the data with zero's and increasing the resolution of the transform.

To test for these effects and to evaluate the algorithm a sinusoidal signal was added to the noise, and the power spectral analysis applied to this. With no noise a sine wave of variable frequency was fed into the computer.

The sampling frequency was determined by a crystal oscillator at 1.25 kHz. and this meant that the frequency resolution of the transform was  $(1.25 \times 10^3 / 2048 \text{ Hz.})$ . A sine wave ranging from 202.0 Hz. to 202.8 Hz. in .1 Hz. steps was fed in and the results analysed. It was found that the power leakage did not exceed 6% and the picket fence effect did not reduce the power by more than 30%. The sine wave was then added to noise and the signal-noise ratio was measured before analysis, the improvement in signal to noise ratio after analysis was then evaluated and compared with theoretical predictions. The results agreed with the predicted values as estimated in the following section.

In order to decide whether a peak occurring in the power spectrum is caused by chance one has to decide on the value of the standard deviation. Many people<sup>55)56)</sup> have

pointed out that the probability density function of one bin in the power spectrum is that of a  $\chi^2$  distribution of order 2. In a  $\chi^2$  distribution of order  $k$  the standard deviation equals  $\sqrt{(2/k)}$  x mean value. Therefore if only one transform is performed the standard deviation of one frequency value will be equal to its mean value. On the integration of  $m$  power spectra however the distribution will be that of a  $\chi^2$  distribution of order  $2m$  and the standard deviation will be  $\sqrt{\frac{2}{2m}} = \sqrt{\frac{1}{m}}$  times the mean value. If the noise power of the incoming noise is  $P_n$  the average power in each frequency bin (assuming the noise is white) is  $P_n / n$  where  $n$  is the number of frequency channels. Therefore the fluctuation in any one channel is  $P_n / n\sqrt{m}$  where  $n$  is the number of channels and  $m$  the number of integrations. If the signal is sinusoidal then most of the power will appear in one frequency bin so one might expect to be able to detect a power equal to  $P_n / n\sqrt{m}$ .

Any one channel has a chance of exceeding a  $3\sigma$  level with a probability of .0013 (if the number of integrations exceed 30). The probability that any channel may exceed  $3\sigma$  = .0013 x  $n$ , ( $n$  = number of channels). It is therefore sensible to define a new level of significance where the probability that any one of the channels may show an effect is .0013 and this implies a probability of .0013/ $n$ , for each channel exceeding  $3\sigma$ . This probability may then be referred back to a new threshold in terms of the standard deviation for what one might call a ' $3\sigma$  effect'. A graph has been constructed to indicate the standard

deviation that should be set for each bin to give a certain final threshold for the spectrum. The graph is presented in figure 4.5 .

An interesting question is this : given a finite length of data for Fourier analysis, is the best thing to perform one long Fourier transform or integrate several shorter transforms? If the main objective of the experiment is to search for a sinusoidal signal (of constant frequency) in noise, then by the previous analysis it is best to perform one long transform. The estimate of the spectrum will not be very accurate as the standard deviation is of the same order as the mean. Due to the elemental bandwidth being smaller however the noise power in each bin will be reduced, and this more than compensates for the high standard deviation.

If the shape of the spectrum is also of importance a compromise should be reached between the number of integrations to reduce the standard deviation and the length of samples required still to give a high frequency resolution.

THE THRESHOLD TO SET FOR EACH CHANNEL OF A POWER SPECTRUM IN ORDER TO GIVE AN OVERALL EXPERIMENTAL THRESHOLD.

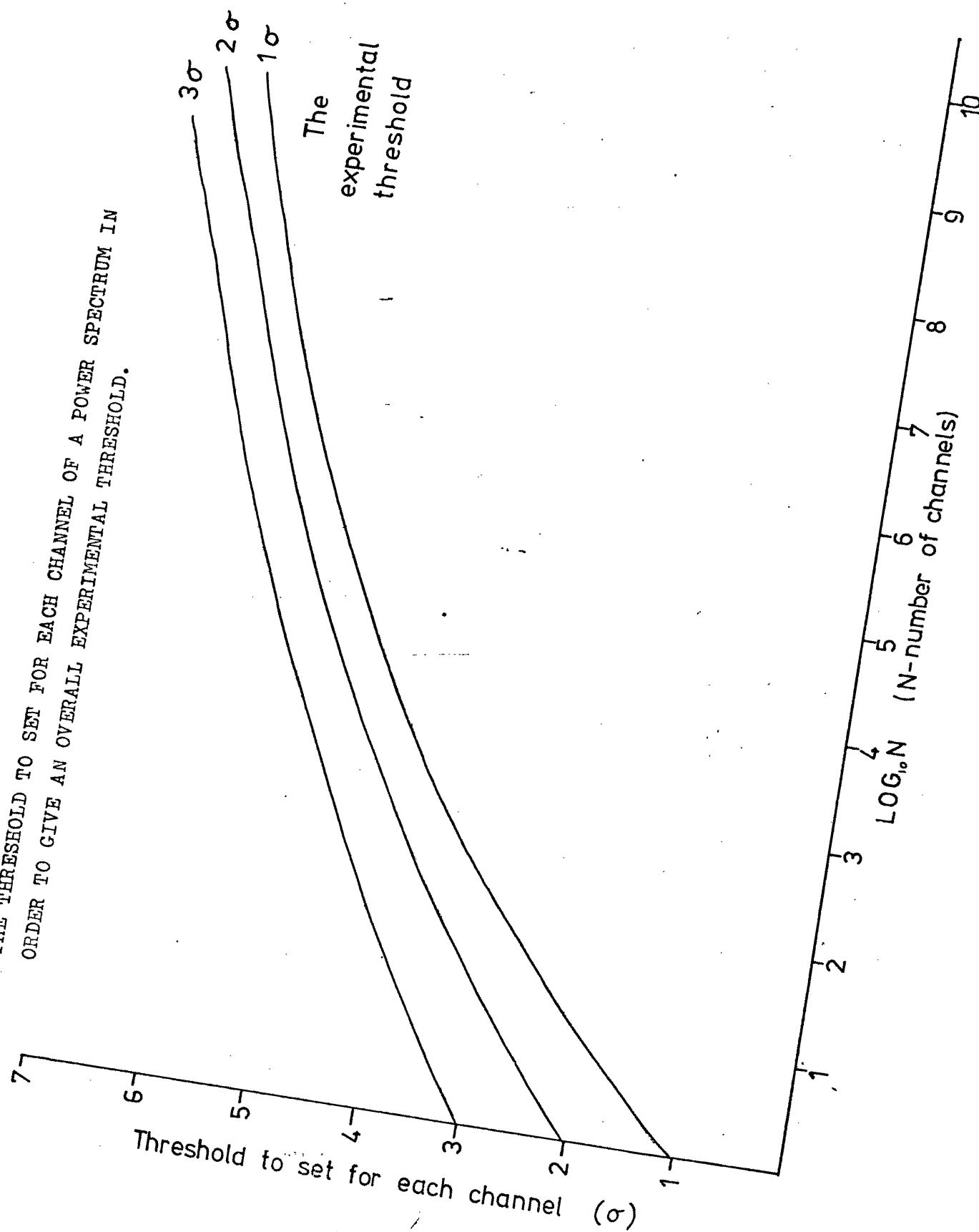


Fig. 4.5.

## Chapter 5

### A Search for Continuous Gravitational Radiation

The object of this experiment was to search for continuous gravitational radiation in a frequency region centred on 1 kHz. Possible forms of continuous radiation include both repetitive waveforms of unknown frequency and continuous random signals. Monochromatic signals in this frequency range might be expected from a rapidly rotating neutron star and broadband radiation could be produced by mass accretion into a black hole. However this has been discussed in a previous chapter. The theoretical predictions, of both strength and the lifetimes of monochromatic sources in this frequency range, indicate that it is unlikely that an effect should be observed at the sensitivity of this experiment. However, as this is a search at a higher sensitivity, (compared with other experiments), it is well worth looking for any effect.

As the nature of the gravitational radiation signals were not known, cross correlation between two detector outputs seemed the best method of detection. Other methods such as cyclic averaging and cross correlation with a standard waveform were ruled out as neither the form nor the frequency of the radiation was known. The experiment was performed in real time and this only allowed time for the cross correlation to be computed and not extended to a cross spectrum analysis technique.

#### The Detector Arrangement

The detection system used for this experiment was essen-

07.

tially the one already in use at Glasgow, searching for pulses of gravitational radiation. Basically one of these detectors consists of two aluminium cylinders linked by piezoelectric transducers to monitor changes in the separation of the two masses. As discussed previously, gravitational radiation impinging on this system would cause a change in the separation. Considering the response of the detection system to external forces one finds that the detector is highly resonant in nature. A technique of extracting the applied driving force from the resonant signal has to be devised and it is discussed later.

Two detectors were operational and they were spaced 50m apart with their axes North-South. The parameters of the detectors are presented in Figure 5.0. The signal from each detector then passes to a low noise field effect transistor amplifier and then through filters F1, F2 and F3. ( Figure 5.1.) Filter F1 is a bandpass filter set at a bandwidth of 160 Hz centred on 985 Hz. The bandwidth was calculated to be optimum for the detection of white noise signals. Filter F2 is an analogue computer which solves the equation relating the motion of an idealised detector to the applied driving force.<sup>59)</sup> ( Figure 5.2.) The filter therefore 'inverts' the resonant frequency response of the detector to give a fairly flat response over the system bandwidth of 160 Hz. ( Figure 5.3.) The signals from Filter F2 therefore represent the effective force signals that have been applied to the detector.

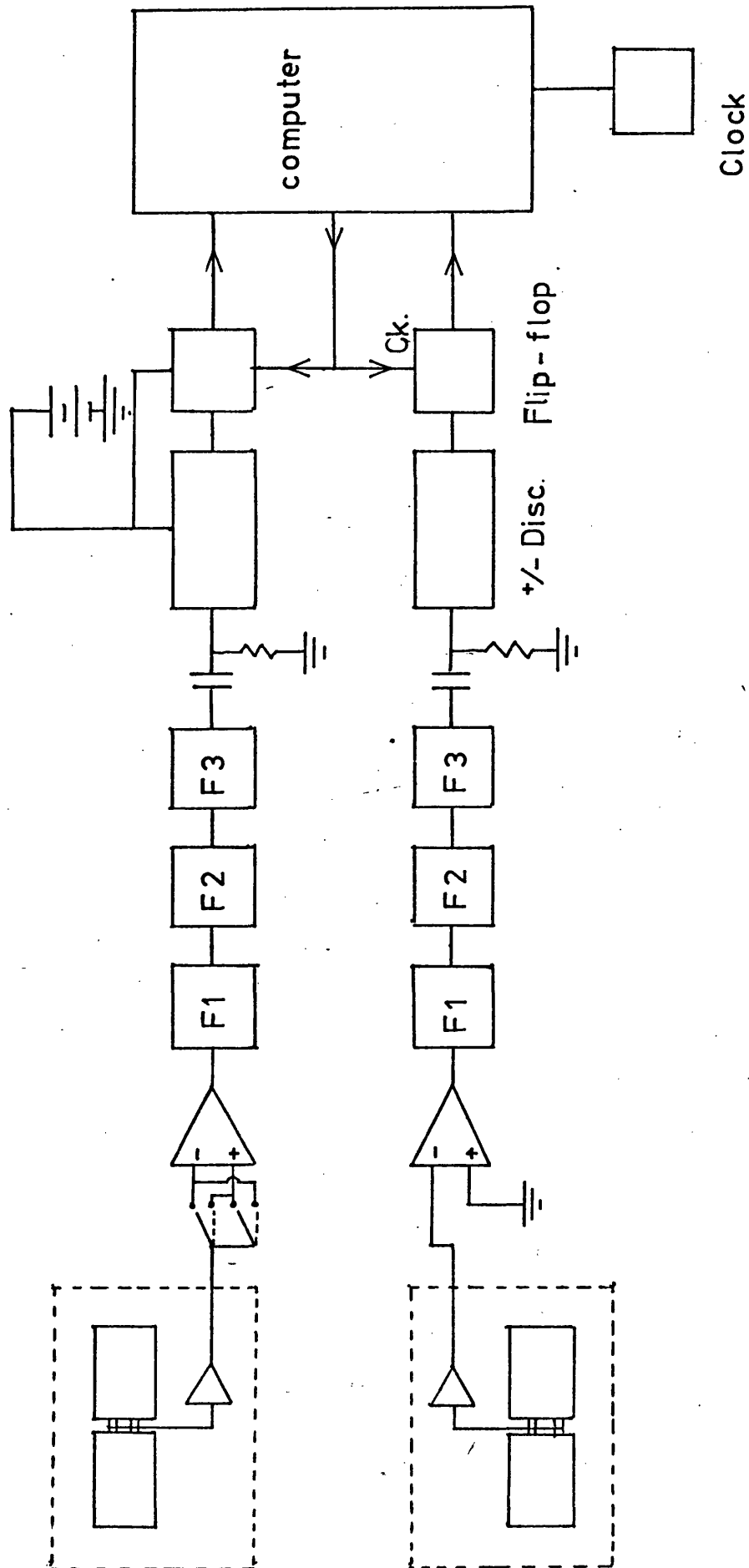
Filter F3 is a bandpass filter primarily to use the response of phase as a function of frequency to produce a



	Detector 1	Detector 2
Total length	1.55 m	1.55m
Total mass	300 kg	300 kg
Resonant frequency	1020 Hz	1120 Hz
Quality factor	1400	2200

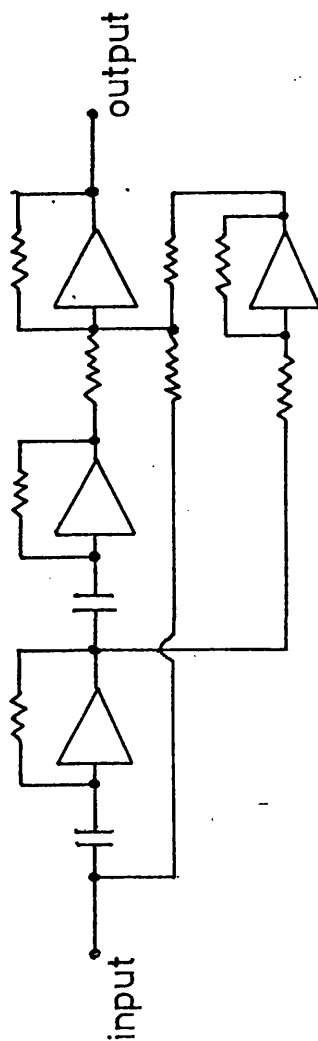
PARAMETERS OF THE DETECTORS AT GLASGOW

Fig. 5.1.



THE CROSS CORRELATION EXPERIMENTAL SYSTEM

# THE INVERSE FILTER



The idealised detector is as follows



The spring constant is such that the resonant frequency is  $\omega$ , i.e.  $k = m\omega^2$ . The equation relating the driving force to the displacement is

$$F = m \frac{d^2 x}{dt^2} + b \frac{dx}{dt} + kx$$

The circuit used to compute  $F$  from  $x$  is shown opposite.

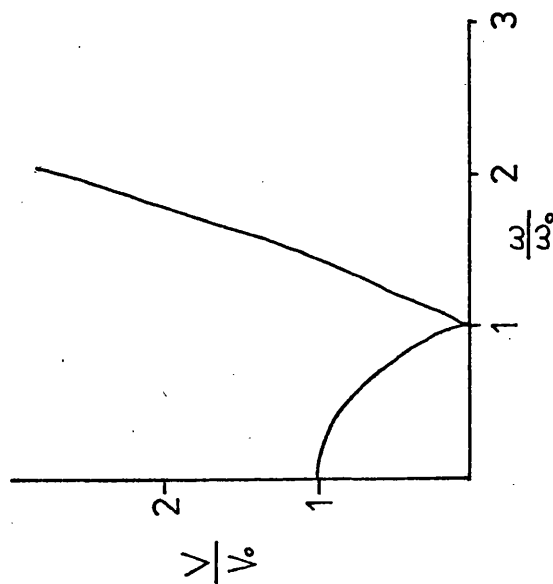
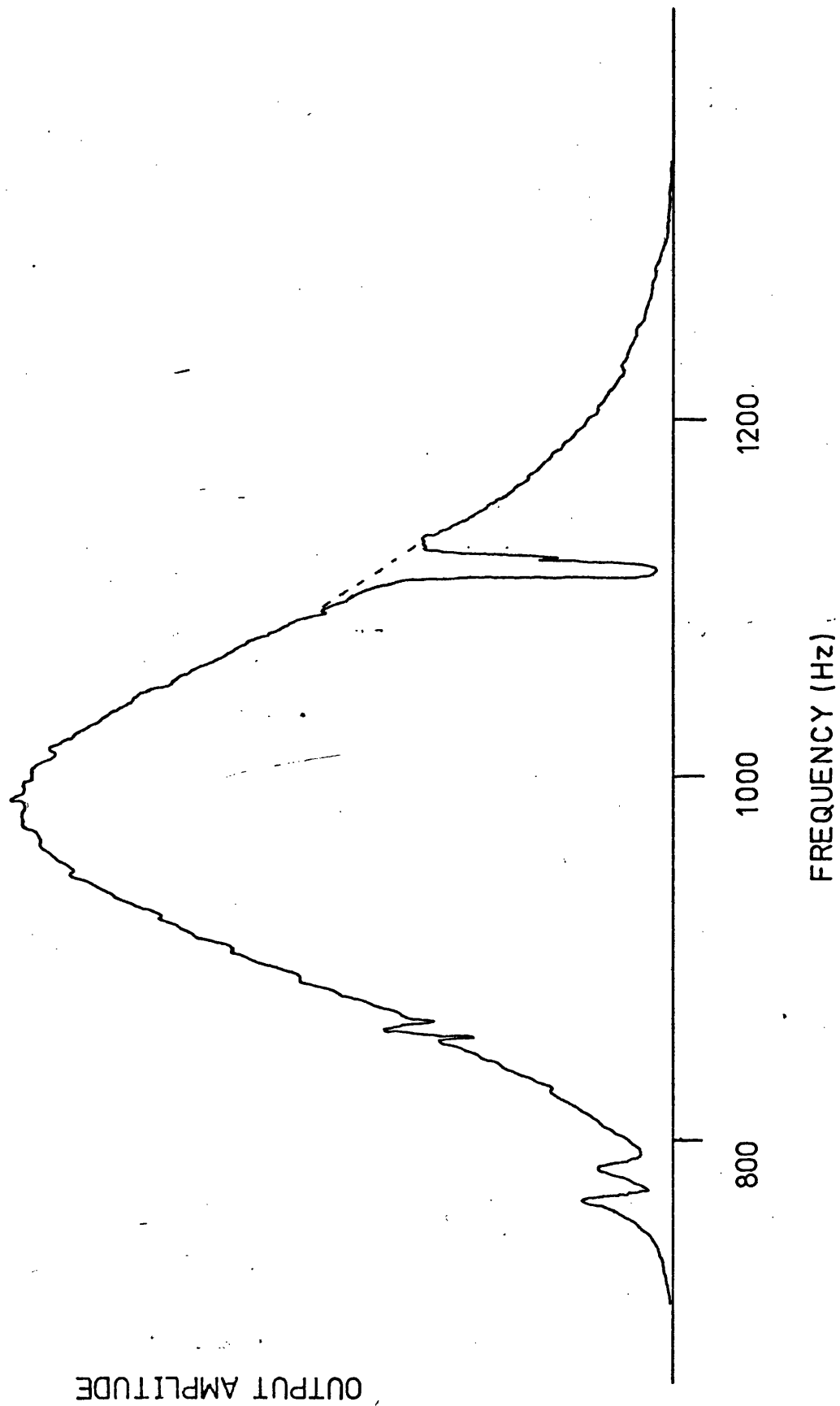


Fig. 5.2.

Fig. 5.3.

THE FREQUENCY RESPONSE OF THE CROSS CORRELATION EXPERIMENT



small time delay. This filter was then adjusted to ensure that signals common to both detectors would not have a phase difference at the output. The filter also proved useful in attenuating any mains hum introduced in the electronics as the correlation technique was very sensitive and only a small amount of hum was required to produce an effect.

These signals then pass into the interface previously discussed in Chapter 4, and the one bit cross correlation is performed on the two signals. During the runs the polarity of one of the signals was periodically reversed at the preamplifier. This experimental technique causes any effect due to correlation between the signals before the preamplifiers to change polarity. Any correlation introduced after the preamplifiers would produce an effect which did not change sign on reversal of the signal polarity. The individual runs were subsequently combined taking into account the polarity reversals to produce a final experimental run.

The cross correlation and its implementation have already been discussed in the previous chapter. The programme used was SFC 6 ( Figure 4.1 ) and this performed a one bit cross correlation on the filtered signals from the two detectors. The maximum possible sampling rate was limited by the length of programme to 2 kHz, and with this 17 delay points each 0.5 ms apart were obtained. Due to the fact that a sampling rate of 2 kHz was barely high enough to satisfy the Nyquist criterion (that the sampling rate is greater than 2x the highest frequency present), some runs were recorded on an analogue tape recorder and

slowed down by a factor of 4 before analysis by the computer.

### Calibration of the Experiment

The experiment was calibrated both for monochromatic and white noise force signals applied to the detector.

The method of producing a force was to apply voltage signals to capacitive end plates situated a small distance from each end of the detector. ( Fig. 5.4.). Assuming an ideal case, the force produced on the end of the detector by this system is:-

$$F = \frac{\epsilon_0 A v^2}{2 d^2}$$

and in the case of  $v = V + dv$

where  $V =$  large D.C. voltage

$dv =$  signal

$$F(t) = \frac{\epsilon_0 A V dv(t)}{d^2}$$

Typical values are  $A = 1.7 \times 10^{-2} \text{ m}^2$  and  $d = 2.3 \times 10^{-3} \text{ m}$

The end plates were therefore furnished with a D.C. voltage of 300 volts and added to this was a variable A.C. signal.

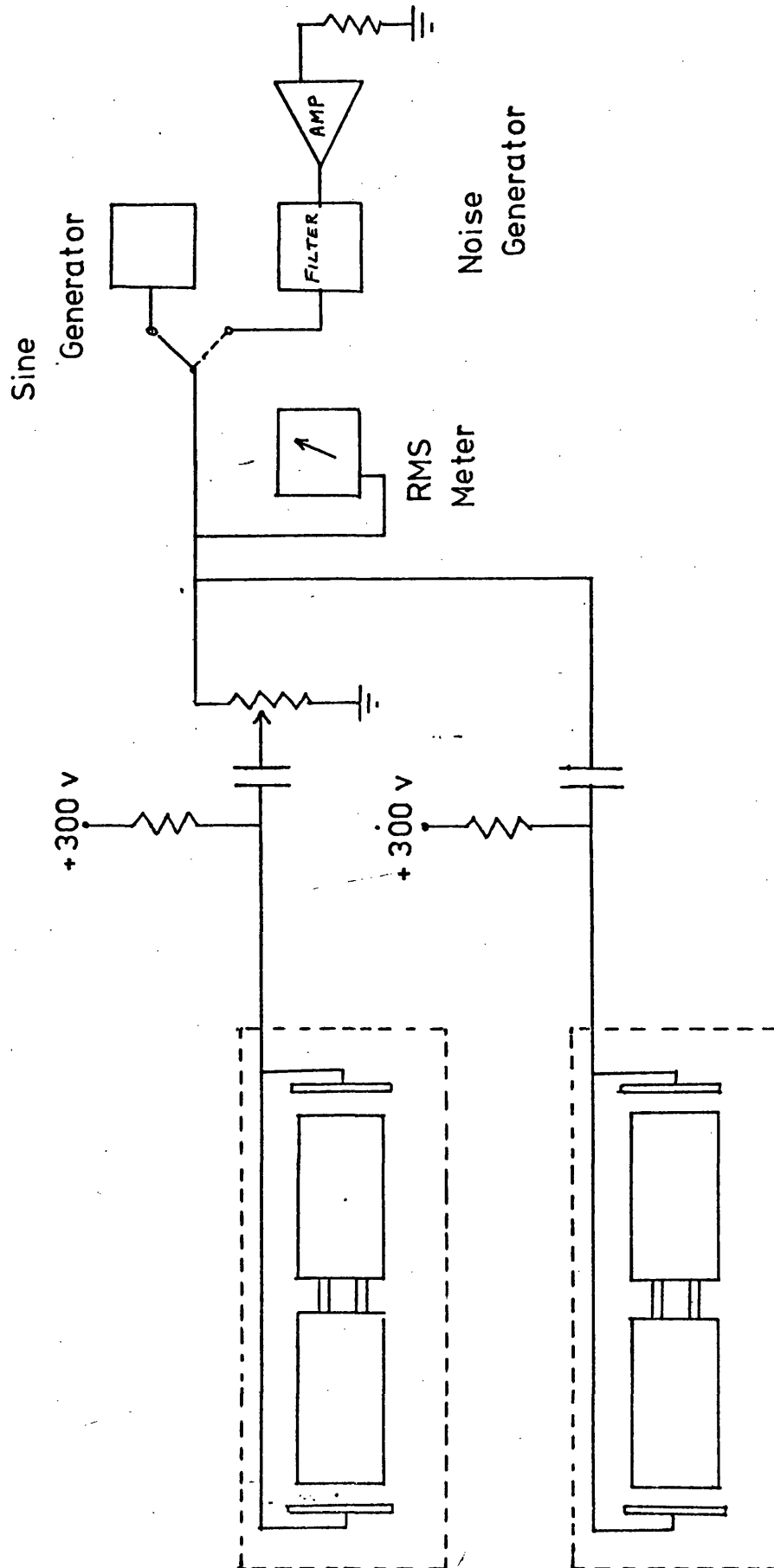
It may be of interest to note that a typical force used for calibration is of the order of  $3 \times 10^{-8} \text{ N}$ , (calculated from the 4 mV signal used in the sinusoidal calibration).

### The Calibration for Sinusoidal Signals

The principle of the calibration of sinusoidal signals was to establish a relationship between the size of the effect measured, by the cross correlation technique, and the incident monochromatic gravitational wave flux.

Fig. 5.4.

THE CALIBRATION SYSTEM



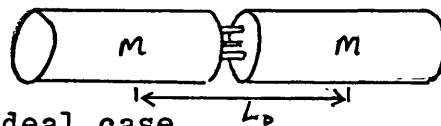
this was achieved in the following way:-

- 1) A sinusoidal force was applied to the detector at several frequencies, by use of the capacitive end plates, and a relationship between the RMS voltage and the size of the effect was found (after cross correlation).
- 2) The amount of energy deposited into the detector as a function of sinusoidal voltage applied, at the detector resonant frequency, was measured.
- 3) The amount of energy that would be deposited by a sinusoidal force on resonance was calculated and this force was related to the Riemann curvature tensor and hence to gravitational wave flux.

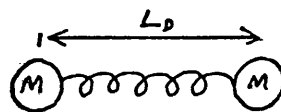
Using the information of steps 2 and 3 a relationship was found between voltage applied to the end plates and the gravitational wave flux. Combining this with the result of step 1 the final relationship is established.

The Theoretical Relationship between Gravitational Wave Flux at the Resonant Frequency and the Energy Deposited:-

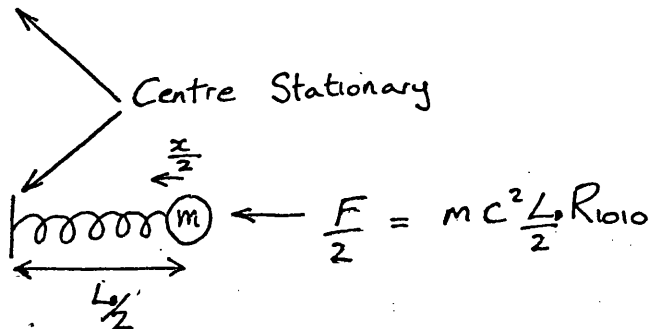
An Actual Detector



Considering the ideal case



Consider a half system





The equation of motion is

$$\frac{d^2 x}{dt^2} + \frac{\omega_m}{Q_m} \frac{dx}{dt} + \omega_m^2 x = \frac{F(t)}{m} \quad -(5.1)$$

Assuming  $F = F_0 \sin \omega t$

and solving the equation yields

$$x(t) = \frac{F_0 \sin \omega t}{\sqrt{(k - m \omega^2)^2 + (C_d \omega)^2}} \quad C_d = \frac{m \omega_m}{Q_m}$$

$$\text{at resonance } x = \frac{F_0 Q_m}{m \omega_m^2}$$

and in terms of  $R_0$  where  $R_{1010} = R_0 \sin \omega t$

$$x = \frac{L_p Q_m c^2 R_0}{\omega_m^2} \quad -(5.2)$$

The average energy of the harmonic system under consideration

$$\text{is } \mathcal{E} = \frac{1}{2} m \omega_m^2 X_{max}^2$$

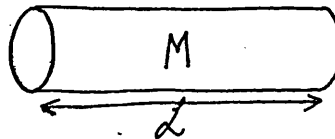
and substituting for  $x$  from Equation 5.2

$$\mathcal{E} = \frac{m \omega_m^2 L_p^2 Q_m^2 c^4 R_0^2}{4 \omega_m^4} \quad -(5.3)$$

The continuous aluminium cylinder has been analysed by

<sup>57)</sup> Piezella and <sup>58)</sup> Kafka among others and the result is:-

$$\mathcal{E} = \frac{4 M \mathcal{L}^2 c^4 R^2 Q_m^2}{\omega_m^2 \pi^4}$$



However  $M = 2 m$

$$\mathcal{L} = 2 L_0$$

to apply to the above case

$$\mathcal{E} = \frac{4 \times 2 \times 4 \times m L_0^2 c^4 R_0^2 Q_m^2}{\pi^4 \omega_m^2}$$

$$\mathcal{E} = \frac{32 m L_0^2 c^4 R_0^2 Q_m^2}{\pi^4 \omega_m^2}$$

$$= \frac{1}{3.04} \frac{m L_o^2 c^4 R_o^2 Q_M^2}{\omega_M^2}$$

-(5.3 A)

$$\text{cf. } \frac{1}{4} \frac{m L_o^2 c^4 R_o^2 Q_M^2}{\omega_M^2}$$

for the two masses

The actual system used lies between the idealised "dumb-bell" and the cylinder. As the numerical factor between the two extremes is small, the ideal dumb-bell will be adopted, as the model.

$$R_{RMS}^2 = \frac{2 \omega_M^2 \mathcal{E}}{m L_o^2 c^4 Q_M^2} \quad \text{-(5.4.)}$$

$$\mathcal{F} = \frac{c^3}{16 \pi G} \langle \dot{h}_+^2 + \dot{h}_x^2 \rangle$$

(Ref. Eqn. 1.7.)

Now assuming unpolarised radiation

$$\mathcal{F} = \frac{c^3}{8 \pi G} \dot{h}_{RMS}^2$$

To relate  $\mathcal{F}$  to  $R_{RMS}^2$

$$\text{as } \frac{1}{2} \ddot{h} = c^2 R$$

$$\text{and as } R_{1010} = R_o \sin \omega t$$

$$\dot{h} = \frac{2 c^2 R_o}{\omega}$$

$$\dot{h}_{RMS}^2 = \frac{4 c^4 R_{RMS}^2}{\omega^2}$$

$$\therefore \mathcal{F} = \frac{c^7 R_{RMS}^2}{2 \pi G \omega^2}$$

$$\Rightarrow \mathcal{F} = \frac{c^3}{2 \pi G \omega_M^2} \frac{2 \omega_M^2 \mathcal{E}}{m L_o^2 Q_M^2}$$

The equation relating energy deposited into the detector with equivalent unpolarised gravitational wave flux incident normally to the detector is

$$\mathcal{F} = \frac{c^3 \mathcal{E}}{\pi G m L_b^2 Q_m^2} \quad \text{-(5.5.)}$$

The Relationship between the Calibration Voltage Applied and the Energy Deposited. With no excitation signal the on line computer was used to measure the mean square value of the signals from the detectors after F1 and before F2. ( See Fig. 5.1.). This signal corresponds to the thermal motion of the detector, caused by the detector not being at absolute zero temperature. As only one normal mode of the detector is included in the bandpass filter F1 (see Fig. 5.3.), the signal corresponds to an average energy of  $kT$  in the detector. The number obtained from the computer for the mean square value of this signal therefore corresponds to an energy of  $kT$ .

With a D.C. voltage of 300 volts applied to the capacitive end plates an A.C. signal of known RMS value was added to this. ( Figure 5.4.). An oscillator was then tuned to the detector resonance and a few seconds were allowed for the detector to reach equilibrium. The mean square value of the signal from F1 was again measured by the on line computer. The RMS value of the A.C. sinusoidal signal was then changed and the detector allowed to come to equilibrium before measuring the new mean square value. These values were then compared to that of the  $kT$  energy. It should be noted that the A.C. signal was attenuated (by a

factor of .25 in voltage) before being applied to detector 2. The reason for this was to allow for differences in the calibration apparatus between the two detectors. It was adjusted to present to both detectors an equal effective gravitational wave flux. The relationship between RMS voltage, applied on resonance, and energy deposited is presented in Figure 5.5

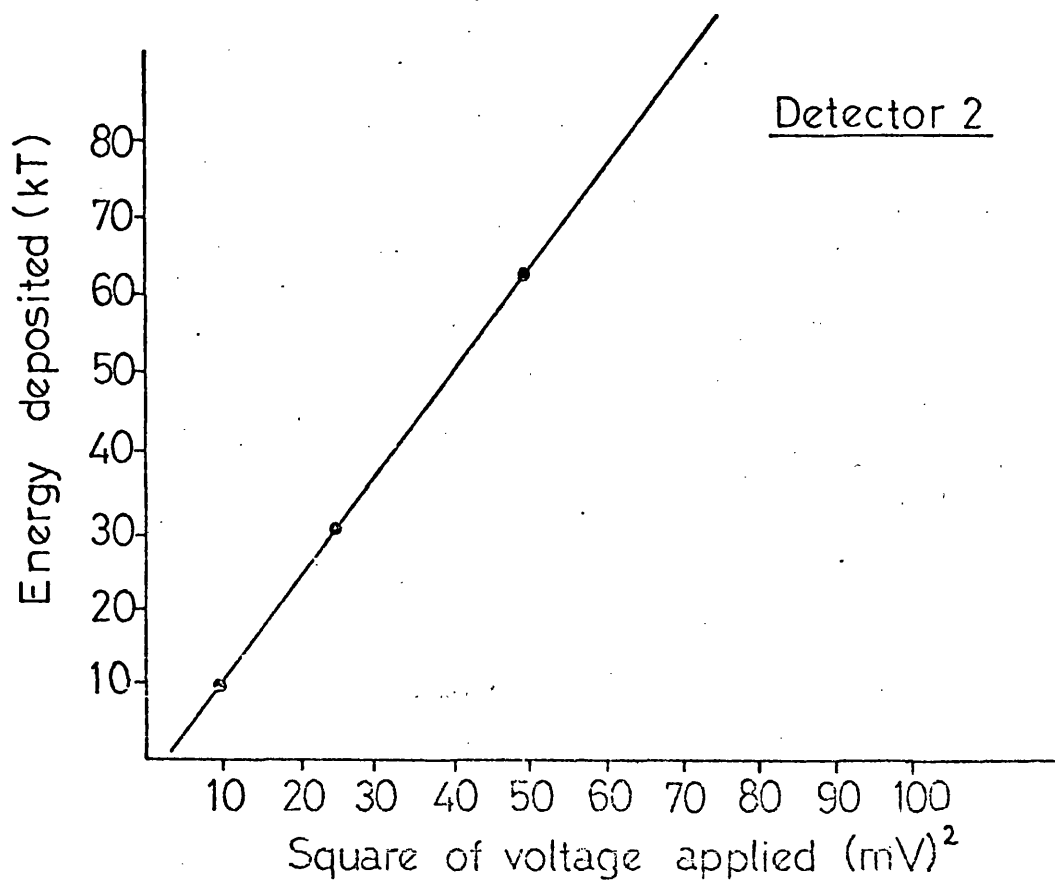
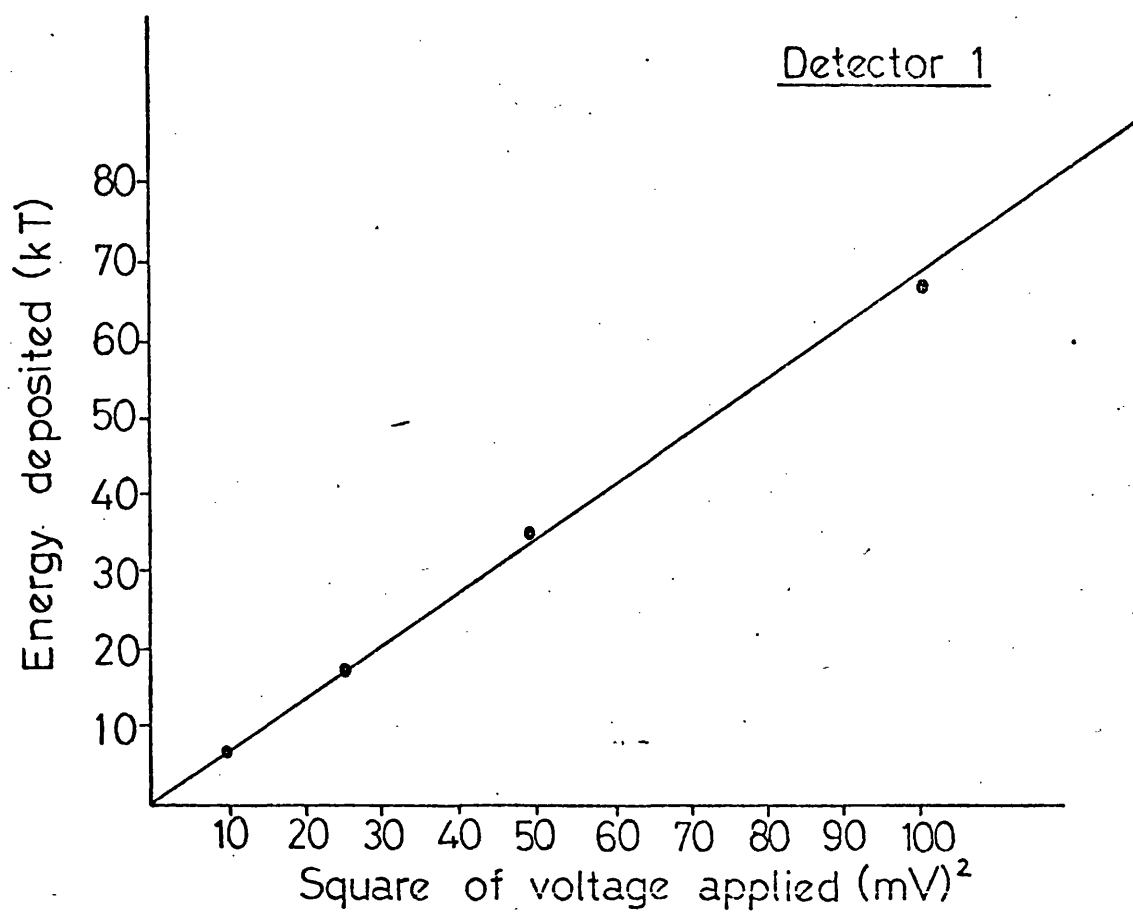
The Relationship between Calibration Voltage and Effective Gravitational Wave Flux. The calculation is done for a 4 mV signal as this amplitude was used in the next section.

From Fig. 5.5. it was concluded that a 4 mV signal, on resonance, deposited 11 kT into detector 1 and 19 kT into detector 2. Using Equation 5.5 this corresponds to an unpolarised gravitational radiation flux, in a normal direction, of  $3.2 \times 10^7 \text{ W.m}^{-2}$  incident on detector 1 and  $2.3 \times 10^7 \text{ W.m}^{-2}$  onto detector 2. The reason why these fluxes are not equal is that the attenuation of the calibrating signal to detector 2 was adjusted correctly for white noise (described later) and was not altered. However it is assumed for measurements of the sensitivity of the cross correlation experiment that a 4 mV RMS sinewave corresponds to a flux of  $2.8 \times 10^7 \text{ W.m}^{-2}$ .

The Size of Effect Measured as a Function of Sinusoidal Gravitational Wave Flux. The computer was then used to measure the cross correlation function with 4 mV into the calibration system, and the result is shown in Figure 5.6A, for a run lasting 52.5 minutes. The frequency of the sine wave was chosen to be 910 Hz, (off the resonant freq-

Fig. 5.5.

ENERGY DEPOSITED AS A FUNCTION OF SINUSOIDAL VOLTAGE AT THE  
RESONANT FREQUENCY

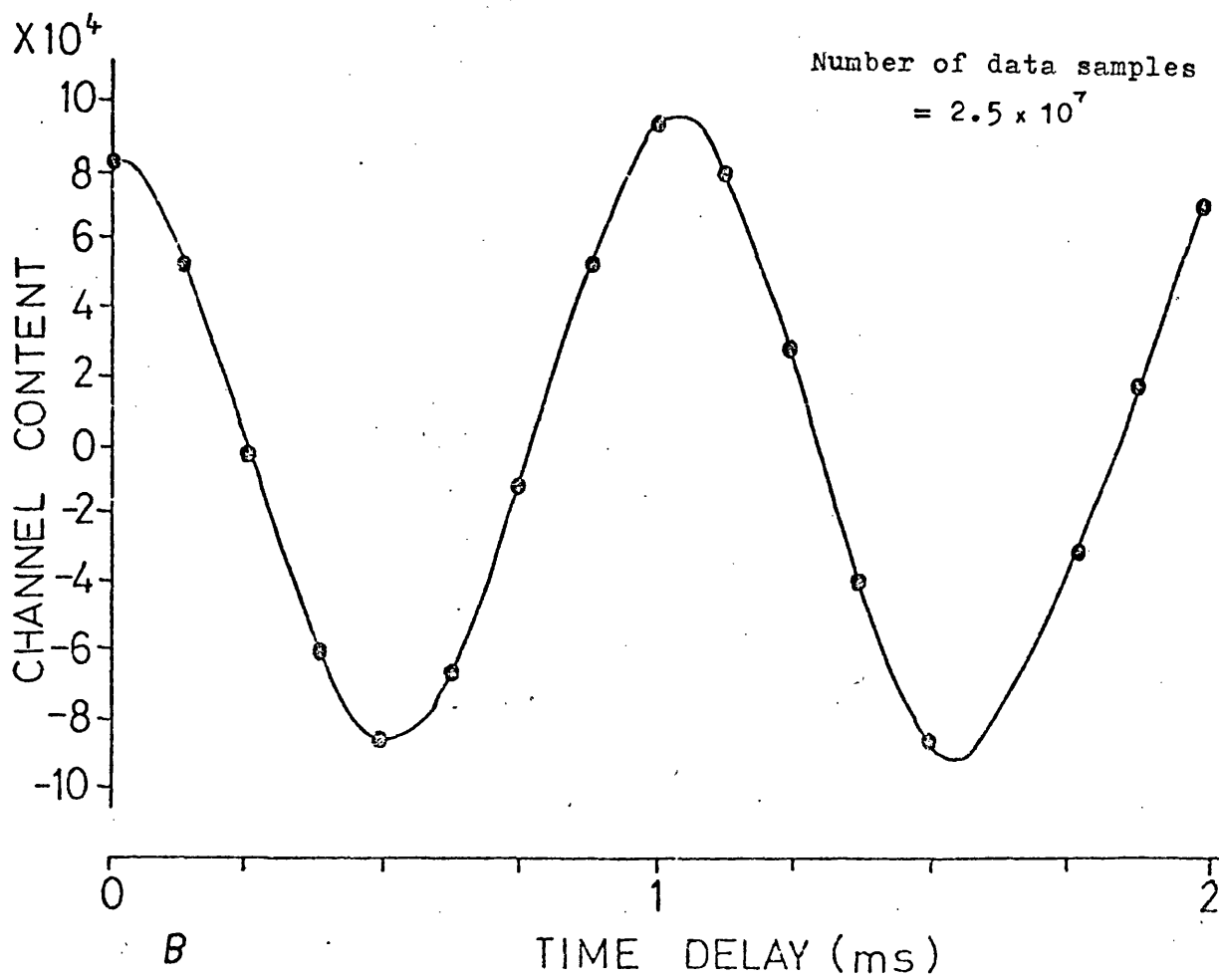
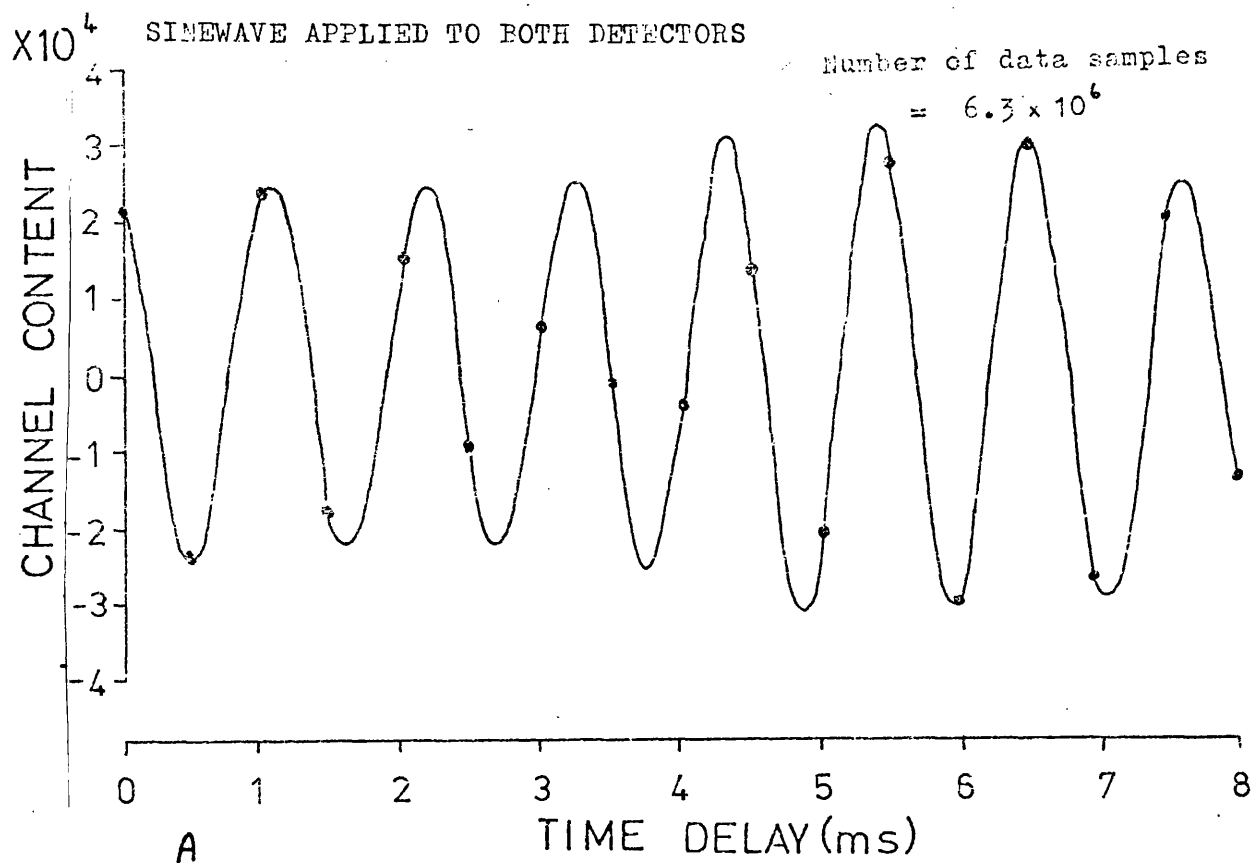


Note: The smooth curve was obtained by the superposition  
of  $\text{sinc}(t)$  functions<sup>82</sup>.



THE CROSS CORRELATION FUNCTION FOR A  
SINEWAVE APPLIED TO BOTH DETECTORS

Fig. 5.6.



uency) which is the lower cut off frequency for the experiment. ( Figure 5.3.). The equivalent unpolarised gravitational wave flux for this effect is  $2.8 \times 10^7 \text{ W.m}^{-2}$  acting in a normal direction to the detector.

The signals from the two detectors were recorded onto analogue tape with 4 mV fed onto the endplates. The tape was then slowed down by a factor of 4 before analysis by the computer. The results of this are shown in Figure 5.6B and the form of the cross correlation function is as expected, and is a sine wave of frequency 910 Hz.

#### The Calibration for White Noise Signals

The principle of the calibration for white noise signals was similar to that for sinusoidal signals. The steps followed in establishing a relationship between the size of the effect measured and the incident white noise gravitational wave flux were as follows:-

- 1) The size of the effect, after cross correlation, was measured as a function of the white noise voltage /  $\sqrt{\text{Hz}}$  applied to the end calibration plates.
- 2) The amount of energy deposited into the detector was evaluated as a function of the noise voltage /  $\sqrt{\text{Hz}}$  applied.
- 3) A theoretical relationship was established between the energy increase in a detector and the applied white noise force /  $\sqrt{\text{Hz}}$ . This was then extended to a value of the Riemann curvature tensor and to the gravitational wave flux.

As before using the steps 2 and 3 the relationship between gravitational wave flux and applied voltage is

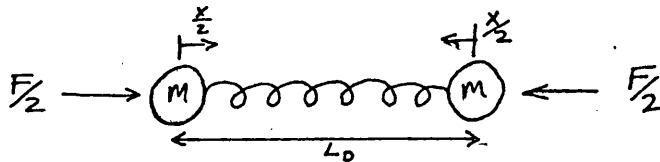


found, and using this result the desired relationship is established.

### The Theoretical Relationship between White Noise

#### Gravitational Wave Flux and the Energy Deposited in a

Detector. As in the sine wave case a theoretical relationship between gravitational wave flux and the energy deposited into the detector had to be derived. This will be done for the ideal dumb-bell case, as it was previously shown in the sinusoidal case that the errors introduced by this approximation are small. The system is as before



The equation of motion is as before (Eqn. 5.1.)

$$\frac{d^2 x}{dt^2} + \frac{\omega_m}{Q_m} \frac{dx}{dt} + \omega_m^2 x = \frac{F(t)}{m} \quad - (5.6)$$

where in this case  $F(t)$  is a white noise force signal.

The response of the system as a function of frequency is:-

$$x(\omega) = \frac{F_0}{k \left\{ (1 - (\frac{\omega}{\omega_m})^2)^2 + \frac{1}{Q_m^2} (\frac{\omega}{\omega_m})^2 \right\}^{1/2}} \quad - (5.7)$$

The Potential Energy of the half system is equal to

$$\frac{1}{2} k \left( \frac{x}{2} \right)_{RMS}^2$$

and from equipartition of energy the total energy of the half system is:-

$$= k \left( \frac{x}{2} \right)_{RMS}^2 \Rightarrow \mathcal{E} = \frac{1}{4} m \omega_m^2 x_{RMS}^2 \quad - (5.8)$$

for the whole system  $\mathcal{E} = \frac{1}{2} m \omega_m^2 x_{RMS}^2$

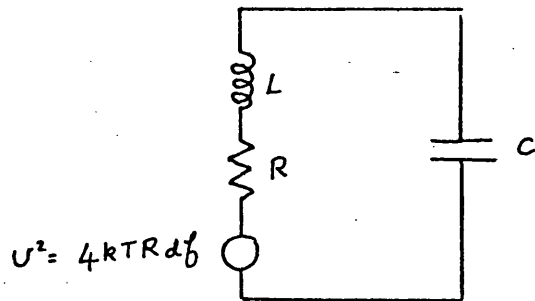
$$\therefore \mathcal{E} = \frac{\frac{1}{2} F_{rms}^2}{M \omega_m^2} \int_0^{\infty} \frac{d\omega}{(1 - (\frac{\omega}{\omega_m})^2)^2 + \frac{1}{Q_m^2} (\frac{\omega}{\omega_m})^2} \quad -(5.9)$$

where  $F_{rms}^2$  is the mean square value of the force per unit rad/sec

The integral  $\int_0^{\infty} \frac{d\omega}{(1 - (\frac{\omega}{\omega_m})^2)^2 + \frac{1}{Q_m^2} (\frac{\omega}{\omega_m})^2}$

may be solved in the following way:-

By analogy with the following electrical circuit



$$E = \frac{1}{2} C \langle v_c^2 \rangle \text{ in the capacitor}$$

and by equipartition of energy

$$E_{tot} = C \langle v_c^2 \rangle$$

$$v_c^2 = \frac{v^2}{(1 - (\frac{\omega}{\omega_0})^2)^2 + \frac{1}{Q^2} (\frac{\omega}{\omega_0})^2}$$

$$E_{tot} = \frac{C 4 kT R}{2\pi} \int_0^{\infty} \frac{d\omega}{(1 - (\frac{\omega}{\omega_0})^2)^2 + \frac{1}{Q^2} (\frac{\omega}{\omega_0})^2}$$

the oscillator

But as  $E = kT$  due to the fact that ~~it~~ <sup>the oscillator</sup> has two degrees of freedom

$$\Rightarrow \int_0^{\infty} \frac{d\omega}{(1 - (\frac{\omega}{\omega_0})^2)^2 + \frac{1}{Q^2} (\frac{\omega}{\omega_0})^2} = \frac{\pi \omega_0 Q}{2} \quad (5.10)$$

Applying this to Eqn. 5.9.

$$\mathcal{E} = \frac{\frac{1}{2} F_{rms}^2 \pi Q_m}{m \omega_m 2} \quad \text{where } F = m c^2 L_0 R_{rms}$$

$$\mathcal{E} = \frac{m^2 c^4 L_0^2 R_{rms}^2 \pi Q_m}{m 4 \omega_m} \quad \text{where } R_{rms}^2 = \text{Mean Square value / rad.s}^{-1}$$

Now in terms of  $R^2 / \text{Hz}$

$$\mathcal{E} = \frac{c^4 m L_0^2 R_{rms}^2 Q_m}{8 \omega_m}$$

$$R_{rms}^2 = \frac{8 \omega_m \mathcal{E}}{c^4 L_0^2 Q_m} \quad (5.11)$$

Now for unpolarised radiation the flux  $\mathcal{F}$  is:-

$$\mathcal{F} = \frac{c^3 \hbar^2 R_{rms}^2}{G 8 \pi} = \frac{c^7 R_{rms}^2}{2 \pi G \omega^2} \quad (5.12)$$

where  $\mathcal{F}$  = flux per Hz.

$$\mathcal{F} = \frac{4 c^3 \omega_m \mathcal{E}}{\pi G \omega^2 m L_0^2 Q_m} \quad (5.13)$$

The Relationship between the Voltage Applied and the

Energy Deposited. The "white noise" signal for the

calibration was generated by a resistor connected to the input of a low noise amplifier, and the resulting signal was then fed through a bandpass filter set at 150 Hz - 10 kHz. This signal was then added to a 300 volt D.C. bias voltage. ( Fig. 5.4.). An A.C. voltmeter was used to

monitor the signal input level. The on-line computer was used to measure the mean square value of the signals from the gravitational wave detectors with no white noise fed onto the calibration plates, thus determining the value corresponding to a detector energy of  $kT$ . The point in the circuit where the signals were measured was at the output of filters  $f_1$  of Figure 5.1. Several values of white noise were applied and a relationship established between the magnitude of applied signal and the energy deposited, and the results are shown in Figure 5.7. The potentiometer ( Fig. 5.4.) on the detector 2 side was adjusted to give an energy ratio between the two detectors of approximately  $\frac{Q_2 f_1}{Q_1 f_2}^*$ , indicating an equal effective gravitational wave flux incident on both detectors. (See eqn. 5.13.).

#### The Relationship between the Magnitude of Applied

Voltage and Gravitational Wave Flux. The flux corresponding to 14.3 mV RMS will be calculated as this voltage was used to measure the effect of cross correlation.

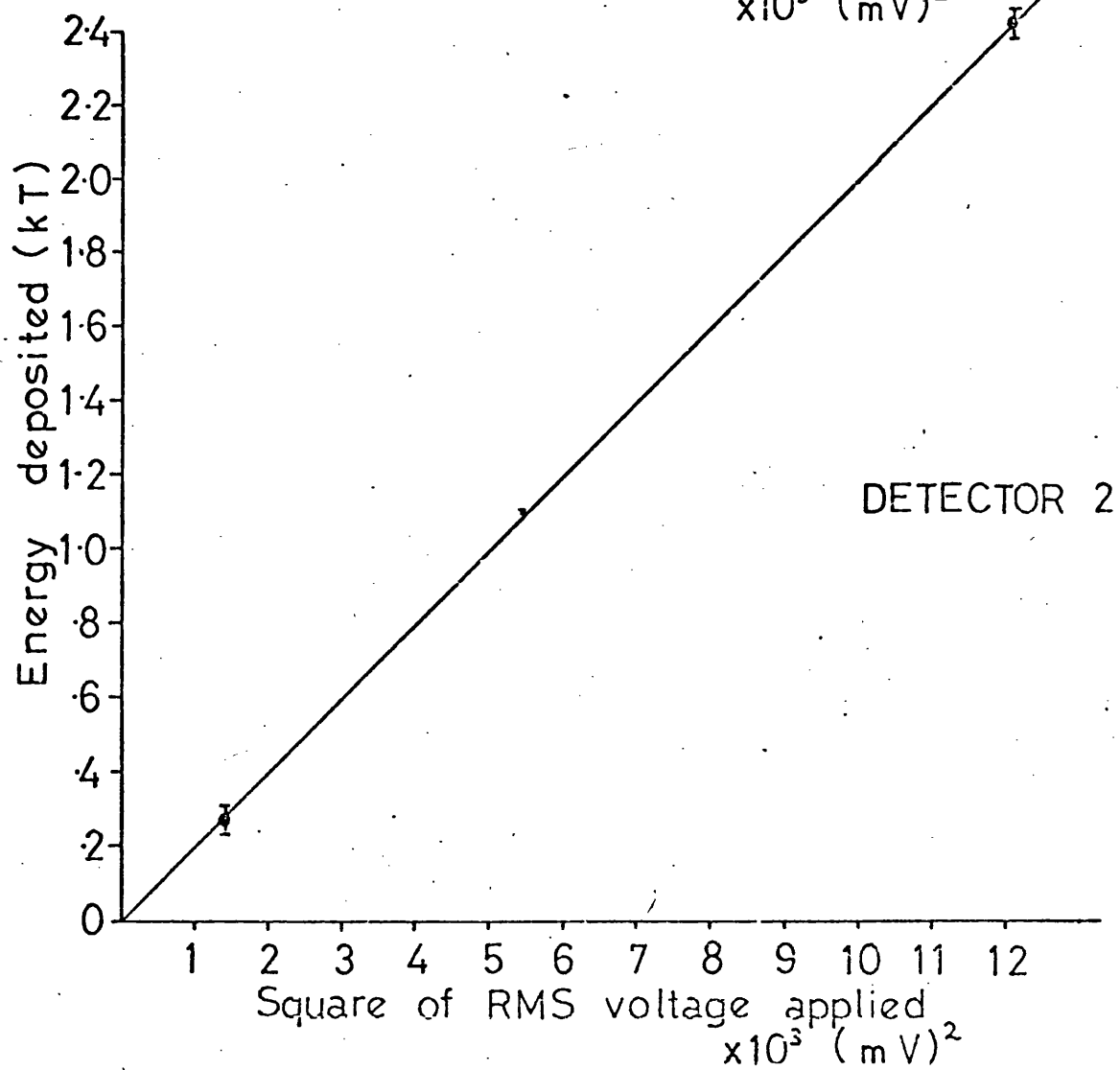
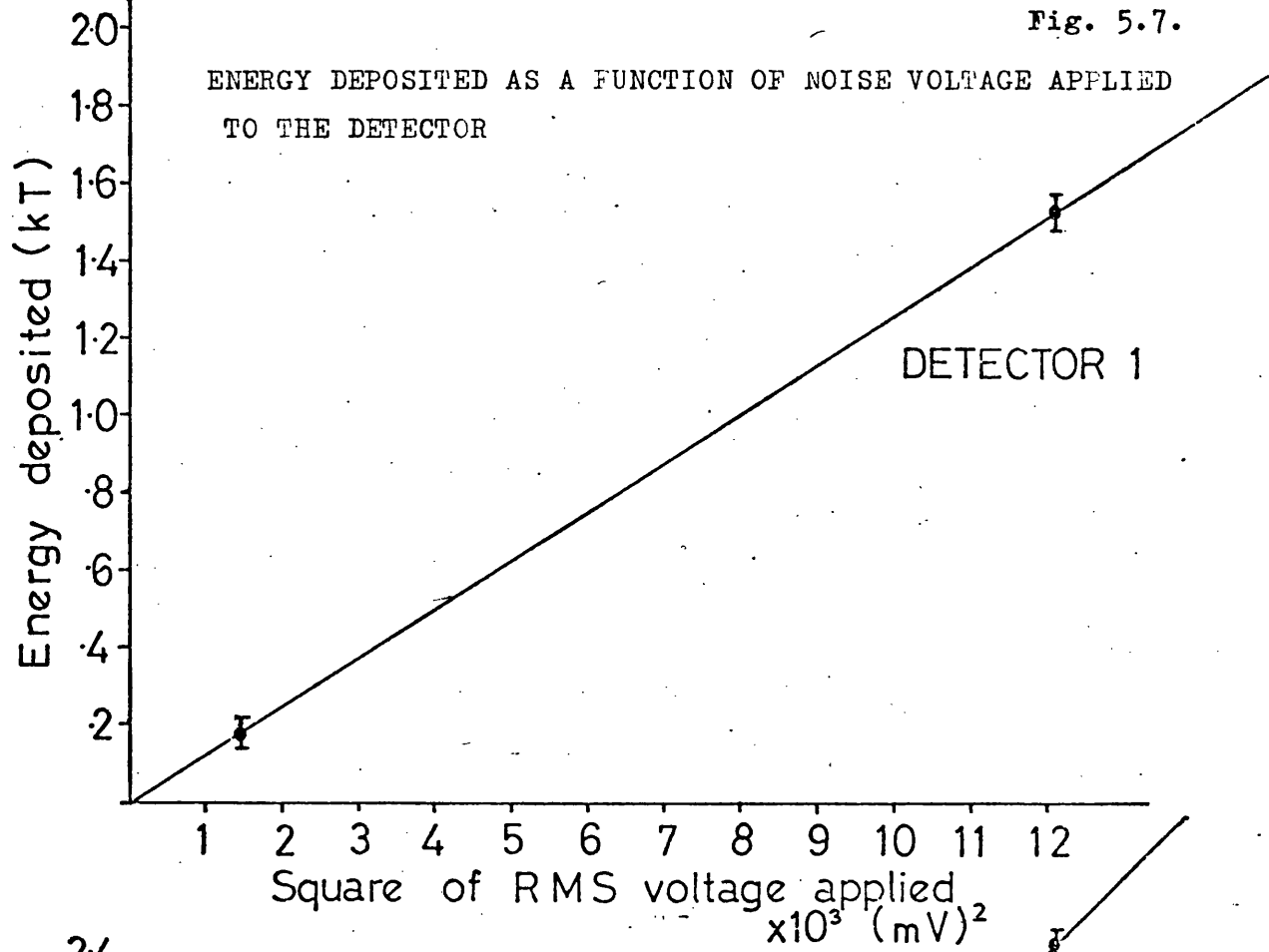
Using the results of Fig. 5.7. it may be concluded that 14.3 mV of white noise deposits 0.026  $kT$  into detector 1 and 0.041  $kT$  into detector 2. Use of Equation 5.13. implies that this voltage is equivalent to a gravitational wave flux of  $7.2 \times 10^4 \text{ W m}^{-2} \text{ Hz}^{-1}$  (This is a mean value as the actual values were  $6.8 \times 10^4 \text{ W m}^{-2} \text{ Hz}^{-1}$  incident on detector 1 and  $7.5 \times 10^4 \text{ W m}^{-2} \text{ Hz}^{-1}$  on detector 2).

The Size of Effect Measured as a Function of Gravitational Wave Flux. The computer was used to cross correlate the

\*  $f_1$  and  $f_2$  are the resonant frequencies of detectors 1 and 2 respectively.

Fig. 5.7.

ENERGY DEPOSITED AS A FUNCTION OF NOISE VOLTAGE APPLIED  
TO THE DETECTOR



output from the detectors with 14.3 mV of white noise fed onto the endplates, and the result (for a 52.5 minute run) is shown in Figure 5.8. This is the magnitude of effect expected from a white noise gravitational flux of  $7.2 \times 10^4 \text{ W m}^{-2} \text{ Hz}^{-1}$  incident on the detectors.

The detector signals were also recorded on an analogue tape recorder and slowed down by a factor of 4 on playback. Analysis of this signal gave further information on the shape of the cross correlation function. The shape of the curve is very characteristic, being that of a decaying sinusoid where the decay time is related to the bandwidth of 170 Hz.

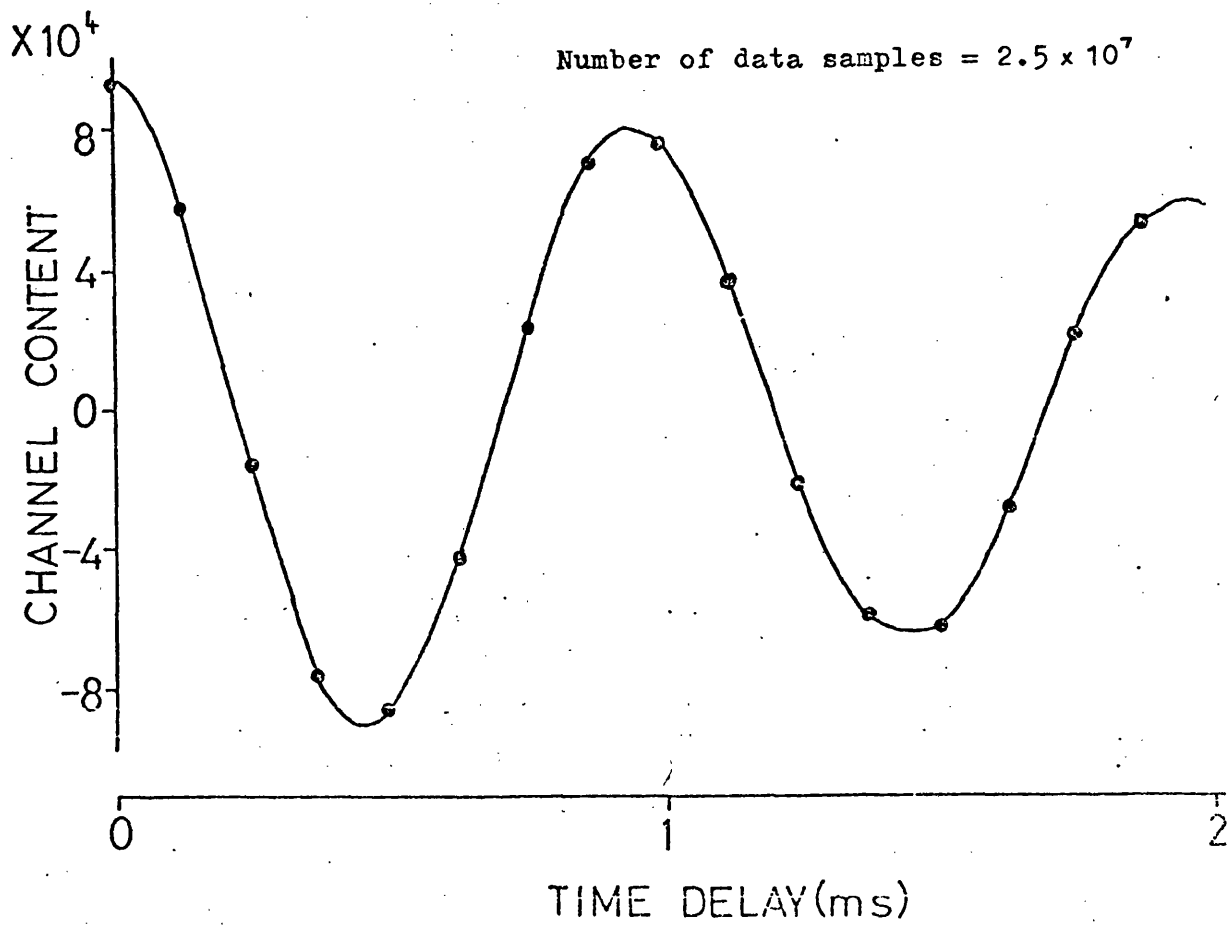
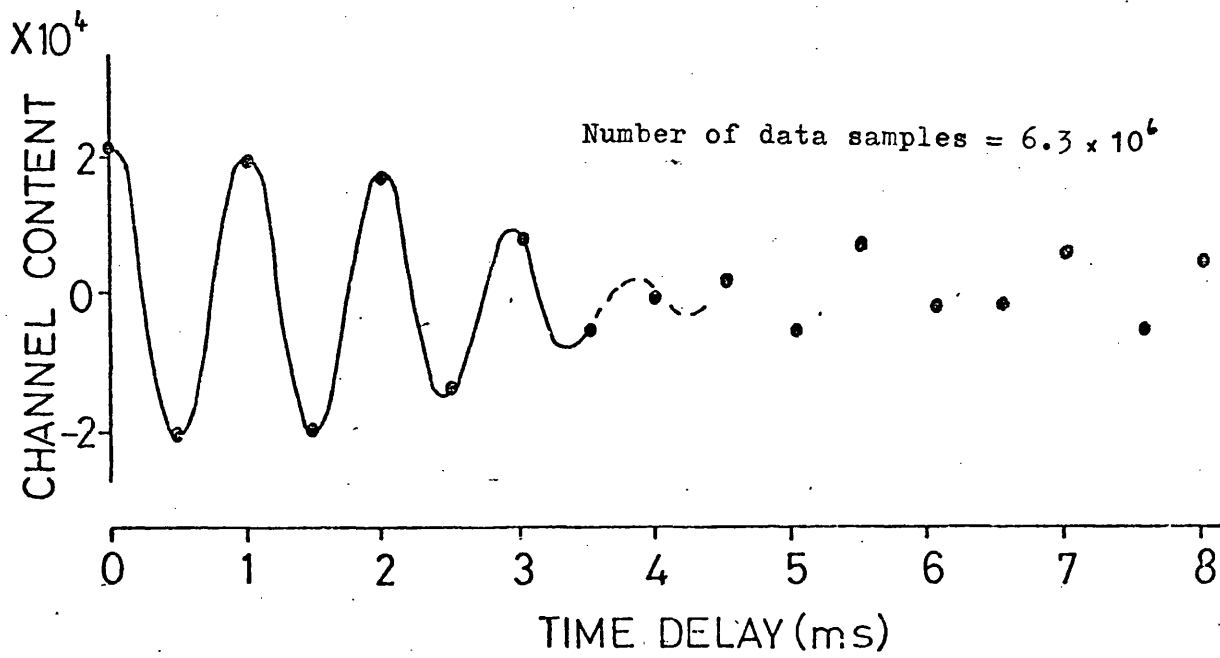
#### An Evaluation of the Standard Deviation of the Experiment.

In order to decide whether the "one bit" cross correlation function indicates the presence of a common signal to both channels, the standard deviation of such a technique has to be determined.

The operation of the cross correlation programme has already been discussed in the previous chapter. The value at any one delay is an addition of +1's or -1's depending on whether the two binary signals, separated by this delay, are similar or different. For uncorrelated signals, (both with a mean of zero), it is reasonable to assume that the probabilities of a +1 or -1 are equal. This assumption therefore leads to the conclusion that the value of a delay point in the cross correlation function will have a probability density function closely related to that of a binomial distribution.

Fig. 5.8.

CROSS CORRELATION FUNCTION FOR NOISE APPLIED TO BOTH  
DETECTORS



The binomial distribution may be defined by considering the following experiment E. Let A be some event associated with E and suppose the probability of the occurrence of A = p. Assuming n independent trials, and defining X as the number of times A has occurred, the probability that X = k is

$$p(X = k) = \binom{n}{k} p^k (1 - p)^{n-k} \quad k = 0, 1, \dots, n$$

and this is known as the binomial distribution.

If X has a binomial distribution with parameters n and p then for large n \* p (i.e. n \* p ≥ 25) X will approximate to a normal distribution, with mean = np

$$\text{and } \sigma = \sqrt{n p (1 - p)}$$

This treatment has so far applied to the random variable X, the number of events, which is a 0 or 1 situation. To apply it to the -1 or +1 situation of the cross correlation a new random variable has to be defined.

$Y = 2(X - n p)$  and this will have a Normal distribution of mean = 0 and standard deviation =  $2\sqrt{n p (1 - p)}$ .

Therefore applying this analysis to the cross correlation case where  $p = \frac{1}{2}$ , the mean of a channel = 0 and the standard deviation is  $\sqrt{n}$ . Both signals are simultaneously sampled n times. However, as the time between samples is less than the autocorrelation time of the individual signals (due to the bandwidth), each sample will be correlated with the previous one. This means that the assumption of independence, used in applying the situation to that of a binomial distribution, was not valid and the standard deviation will exceed  $\sqrt{n}$  by a numerical factor.



The standard deviation of the data was therefore measured experimentally.

The cross correlation was performed on the same signal seventy times (the number integrations set at  $\sim 10^6$ ) and the values from two uncorrelated delay points recorded each time. The length of the run was chosen short enough to ensure no bias could be introduced by a possible correlation. The standard deviation and mean of the two data sets were evaluated and it was found that

$$\sigma = \sqrt{n} \cdot (1.4 \pm .1) \text{ for both data sets.}$$

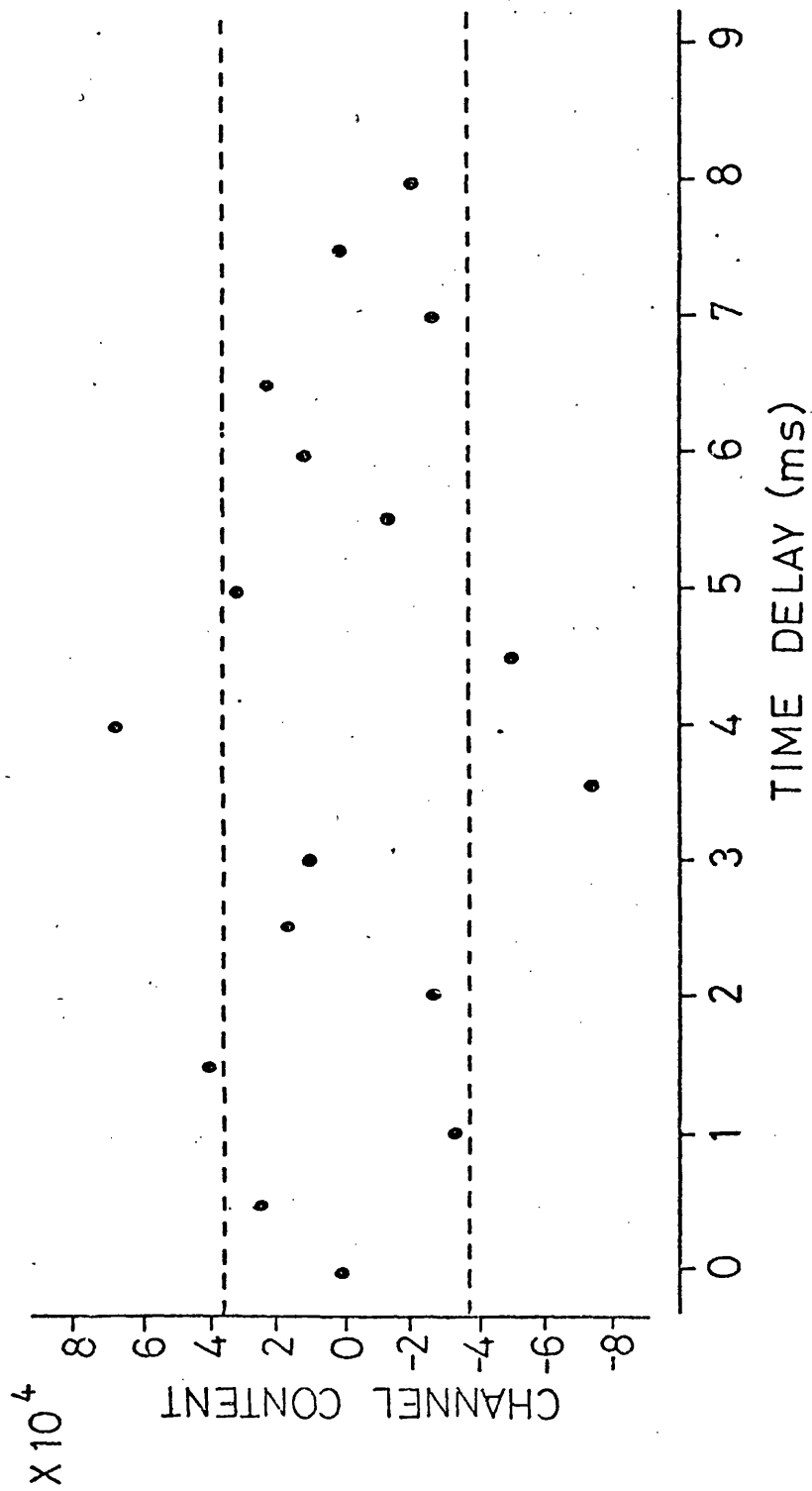
This is the value of the standard deviation for the direct runs; however, if the data are recorded and slowed down before analysis the standard deviation changes. Slowing down the data, by a factor  $m$ , may be considered as sampling the signal faster. If this is done the standard deviation will change to  $1.4 \sqrt{n \cdot m}$  where  $n$  still remains the number of samples taken and  $m$  the factor by which the data have been slowed down.

#### The Experimental Runs and Evaluation of the Sensitivity of the Experiment

A one bit cross correlation was performed on the detector signals for 90 hours, from the 6th - 10th September 1974 and the result is shown in Figure 5.9. The polarity of the preamplifier was reversed during the run and the curve shown takes account of this.

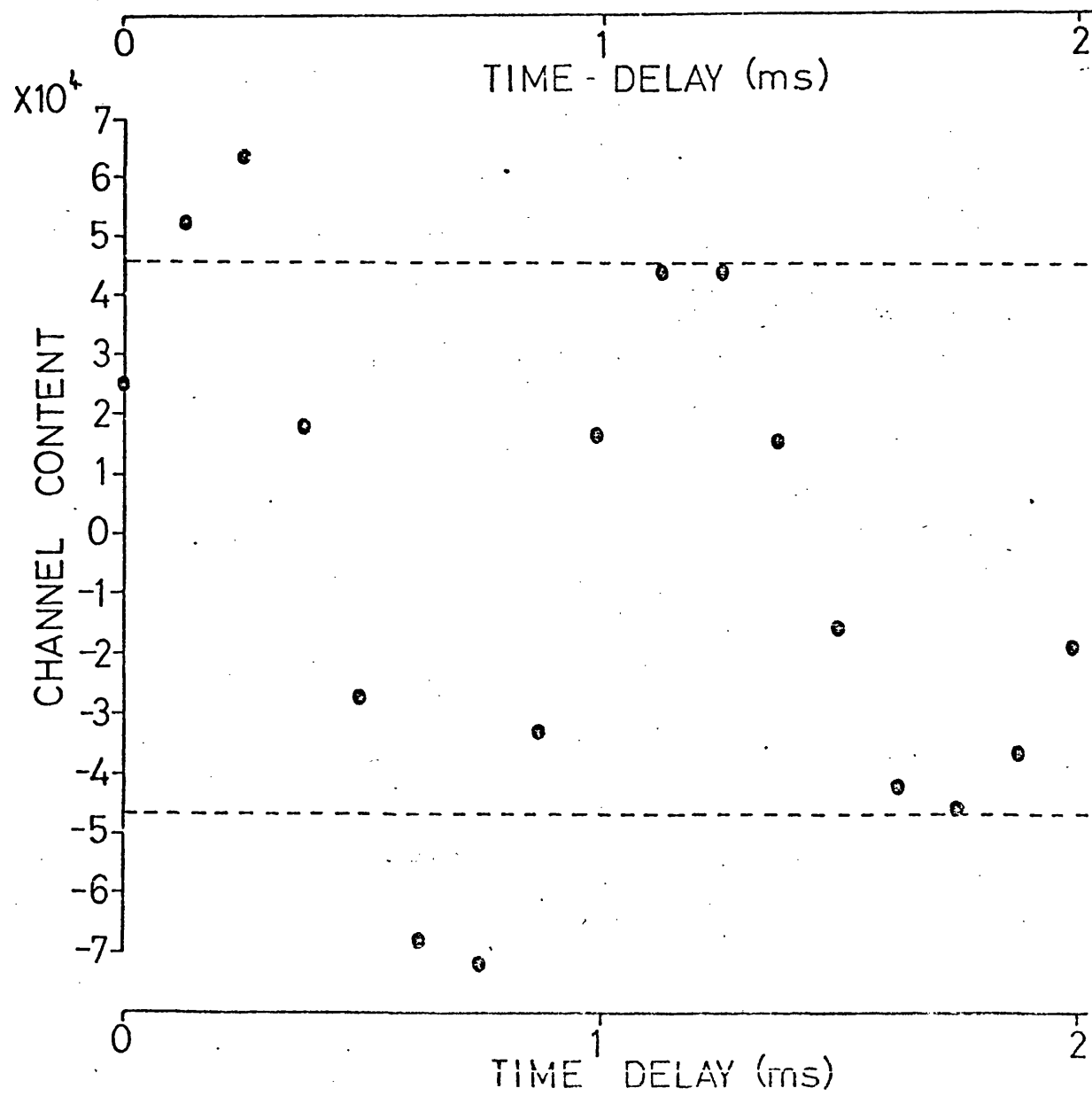
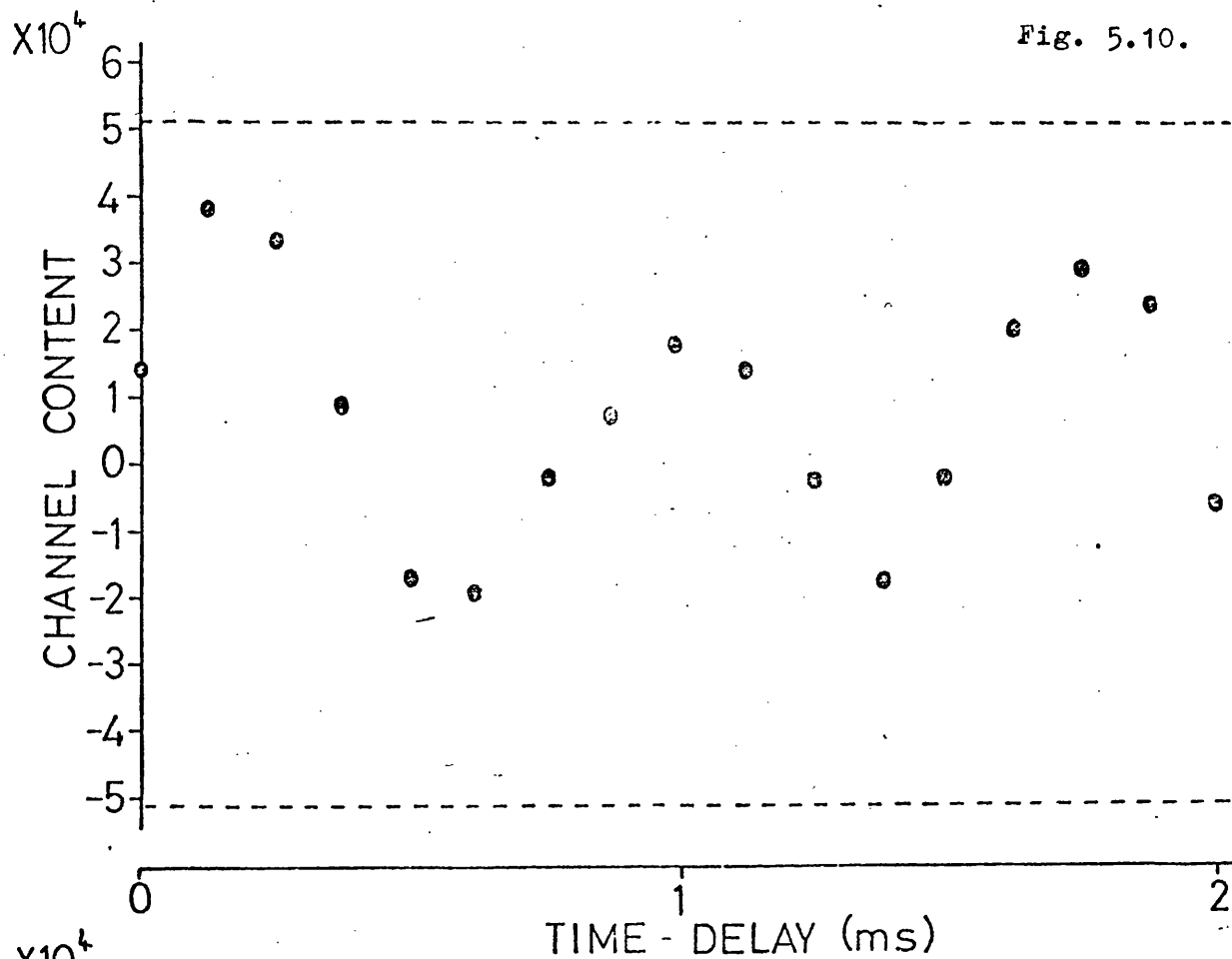
A continuous run of 24 hours between 6th - 7th August 1974 was recorded onto an analogue tape recorder. The tape was then slowed down by a factor of 4 for analysis by the computer, the results are shown in Figure 5.10.

Fig. 5.9.



THE EXPERIMENTAL RUN LASTING 90 HOURS

Fig. 5.10.



the polarity of the preamplifier was also reversed during this run.

The reason why the curves for the experimental run have a decaying 'sinusoidal' shape is due to the autocorrelation of the data points. It was noted that the pattern was not persistent from one part of the run to the next. The lines on the graph indicate the standard deviation level and it is noted that no number exceeds a level of  $3\sigma$ . It is therefore concluded that there were no signals common to both detectors, at this level of significance.

Using the calibration figures obtained, an upper limit may be set for the flux of gravitational radiation incident on the detector.

#### The Upper Limit for Sinusoidal Signals.

From the calibration runs a flux of  $2.8 \times 10^7 \text{ W m}^{-2}$  incident on the detector produced an effect 7.4 times the standard deviation. The run consisted of the integration of  $6.3 \times 10^6$  samples.

As the ratio of effect to standard deviation of the cross correlation is proportional to  $\sqrt{n}$  the sensitivity at a  $3\sigma$  level in a 90 hour run is  $1.1 \times 10^6 \text{ W m}^{-2}$  for sinusoidal signals.

The values for flux have assumed the radiation to be incident normally to the axis of the detector. The sensitivity of the experiment however reduces if the radiation is incident off the normal direction. The equivalent isotropic flux is not calculated, as an isotropic monochromatic source is unlikely.

### The Upper Limit for Noise Signals

The calibration runs indicated that a flux of  $7.2 \times 10^4 \text{ W m}^{-2} \text{ Hz}^{-1}$  incident on the detector produced an effect 6 times the standard deviation. Following the arguments of the sensitivity depending on  $\sqrt{n}$  as used previously, the flux of wideband radiation that should have produced a  $3\sigma$  effect for the 90 hour run was  $3.6 \times 10^3 \text{ W m}^{-2} \text{ Hz}^{-1}$ .

This radiation is also assumed normal to the detector axis. An isotropic flux of  $6.8 \times 10^3 \text{ W m}^{-2} \text{ Hz}^{-1}$  would also produce a  $3\sigma$  effect in the 90 hour run, this is calculated from the angular dependence of the detector cross section.

### A Comment on the Pulses Reported by Weber

As stated previously this experiment implies that the events reported by Weber were not due to a large flux of small gravitational radiation pulses, and although this was not the object of the experiment, this result has proved extremely useful. The sensitivity of the experiment was such that a flux consisting of 5000 or more pulses per day depositing an aggregate energy of about 500 times the mean thermal energy per mode in one of the detectors, would have been observed at a three standard deviation level. From an analysis of Weber's sensitivity if the coincidences were due to small pulses of .2 kT or less the rate of occurrence would have to be greater than the limit set by the above experiment. This type of signal had not previously been excluded.

## Chapter 6

### Conclusion

Summary: In the introduction it was stated that the sensitivity of gravitational radiation detectors had to be increased in order to attain a reasonable rate of detection. Various ways of improving this sensitivity have been considered in this thesis and one of the first fields investigated was the low noise amplification of signals from gravitational wave detectors. Experiments have shown that in a frequency region around 1 kHz the noise reduction produced by the cooling of F.E.T.s was a significant but not large factor, and therefore another method of low noise amplification was investigated. Measurements were made on the noise performance of a SQUID and the major noise component was identified. The basis for initiating the work on the SQUID was that as it was a superconducting device, and hence maintained at a low temperature, the thermal noise of the device would be small, and indeed this was found to be the case. However, the majority of the noise was found to be produced in the RF Biasing and sensing circuit and the amount of backward fluctuation from the circuit had to be calculated. This problem was considered, by J. Hough and the author, and the amount of flux available for back reaction was estimated. While the thesis was being written similar conclusions have been drawn by Rudenko<sup>60)</sup> and Giffard.<sup>61)</sup>

As well as an investigation into possible improvements that may be made in detector sensitivity a search was performed for continuous gravitational radiation in the

frequency region around 1 kHz. No effect was found, however the experiment proved worthwhile in providing a more sensitive limit for radiation of this nature. This work led onto a more general consideration of various techniques concerned with the extraction of continuous signals from the noise of gravitational wave detectors.

It is envisaged that these programmes and similar ones will be of great use when the new generation of detectors come into operation. The Fourier analysis programme developed for experiments concerned with the detection of gravitational radiation were used on an unrelated experiment on the detection of celestial x-rays by a ground based technique(Appendix A).

Future work: Using the measurements on various low noise amplification systems the sensitivity of various detection schemes was calculated. Of all the possible experiments considered by the group at Glasgow, two systems were found to be most sensitive. Firstly a detector consisting of a maser amplifier coupled to a cooled aluminium bar (1°K) was possible, as the backward fluctuation was thought to be small enough to make cooling worthwhile. Secondly a system using a laser to monitor the separation of the masses was found to be as sensitive. This type of system is similar in principle to the detector of Forward<sup>36)</sup>, and the proposed systems of Weiss<sup>37</sup> and of Billing<sup>8</sup> et al.

It was thought that the laser technique posed fewer technical difficulties, and an extension of this type of detector is now under construction here at Glasgow. This

detector should be sensitive to the low frequency pulses predicted from very heavy black holes. Other systems under construction include low temperature experiments by Fairbank et al.<sup>63</sup>, Hamilton et al.<sup>63</sup> and the group at Rome.<sup>64-65)</sup> Fairbank et al intend to use a SQUID coupled to an aluminium bar by means of a resonant diaphragm. They propose to use a much higher bias frequency for the SQUID compared with the 20 MHz considered in the thesis, and it is thought that the SQUID will have a much lower noise hence making it worthwhile to cool the detector to a few mK. Hamilton et al. intend to use a parametric device similar to the one described in Chapter 3. Due to the limiting effect of the backward fluctuation he only intends to cool the detector down to a few-degrees Kelvin. The sensitivity of these detectors is now reaching a value where detection of gravitational radiation from the Virgo cluster seems a possibility in the not too distant future. The time when these experiments will come into operation is not known exactly, however within one year it is expected that intermediate experiments will be underway.

A suitable sentiment of what may lie ahead has been expressed by Thorne:<sup>35</sup>

"I look forward with particular excitement to the time, perhaps eight years hence, when detectors will study bursts of waves from supernovae in the Virgo cluster of galaxies (about three supernovae per year!). Such bursts will be a direct probe of the guts of stellar collapse, as well as a powerful tool for distinguishing between competing theories of gravitation."



## Appendix 1

### An Investigation into the Possibility of Detecting Periodic Celestial X-rays by a Ground Based Technique

#### Introduction

The Fourier transform programmes developed in connection with experiments on the detection of gravitational radiation have previously been discussed. The experiment described in this appendix although not related to the detection of gravitational radiation has proved useful in its own right and in providing a good test of the Fourier transform programmes.

The experiment described is an investigation into the possibility of detecting periodic extra-terrestrial x-rays of unknown period by a ground based technique.

Several groups have been involved in experiments to detect x-ray transient effects <sup>(66-70)</sup> including the group led by Drever at Glasgow University.

The basic idea is to monitor the phase of a distant VLF radio signal arriving at the receiver. The mode of transmission is such that the signal is 'reflected' from the ionosphere before reception.

X-rays impinging on the ionosphere cause the ionisation density to change and thus the 'reflection' height of the signal. This in turn causes a change in distance travelled by the wave and hence a phase change. The method of measuring the phase change will be discussed followed by the results of a search for periodic fluctuations in the phase. The amount of change expected as a

function of x-ray flux will then be discussed.

### Experimental Method

The low frequency radio signal chosen for the experiment was transmitted from the Prangins HBG timing station. This station is situated in Switzerland and transmits on 75 kHz with a power of 20 kW. The form of the time signal is a short interruption of the carrier every second with a double interruption every minute.

Two types of antenna were tested, a fixed long wire (100m) and a rotatable multi-turn loop aerial. The loop was found to be best for reception of the Swiss station.

A variable capacitance was connected in parallel with the inductive loop and this resonant circuit was tuned to 75 kHz. To avoid damping the circuit a high input impedance amplifier was connected at this point. Signals from the output of the amplifier were then again filtered with an LC resonant circuit, the circuit being connected to a preamplifier.

A resonant circuit was used to give selective positive feedback on the main amplifier to produce a regenerative type of receiver, the positive feedback being used to narrow the bandwidth. Indeed by this method bandwidths of a few tens of hertz were obtained, the only limit being that with too much feedback the receiver became unstable.

The phase of the incoming radio signal was measured by comparing it with a 75 kHz signal generated from a 5 MHz oven crystal oscillator. The crystal oscillator was 'locked' in frequency over the long term to the incoming radio signal.

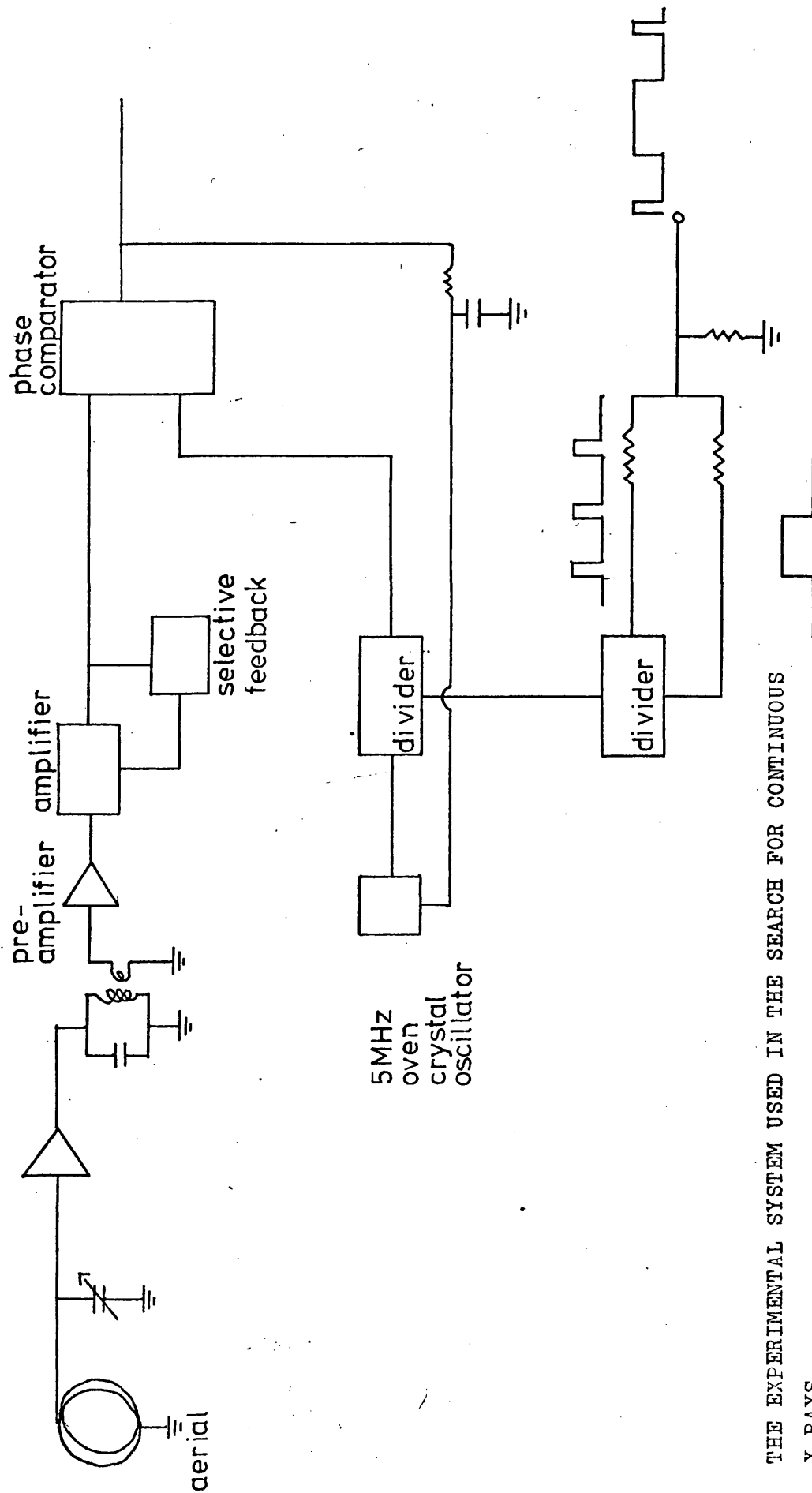
The 75 kHz reference was fed into one input of a phase comparator, Fig. A.1., the radio signal being fed into the other input. The output voltage of the phase comparator is a measure of the phase difference between the two signals, and the output is zero when the phase between signals is  $90^\circ$  and reaches the extremes at  $0^\circ$  and  $180^\circ$ . The output voltage as well as being used as the signal to be analysed was smoothed with a long time constant and fed as a control signal to the crystal oscillator to lock the frequency.

The output of the phase comparator was fed onto the input of the computer A.D.C. As the signal had to be sampled in order to compute the power spectrum by the digital computer, attention had to be paid to the sampling theorem as described in Chapter 4.

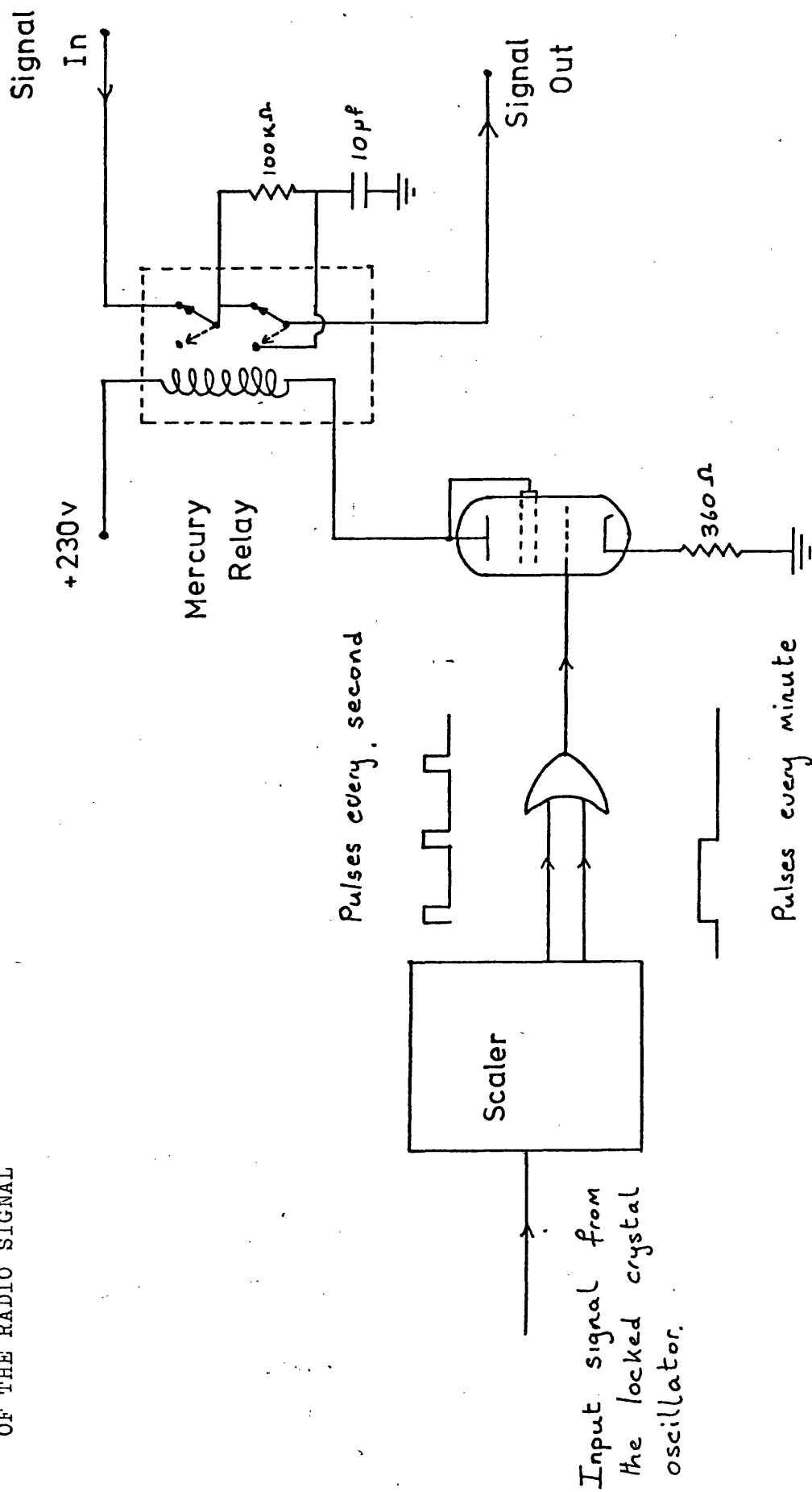
The signal was therefore filtered to an upper cut off frequency of just less than half of the sampling frequency.

Two methods of processing the data were used, one was to compute the power spectrum of the signal direct using the F.F.T. programme previously described. The other method was to record the output of the phase comparator in a digital form onto magnetic tape and then analyse the data at a later stage.

As mentioned previously the signal from the Swiss station was that of a constant amplitude carrier interrupted every second with a double interruption at the minute. This abrupt change in the carrier caused a transient every second in the phase comparator output and this was eliminated by the circuit shown in Fig. A.2.



THE METHOD OF EXCLUDING THE TRANSIENTS CAUSED BY THE INTERRUPTION  
OF THE RADIO SIGNAL



The principle was to use the locked crystal oscillator to generate a pulse every second, and a longer one at the minute. This voltage was used to gate out the transient by use of the mercury relays as shown. The mean voltage up to gating is stored and presented to the input of the A.D.C. while the signal is gated out, this procedure avoiding a change in the mean voltage on gating.

#### The Results of the Experiment.

Preliminary experimental runs were performed on the signal with sampling frequencies of 50 Hz and 500 Hz. Pronounced peaks were noted at 50 Hz due to mains hum and at 1 Hz (and harmonics) due to the gating of the signal. A peak however was noted at  $6.27 \pm .02$  Hz (and harmonics) in the runs with a sampling frequency of 50 Hz. The origin of this peak had to be clearly identified before further search, for other less obvious peaks, could be done.

In order to check whether the peaks were concerned with the sampling frequency, a simultaneous run was performed on two computers with the sampling frequency set in one case at 50 Hz and in the other at 42.31 Hz. The peaks occurred in both spectra at the same frequency. To test whether the effect was generated within the apparatus an artificial carrier at 75 kHz was injected to the radio with white phase noise introduced onto it. The apparatus for producing the artificial carrier with phase signals present is described in the section on calibration. The analysis however did not present any peaks at the required frequency.

In order to determine the frequency of the peaks with higher resolution and to investigate the frequency stability of them the following experiment was performed.

The signal from the phase detector was filtered to a frequency band of 4 - 8 Hz, and the signal was fed into 1 input of an analogue multiplier. A sine wave of frequency 5.95 Hz was applied to the other input. The product of the two signals was then passed through a low pass filter with a cut at 0.4 Hz. The signal was then fed to the computer and analysed with a sampling rate of 1 Hz. The frequency of the peaks due to the difference frequency of the effect with 5.95 Hz was measured and the frequency of the effect was found to be  $6.2737 \pm .0005$  Hz.

By comparing the peaks with the <sup>measured</sup> frequency of the mains divided by 8 it was found that, compared with the mains, the frequency of the effect was much more stable.

It was thought that the effect was due to an interfering station and the loop aerial was rotated in order to try to null out the effect, however this was not successful. To investigate the hypothesis further the system was changed to receive other stations including the German timing station Mainflingen transmitting at a frequency of 77.5 kHz. On analysis of the phase signal of this station peaks were found separated by  $6.27 \pm .1$  Hz, but displaced from the previous peak by  $3.1 \pm .1$  Hz. This is a result consistent with an interfering signal. To prove this further the system was tuned to  $\frac{1}{13}$  MHz and an artificial carrier was injected at this frequency. With the aerial also connected the peaks were observed at a

separation of 6.27 Hz and displaced by  $3.0 \pm .1$  Hz.

This result confirmed the conclusion made from the previous results, and a possible model for the effect is presented in Fig. A.3.

Knowing that the effect was not of extra-terrestrial origin a 24 hour continuous recording was performed from 10.00 GMT on 2/3/76 to 12.00 GMT on 3/3/76. The clock frequency for this run was set at 250 Hz and the signal was low pass filtered with a cut off frequency of 92 Hz. The data were analysed, in  $3\frac{1}{2}$  hour sections, for a peak occurring above 3 times the standard deviation of the data. The fact that there were many channels meant that Graph 4.5 . was used to determine the effective level for a ' $3\sigma$ ' effect. No peaks were found at this level except those related to the mains frequency, the 1 Hz chopping frequency and the 6.27 Hz interference.

#### The Upper Limit Implied

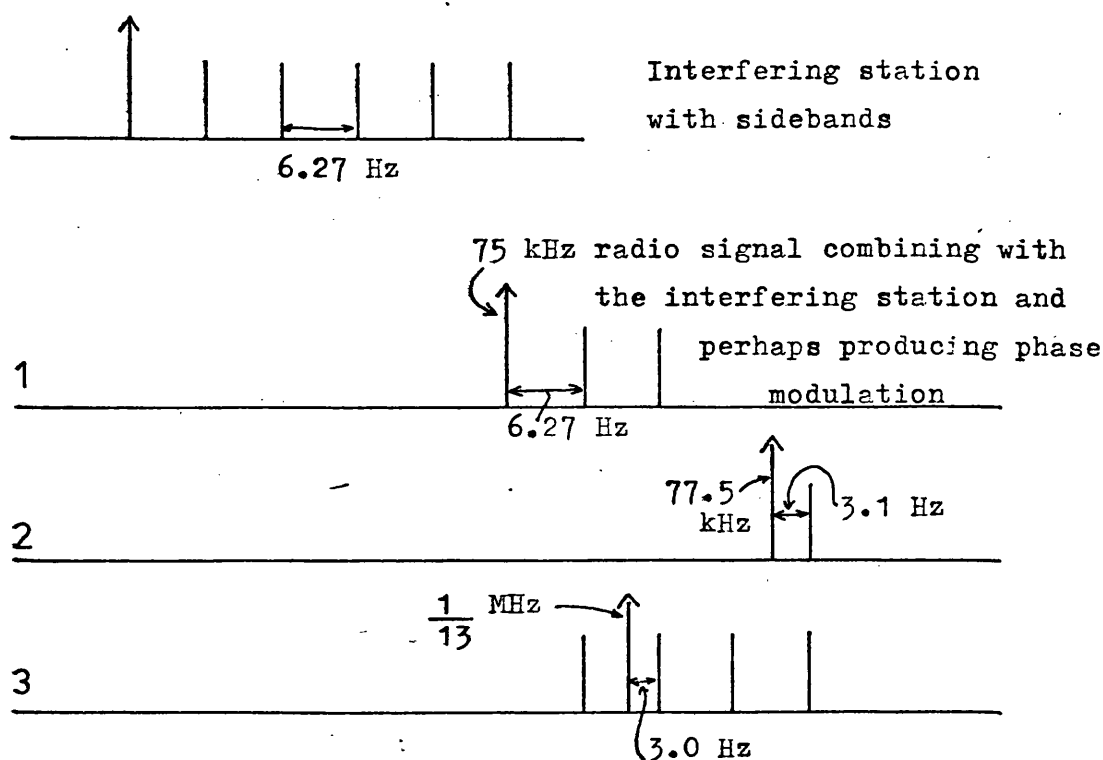
This information may be used therefore to set an upper limit for this experiment to the periodic x-ray flux (in the frequency range up to 60 Hz) incident on the ionosphere.

In order to do this the experiment has to be calibrated. Firstly an empirical relationship between the phase change amplitude and the power spectrum analysis has to be obtained. Secondly the relationship between x-ray flux and the phase change expected, in the radio signal, is derived.

#### The Relationship between the Phase Change of the Radio Signal and the Magnitude of Effect Measured. The first



Fig. A3.



Therefore for the model to work

- 1)  $75 \text{ kHz} - f = m (6.27 \text{ Hz})$
- 2)  $77.5 \text{ kHz} - f = n (6.27 \text{ Hz}) \pm 3.1$
- 3)  $76.923 \text{ kHz} - f = l (6.27 \text{ Hz}) \pm 3.0$

Subtracting 1) from 2)

$$(77.5 - 75) \text{ kHz} = k(6.27 \text{ Hz}) \pm 3.1$$

Subtracting 1) from 3)

$$(76.923 - 75) \text{ kHz} = j(6.27 \text{ Hz}) \pm 3.0$$

and with  $k = 398$  and  $j = 306$  these equations are true.

The model therefore seems correct.

THE PROPOSED MODEL TO EXPLAIN THE 6.27 Hz PEAKS IN THE  
POWER SPECTRUM

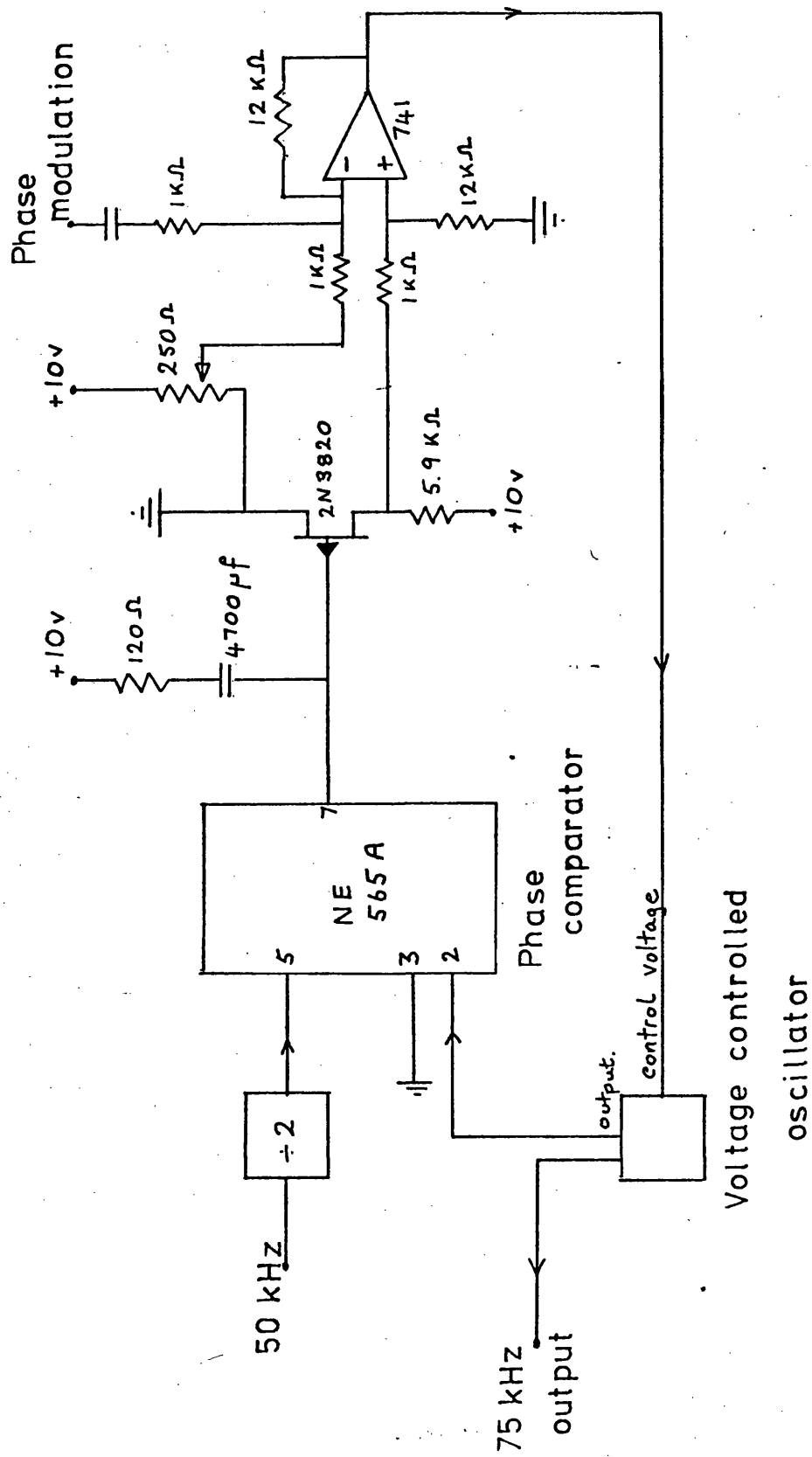
stage in the calibration was to establish the relationship between amplitude of sinusoidal phase change of the radio signal and the Fourier transform output signal power.

The artificial radio signal was phase modulated by the method shown in Fig. A.4. A crystal oscillator, separate from the system, was used to generate a 25 kHz signal and a phase locked loop was locked to the 3rd harmonic of this.

By introducing a signal voltage to the feedback loop of the phase locked loop a phase signal was introduced to the 75 kHz carrier signal. The phase change introduced as a function of the voltage applied to the feedback loop was determined, and the result is presented in Fig. A.5. The relationship was independent of frequency up to a frequency of several hundred hertz. This signal was used to measure the bandwidth of the experiment and it was found to be 60 Hz. Sinusoidal signals of variable amplitude and at frequencies of 20 Hz and 60 Hz were applied to the feedback of the phase locked loop. The power spectrum of the phase detector output was then determined. The power registered by the Fourier transform programme was then related to the RMS input voltage and then (using Fig. A.5. ) to the phase change of the radio carrier. A graph of the relationship between mean power and incoming phase change is presented in Fig. A.6., for both 20 Hz and 60 Hz, 60 Hz being the high frequency cut of the experiment.

As stated previously, the analysis of the recorded data did not yield any peaks of extra-terrestrial origin

Fig. A4.



THE CALIBRATION SYSTEM

Fig. A5.

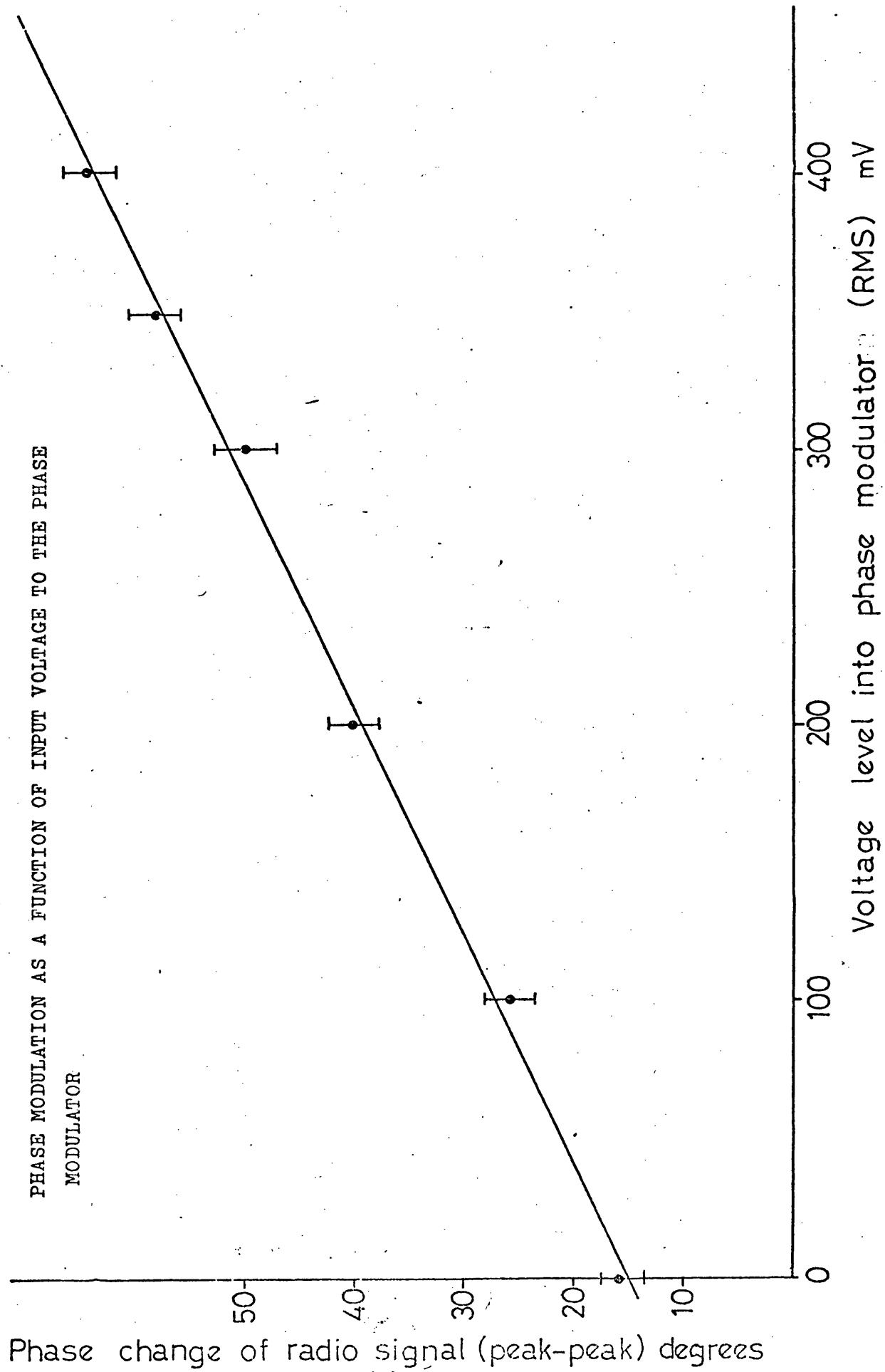
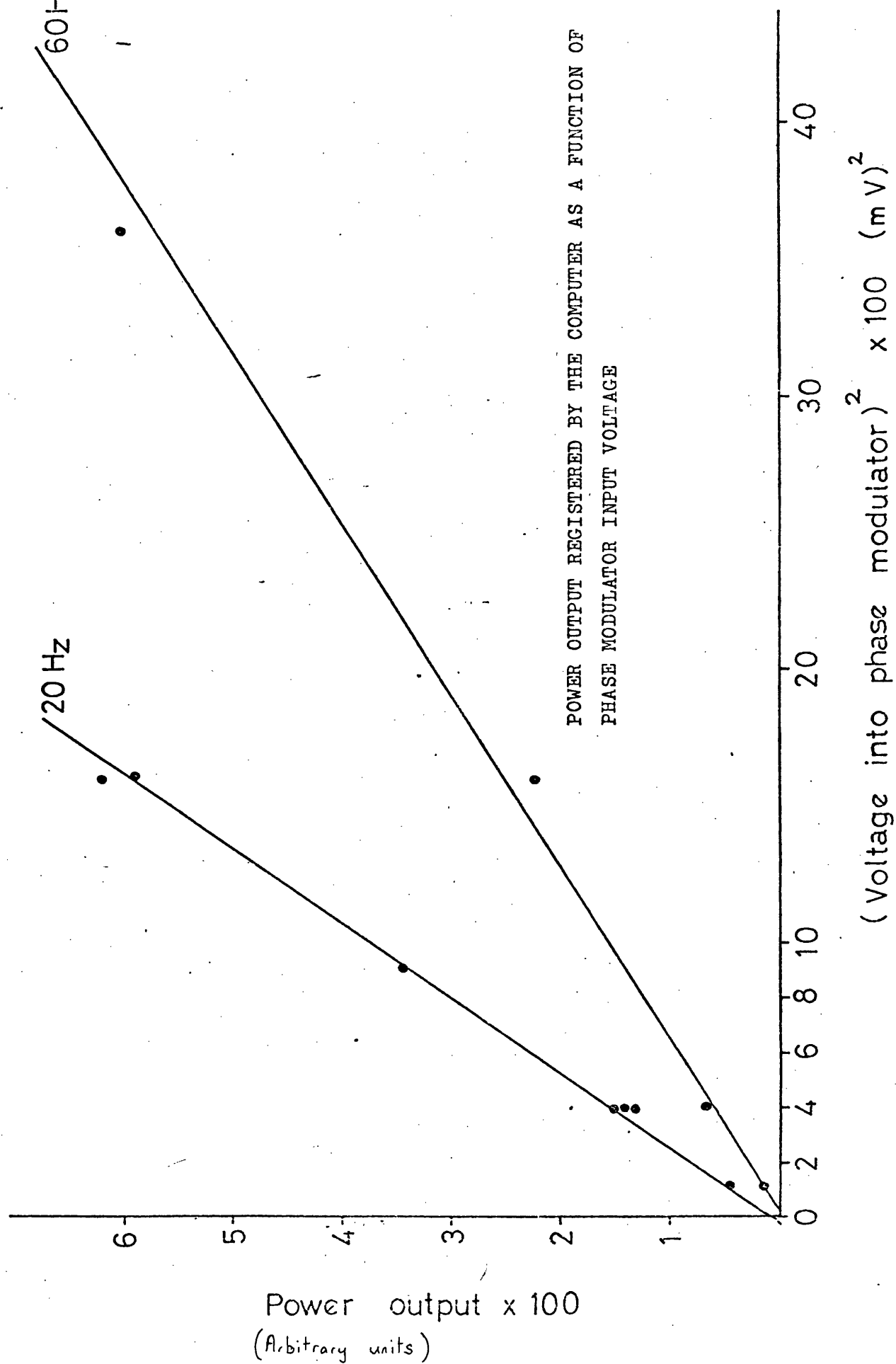


Fig. A6.



above a ' $3\sigma$ ' level. The  $3\sigma$  level in terms of the power output was calculated for the experimental runs. The 24 hour run was analysed in seven sections each 3 hours 27½ minutes long. The standard deviation for each section being measured both at the region around 20 Hz and at 60 Hz.

For the section from 20.22½ GMT to 23.50 GMT the standard deviation was found to be  $1 \pm .3$ , at 20 Hz and  $.7 \pm .3$  at 60 Hz, and this was the quietest section. The other values are presented in Figure A.7. The run from 3.27 GMT to 6.55 GMT was particularly noisy, with a standard deviation of  $13 \pm 3$ , at 20 Hz.

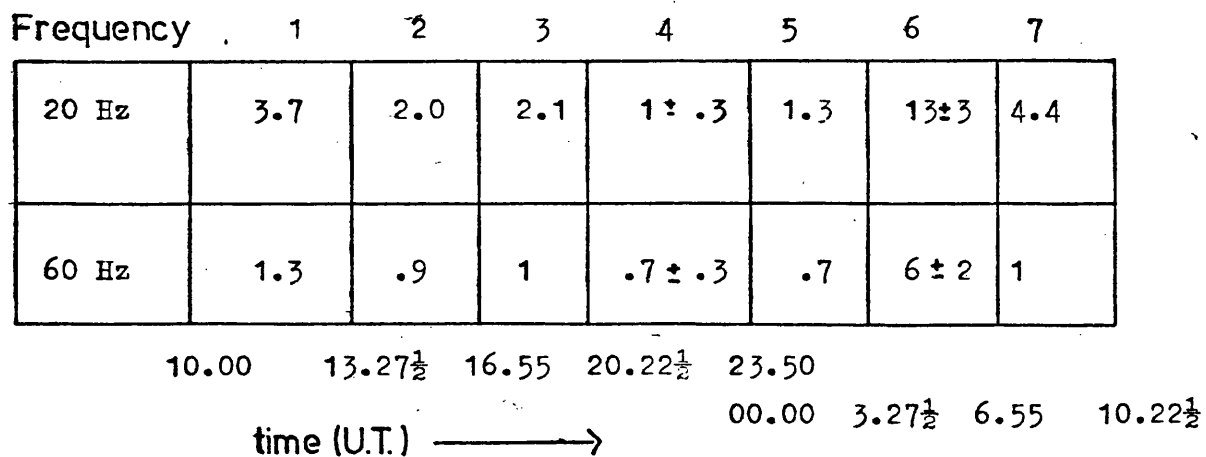
The sensitivity of the experiment in terms of the phase change at the input is calculated for the best section as the sensitivity for the other runs may be scaled accordingly.

Taking into account the different programme scaling factor, on recording the data and performing the calibration, the sensitivity of the system to phase change at 20 Hz was  $.7 \pm .2$   $\mu$ S RMS level and  $.9 \pm .2$   $\mu$ S at 60 Hz.

#### The Relationship between the X-ray Flux and the Phase Change Expected.

The effect of celestial x-rays in the energy region of 5 - 10 keV in terms of increasing the electron production rate has been predicted by O Mongain and Baird<sup>(6)</sup> and Baird<sup>(6)</sup>. They predict that for the strongest celestial x-ray source SC0 X-1 the electron production rate peaks at a value of  $4 \times 10^{-3}$  electrons  $\text{cm}^{-3} \text{s}^{-1}$  at a height of 80 km. The electron lifetime at the height of 80 km predicted by Baird<sup>(6)</sup> is 100 seconds, and this may be combined with the above production rate to give a mean

Fig. A7.



THE STANDARD DEVIATION (AT TWO FREQUENCIES) AS A FUNCTION OF TIME, FOR A 24 HOUR RUN.

Note: Divide the numbers above by 16 in order that the standard deviations are in terms of the arbitrary units of Fig. A.6.

electron density due to SCO X-1 of  $0.4 \text{ electrons cm}^{-3}$ .

Using the graphs of electron density as a function of height, (in the region of 80 km), a change in reflection height of .3 km would be expected. Measurements performed by Edwards et al<sup>70)</sup> indicate a drop in reflection height of .5 km at 80 km, and this value is used in the following calculation.

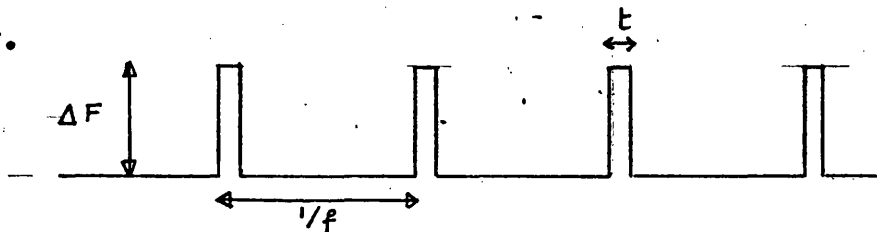
Consider a periodic x-ray source at a frequency of  $f$ .

The time averaged periodic x-ray flux from the source

=  $F$ .

The x-ray pulses will be assumed short compared with the time between pulses.

e.g.



The number of electrons produced ( $\Delta N$ ) by each pulse

is  $= k_1 \Delta F t$   $k_1$  - factor relating -(A.1.)  
production rate to x-ray  
flux.

The time averaged value  $F$  may be defined by

$$F = \Delta F t f$$

and using A1.

$$\Delta N = \frac{k_1 F}{f} \quad \text{-(A.2.)}$$

The flux from SCO X-1 is known, and let this be equal to  $F_0$ .

As it is a continuous source the number of electrons



produced (N) is given by the following formula

$$N = k_2 F_0 T_{\text{Decay}}$$

-(A.3)

$k_1$  - factor relating  
production rate to  
x-ray flux

$T_{\text{Decay}}$  - lifetime of  
electrons

assuming  $k_1 = k_2$  i.e. x-ray energy spectrum is the same.

$$\frac{\Delta N}{N} = \frac{F}{F_0 f T_{\text{Decay}}} \quad \text{-(A.4)}$$

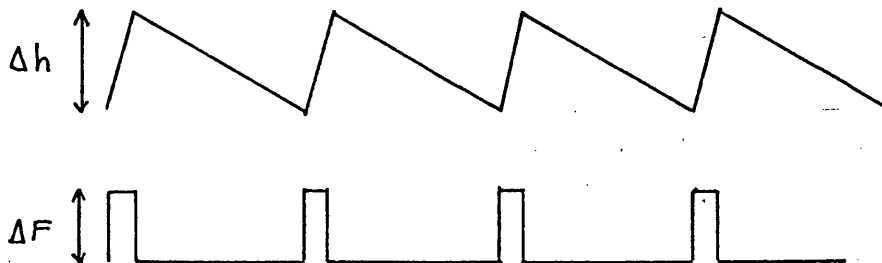
and assuming a linear relationship  $\Delta h$  - height change  
between N and h (over a small region) due to source

$$\frac{\Delta h}{h} = \frac{F}{F_0 f T_{\text{Decay}}} \quad \text{h - height change due to SCO X-1}$$

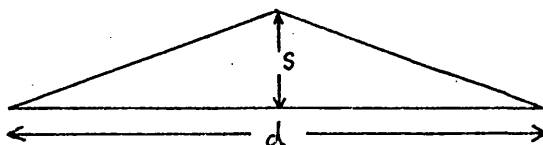
= .5 km.

$$\Delta h = \frac{F}{F_0 f T_{\text{Decay}}} h \quad \text{-(A.5)}$$

where  $\Delta h$  - the change in height will have the following form.



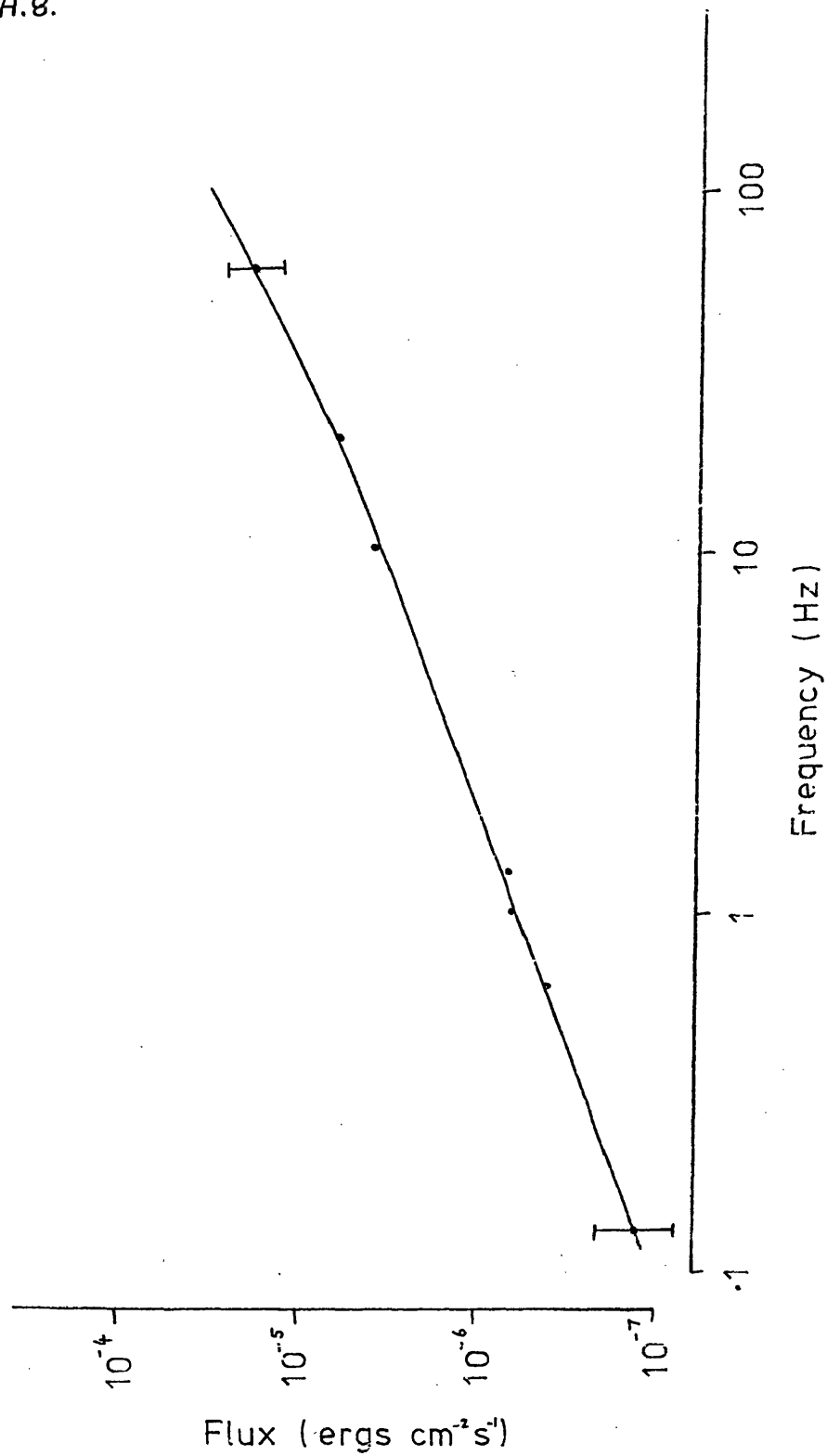
Assuming the following model for the reflection



$$s = 80 \text{ km}$$

$$d = 1500 \text{ km}$$

Fig A.8.



The X-ray flux necessary to produce a  
one standard deviation effect.

The length of the path =  $l$

Height of the ionosphere =  $s$

$$\left(\frac{l}{2}\right)^2 = s^2 + \left(\frac{d}{2}\right)^2$$

$$2 l dl = 8 s ds$$

$$dl = \frac{4 s ds}{l}$$

This path-length change corresponds to a phase change of

$$dt = \frac{dl}{c} \quad c - \text{velocity of light}$$

$$dt = \frac{4 s}{c l} \frac{F}{F_0} \frac{h}{f T_{\text{decay}}}$$

and this leads to an RMS value of

$$dt = \frac{1}{\sqrt{2} \pi} \frac{4 s F h}{c l F_0 f T_{\text{decay}}} \quad \text{---(A.6)}$$

#### The Sensitivity of the Experiment in terms of X-ray Flux

The RMS phase change of the radio signal required to give a one standard deviation effect ( in the section from 20.22 to 23.50 U.T.) was found to be 0.7ns at 20 Hz and 0.9ns at 60 Hz.

The sensitivity of the experiment to time averaged periodic X-ray flux is frequency dependent. By use of equation A.6, the experimental sensitivity in terms of phase change is related to time averaged X-ray flux. This equation gives the flux sensitivity in terms of the continuous flux from Sco X1, and by using known values of this flux<sup>71</sup>, the sensitivity in absolute units is found. Figure A.8 is a graph of the X-ray flux that would cause an effect corresponding to one standard deviation plotted

as a function of the frequency of the periodic flux. The frequencies considered range from 60 Hz ( the high frequency cut off) to 0.12 Hz, which was determined by the resolution of the Fourier transform.

As an indication the time averaged periodic flux from the Crab pulsar (NP 0532) at 60 Hz is  $1.34 \times 10^{-9}$  ergs  $\text{cm}^{-2}\text{s}^{-1}$ .

### Conclusion

On analysis of the data no effect was found to exceed a  $3\sigma$  level of significance, other than the frequencies identified as interference. This sets an upper limit to the periodic X-ray flux over a frequency range from 0.12 Hz to 60 Hz. The upper limit ranges from  $9 \times 10^{-5}$  ergs  $\text{cm}^{-2}\text{s}^{-1}$  (60 Hz) to  $6 \times 10^{-7}$  ergs  $\text{cm}^{-2}\text{s}^{-1}$ ; and it depends on the frequency as shown in Fig. A.8.

The predicted effect of the Crab pulsar is found to be much smaller than the sensitivity of the experiment; however, it should be stated that the calculations are approximate due to uncertainties in the ionospheric parameters.

This was a general search for unknown frequencies. If the object of the experiment had been solely to detect a pulsar of known frequency, such as the Crab, a cyclic averaging technique would have been preferable. However, even with continuous cyclic averaging over 1 week the flux sensitivity would have to be improved by about 2,000 in order to detect the Crab.

Although this type of experiment is not as sensitive as

satellite and rocket borne experiments it is much more convenient and far less expensive. It can also provide a relatively simple technique to search for X-ray pulses. However a difficulty encountered with this technique was that of the identification of periodic signals from terrestrial sources.

## References

1. Weber, J., 1960, Phys. Rev., 117, 306.
2. Weber, J., 1969, Phys. Rev. Lett., 22, 1320.
3. Weber, J., 1970, Phys. Rev. Lett., 25, 180.
4. Braginskii, V.B., Manukin, A.B., Popov, E.I., Rudenko, V.N., and Khorev, A.A., 1972, Soviet Physics - JETP Lett., 16, 108.
5. Drever, R.W.P., Hough, J., Bland, R., and Lessnoff, G.W., 1973, Nature, 246, 340
6. Garwin, R.L., and Levine, J.L., 1973, Phys. Rev. Lett., 31, 176.
7. Levine, J.L., Garwin, R.L., 1974, Phys. Rev. Lett., 33, 794.
8. Billing, H., Kafka, P., Maischberger, K., Meyer, F., and Winkler, W., 1975, Lett., Nuovo Cim., 12, 111.
9. Douglass, D.H., Gram, R.Q., Tyson, J.A., Lee, R.W., 1975, Phys. Rev. Lett., 35, 480.
10. Choquet-Bruhat, Y., (Ed.) Colloques Internationaux du CNRS No. 220., Ondes at Radiations Gravitationnelles, Paris, 18-22 June 1973. CNRS
11. Bonazzola, S., Chevreton, M., Felenbok, P., Herpe, G., Thierry-mieg, J., 1973, Page 101 of Ref. 10.
12. Allen, W.D., Christodoulides, C., 1975, J. Phys. A: Math. Gen., 8, 1726.
13. Hirakawa, H., and Narihara, K., 1975, Phys. Rev. Lett., 35, 330.

14. Forward, R.L., Zipoy, D., Weber, J., Smith, S., Benioff, H., 1961, Nature, 189, 473.
15. Levine, J., and Stebbins, R., 1972, Phys. Rev. D, 6, 1465.
16. Mast, T.S., et al., 1972, Nature, 240, 140.
17. Sadeh, D., and Meidav, M., 1972, Nature, 240, 136.  
Sadeh, D., 1972, Nature, 240, 139.
18. Tuman, V.S., 1971, Nature Physical Science, 230, 101  
Tuman, V.S., 1973, G.R.G., 4, 279.
19. Mast, T.S., Nelson, J.E., and Saarloos, J.A., 1974, Astrophys. J., 187, L49.
20. Forward, R.L., Private Communication as referenced in Burke, W.L., 1973, Phys. Rev. D, 8, 1030.
21. Weber, J., General Relativity and Gravitational Waves, 1961, Interscience Publications, New York.
22. Isaacson, R.A., 1968, Phys. Rev., 166, 1272.
23. Misner, C.W., Thorne, K.S., and Wheeler, J.A., 1973, Gravitation, W.H. Freeman and Co. San Fransisco.
24. Braginskii, V.B., and Rudenko, V.N., 1970, Soviet Physics - Usp., 13, 165.
25. Ceapa, A., 1972, Nature Physical Science, 240, 102.
26. Thorne, K.S., - Private Communication.
27. Thuan, T.X., and Ostriker, J.P., 1974, Astrophys. J. 191, L105.
28. ~~Talbot~~ Talbot, R.J., Astrophys. J., 1976, 205, 535. /
29. Ruffini, R., 1973, Phys. Rev. D, 7, 972.
30. Davis, M., Ruffini, R., and Tiomno, J., 1972 Phys. Rev. D, 5, 2932.

31. Rees, M., Ruffini, R., Wheeler, J.A., 1974,  
Black Holes, Gravitational Waves and Cosmology,  
Gordon and Breach Science Publications.
32. Thorne, K.S., and Braginskii, V.B., 1976, Astrophys.  
J., Lett., 204, L1.
33. Mironovskii, V.N., 1965, Sov. Phys. - JETP, 21, 236.
34. Press, W.H., and Thorne, K.S., 1972, Ann. Rev.  
Astron. and Astrophys., 10, 335.
35. Sejnowski, T.J., 1974, Physics Today, January, 40.
36. Moss, G.E., Miller, L.R., and Forward, R.L., 1971,  
Appl. optics, 10, 2495.
37. Weiss, R., Report 105, Res. Lab. Electron., M.I.T.
38. Braginskii, V.B., Manukin, A.B., Popov, E.I.,  
Rudenko, V.N., 1974, Soviet-Physics JETP, 39, 387.
39. Haslett, J.W., and Kendall, E.J.M., 1972, IEEE  
Trans. Electron Devices ED-19, 943.
40. Klaassen, F.M., and Robinson, J.R., 1970, IEEE  
Trans. Electron Devices ED-17, 852.
41. Giffard, R.P., Webb, R.A., and Wheatley, J.C.,  
1972, J. Low Temp. Phys., 6, 533.
42. Zimmerman, J.E., 1972, Cryogenics, 12, 19.
43. Donaldson, G., Private Communication.
44. Peek, J.B.H., 1968, Philips Research Supp. 1.
45. Bleaney, B.I., and Bleaney, B., Electricity and  
Magnetism, Oxford University Press 1965, Page 244.
46. Kurkijärvi, J., 1973 J. Appl. Phys., 44, 3729.
47. Bendat, J.S., 1958, Principles and applications of  
random noise theory, Wiley, New York.



48. Van Vleck, J.H., 1943, Revised and reprinted in 1966, Proc. IEEE 54,1.
49. Davies, R.D., Ponsonby, J.E.B., Pointon, L., de Jager, G., (1969), Nature, 222, 933.
50. Weinreb, S., 1963, M.I.T. Technical Report 412.
51. Cooley, J.S., and Tukey, J.W., 1965, Math. Computation,19, 297.
52. Bergland, G.D., 1969, IEEE Spectrum,6,July, 41.
53. Brigham, E.O., and Marrow, R.E., (1967) IEEE Spectrum,4,Dec, 63.
54. Richards, P.I., 1967, IEEE Spectrum, 4, January, 83.
55. Blackman , R.B., and Tukey, J.W., 1958, The Measurement of Power Spectra,Dover Publications INC. New York.
56. Groth, E.J., 1975, Astrophys. J. Supp.,29, 285.
57. Pizzella, G., 1974, Rivista del Nuovo Cimento, 5,369.
58. Kafka, P., 1975, Lectures presented at the International School of Cosmology and Gravitation, Erice.
59. Drever, R.W.P., (1971), Talk presented at the Sixth International Conference on Gravitation and Relativity - Copenhagen 5th-10th July.
60. Rudenko, V.N., Private communication.
61. Giffard, R.P., Private communication.
62. Dewitt-Morette, C., (Ed), 1974, IAU Symposium No. 64, Gravitational radiation and Gravitational Collapse (Warsaw, Sept. 1973 ). Reidel, Dardrecht.

63. Boughn, S.P., Fairbank, W.M., McAshen, M.S.,  
Paik, H.J., and Taber, R.C. (Stanford University)  
Bernat, T.P., Blair, D.G., Hamilton W.O.,  
(Louisiana State University).

Ref. 58. Page 40.

64. Carelli, P., Cerdonio, M., Giovannardi, U.,  
Lucano, G., Modena, I.,

Ref. 10. Page 257.

65. Carelli, P., Foco, A., Giovanardi, U., Modena, I.,  
Bramanti, D., Pizzella, G., 1975, Cryogenics, 15, 406.

66. Sharma, D.P., Jain, A.K., Chakravarty, S.C.,  
Kasturirangan, K., Ramanathan, K.R., and Rao. U.R.  
(1972), Astrophysics and Space Science, 17, 409.

67. Rumi, G.C., Leschiutta, S., Sabatino, A.,  
(Private Communication).

68. O'Mongain, E., and Baird, G.A., Private communication

69. Baird, G.A., 1974, J. Atmos. and Terres. Phys.,  
36, 1565.

70. Edwards, P.J., Burtt, G.J., Knox, F.,  
Nature, 222, 1053.

71. Giacconi, R., et al., 1974, Astrophys. J. Supp.  
27, 37.

72. Bradt, B., et al., 1969, Nature, 222, 728.

#### Other Publications

73. Bertotti, B., (Ed.). Proceedings of the International  
School of Physics <Enrico Fermi> No. 56, July 1972,  
Academic Press: New York and London.

74. Papini, G., 1974, Can. J. Phys., 52, 880.

75. Gibbons, G.W., and Hawking, S.W., 1971, Phys. Rev. D, 4, 2191.
76. Buckingham, M.J., and Faulkner, E.A., 1973, Radio and Electronic Engineer, 42, 163.
77. Hawking, S.W., 1972, Contemp. Phys., 13, No.3, 273.
78. Fellgett, P.B., Sciama D.W., 1971, Radio and Electronic Engineer, 41, No.9 , 391.
79. Aplin, P.S., 1972, Contemp. Phys., 13, No.3, 283.
80. Paik, H.J., Ph.D. Thesis, 1974, Stanford University.
81. Hough, J., Pugh, J.R., Bland, R., Drever, R.W.P., 1973, Nature, 254, 498.
82. Goodyear C.C., Signals and Information, Butterworths  
London. 1971. Page 48.
83. Gallop, J.C. and Petley, B.W., 1976, J. Phys. E: Sci. Instr., 9, 417.